UNIVERSITY OF HAWAII
LIBRARY
JUN 5 '53

The PHILOSOPHICAL MAGAZINE

FIRST PUBLISHED IN 1798

L. 44 SEVENTH SERIES No. 352 May 1953

A Journal of Theoretical Experimental and Applied Physics

EDITOR
PROFESSOR N. F. MOTT, M.A., D.Sc., F.R.S.

EDITORIAL BOARD
SIR LAWRENCE BRAGG, O.B.E., M.C., M.A., D.Sc., F.R.S.
SIR GEORGE THOMSON, M.A., D.Sc., F.R.S.
PROFESSOR A. M. TYNDALL, C.B.E., D.Sc., F.R.S.

PRICE 15s. 0d.
Annual Subscription £8 0s. 0d. payable in advance

D AND PUBLISHED BY TAYLOR & FRANCIS LTD., RED LION COURT, FLEET ST., LONDON, E.C.4.

Early Scientific Publications

ALERE FLAMMAM

DIARY OF ROBERT HOOKE, M.A., M.D., F.R.S.
1672-1680

25/-
net

Edited by **H. W. ROBINSON** and **W. ADAMS**
Recommended for publication by the Royal Society, London

"This vivid record of the scientific, artistic and social activities of a remarkable man during remarkable years has too long remained in obscurity."—Extract from foreword by Sir Frederick Gowland Hopkins, O.M., President of the Royal Society.

MATHEMATICAL WORK OF JOHN WALLIS, D.D., F.R.S.

12/6
net

By **J. F. SCOTT, Ph.D., B.A.**

"His work will be indispensable to those interested in the early history of The Royal Society. I commend to all students of the Seventeenth Century, whether scientific or humane, this learned and lucid book."—Extract from foreword by Prof. E. N. da C. Andrade, D.Sc., Ph.D., F.R.S.
Recommended for publication by University of London

CORRESPONDENCE AND PAPERS OF EDMOND HALLEY

21/-
net

Arranged and Edited by **EUGENE FAIRFIELD MACPIKE**

First published on behalf of The History of Science Society by Oxford University Press. Now re-issued by Taylor & Francis, Ltd.

MEMOIRS OF SIR ISAAC NEWTON'S LIFE

5/-
net

By **WILLIAM STUKELEY, M.D., F.R.S., 1752**
From an Original Manuscript
Now in the possession of the Royal Society, London

HEVELIUS, FLAMSTEED AND HALLEY

12/6
net

Three Contemporary Astronomers and their Mutual Relations
By **EUGENE FAIRFIELD MACPIKE**
Published by arrangement with The History of Science Society

Established over 150 years

TAYLOR & FRANCIS, LTD.
RED LION COURT, FLEET ST., LONDON E.C.
PRINTERS & PUBLISHERS OF SCIENTIFIC BOOKS

XLVIII. *The Effect of Small Amounts of Cold-Work on Young's Modulus of Copper*

By A. D. N. Smith
Royal Aircraft Establishment, Farnborough*

[Received December 5, 1952; Revised January 5, 1953]

Summary

The effect on Young's Modulus of copper of small amounts of plastic extension (1–8%) and subsequent low temperature annealing (50–100°c) has been studied. The results confirm previous work that there is a reduction of about 11% in the modulus, the greater part of which is recoverable after prolonged annealing at 100°c. The reduction is attributed to the elastic oscillation of the relatively mobile screw components of dislocation loops, recovery being caused by the annihilation of such components in pairs by cross-slip, as suggested by Mott (1952).

In an analysis of the recovery process it is assumed that the activation energy required to move the two screw components together is not unique but is distributed in a Gaussian manner about a mean. This mean value is found to be 25 000 cals/mole for O.F.H.C. copper extended by 1% and 21 500 cals/mole for the same material extended by 8·4%.

§ 1. Introduction

As long ago as 1907 Beilby noticed that the elastic moduli of metals are reduced by small amounts of cold-work, although partial recovery may be effected by low temperature annealing, and this phenomenon has since been confirmed by many investigators (e.g. Kuntze 1928, Kawai 1930, Köster 1940). It has also been noted that while a small amount of deformation reduces the modulus, continuing cold-work may reverse this trend in some cases, and may actually cause the modulus to increase above its original value. While it seems clear that the latter effect is due to the development of preferred crystallographic orientation, coupled with the elastic anisotropy inherent in most metals, the reason for the former has not yet been established although three theories have been put forward, which will be examined in detail in § 4 below. Some experiments have been made to assess which, if any, of these three theories is correct. In these experiments a number of polycrystalline copper bars were stretched plastically by small amounts, Young's Modulus, *E*, being measured dynamically before and after extension. The bars were then annealed for various times in the temperature range 50–100°c, the modulus being measured at sufficiently frequent intervals during the annealing period to establish a series of recovery curves.

---

* Communicated by the Author.

§ 2. Experimental Details

Material : The copper used in these experiments was principally some oxygen-free, high-conductivity copper supplied by Messrs. Thomas Bolton Ltd., in the form of rolled sheet of cross section 6 in. $\times \frac{1}{4}$ in., from which specimens of dimensions approximately 6 in. $\times \frac{1}{4}$ in. $\times \frac{1}{4}$ in. were cut. A typical maker's analysis of material supplied to the same specification as that used here is as follows : Cu 99·984%, Ag 0·002%, Fe 0·0028%, Ni 0·003%, Pb 0·001%, Bi 0·0004%, O_2 0·0045%. No trace was found of Se, Te, As or Sb.

Three experiments were also made using spectrographically pure copper in the form of 6 mm diameter bars, supplied by Messrs. Johnson Matthey and Co. Ltd.

Apparatus : Young's modulus, E, was measured dynamically by determining the fundamental frequency of vibration in the 'free-free' mode, using the relation

$$E=\frac{0{\cdot}0787\,f^2\,l^4\,\rho}{k^2}$$

where f is the natural frequency in cycles per second, l the length of the bar, ρ the density and k the radius of gyration of the section.

The apparatus used to determine the natural frequency followed the design of Förster (1937). Briefly, the specimen was suspended horizontally by two fine cotton threads attached to the bar close to the nodes of the 'free-free' mode, the other ends being attached to the coil of a moving-coil loudspeaker and to a gramophone pick-up, respectively. The loudspeaker, which was driven from an accurately calibrated decade oscillator, induced vibrations in the bar which were detected by the pick-up, amplified and fed to a cathode ray oscilloscope. The oscillator was tuned so that the vibrations increased to a maximum, and the resonant frequency was then read directly from the decade dials.

Experimental Procedure : Each specimen was first annealed in vacuo for 3 hours at 500°c, after which treatment x-ray back reflexion photographs showed that recrystallization was complete, while the grain size of one sample bar was about 0·06 mm. The moduli of the annealed bars were measured and then each bar was given a small amount of plastic strain in a tensile testing machine. Of the O.F.H.C. bars, seven were extended by 1% and seven by 8·4%, while all the three spec. pure bars were extended 1%. The ends of the test piece were then sawn off to remove the scoring made by the grips of the machine. The modulus was measured again and then each bar was annealed in the range 47–100°c, the modulus being measured at suitable intervals during heat treatment. To ensure a close control on the annealing temperature for the longer anneals, the bars were first heated up quickly by immersion in hot water at the appropriate temperature, then transferred to a vacuum flask full of oil at the same temperature, which was itself placed in a thermostatically-controlled oven. The oil served the dual purpose of smoothing out the temperature fluctuations of the oven and reducing the oxidation of the specimen. For short anneals (< 3 minutes), the specimen was kept in hot water for the whole of the annealing period.

Finally when sufficient points on the recovery curve had been obtained, all the bars were given a prolonged anneal at about 100°c, after which treatment it was assumed that all had recovered to approximately the same degree.

§ 3. Results

O.F.H.C. Copper, 1% Extension : The recovery curves are shown in fig. 1, in which the dimensionless parameter $(E_2 - E)/E_2$ is plotted against $\log_{10} t$, where E_2 was the final value of the modulus after a prolonged anneal of 70 hours at 105°c, and E was the modulus after t hours at the given temperature. The error in this parameter due to uncertainty of measurement is probably about $\pm 0{\cdot}003$.

Fig. 1

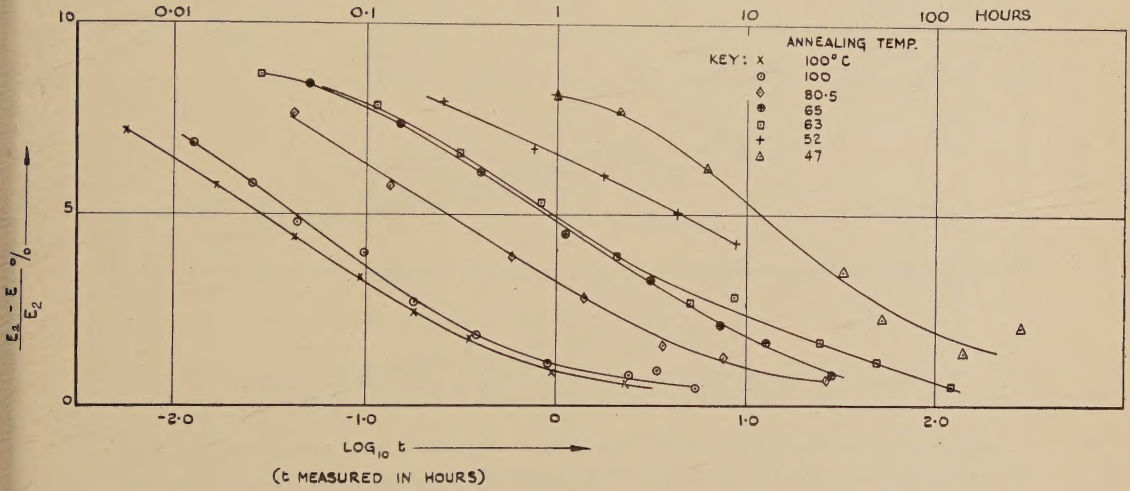

Recovery curves for bars extended 1% : O.F.H.C. copper.

It will be seen from fig. 1 that the recovery curve for the 52°c anneal is incomplete, owing to the accidental dropping of the specimen after it had been annealed for a few hours. It has been assumed however that the value of E_2 was not materially altered by this accident.

O.F.H.C. Copper, 8·4% Extension : The corresponding curves for the seven bars in this group are shown in fig. 2, the final common anneal being for 230 hours at 100°c.

Spectrographically Pure Copper, 1% Extension : Figure 3 shows the recovery curves for the three bars in this group, the final common anneal being for 70 hours at 105°c.

Effect of Stress : One experiment was made to discover whether the recovery process was speeded up by the application of stress. Two bars were extended by 1%, and after measuring the modulus of each, one was driven at resonance by the loudspeaker, while the other was not, both bars being kept at the same temperature (18°c). The amplitude of vibration used in this experiment was about 4 times greater than that normally used to measure the modulus. After about five hours of this treatment the moduli of both bars were measured in the normal manner, and it was found that both had increased by about 0·8%. It was also found that increasing the vibration amplitude by a factor of four did not alter the modulus detectably. Hence the reduction in modulus due to cold work is not influenced by the magnitude of the stress nor by the length of time for which it is applied, under the conditions of this experiment.

Fig. 2

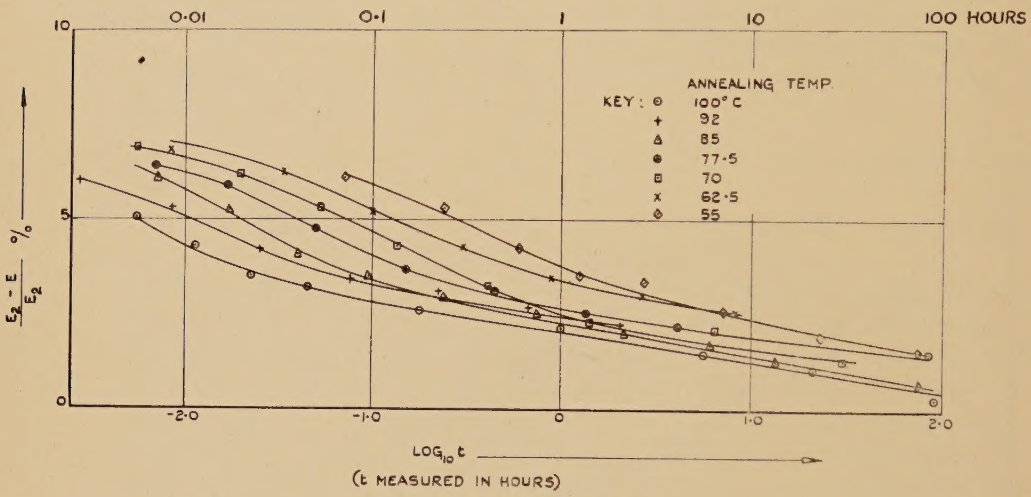

Recovery curves for bars extended 8·4% : O.F.H.C. copper.

Effect of Removal of Ends of Test-Piece : Since it was possible that the working introduced by sawing off the ends of the bars could have a marked effect on the modulus, the ends were sawn off an annealed bar ; it was found that *E* was reduced by 1% after one end was removed, and by a further 0·5% after the other end was taken off. Thus the effect was much smaller than the reduction of about 11·5% due to plastic extension.

Effect of Reduction in Temperature : One bar was cooled down to sub-normal temperature after it had been worked, to see whether there was any substantial increase of the modulus associated with reduction in temperature. The amount of plastic extension was 1% and the values of the modulus were :

Fully annealed		12 700 kg/mm^2
Freshly worked at	19°c	11 440 kg/mm^2
	−15°c	11 650 kg/mm^2
	−41°c	11 840 kg/mm^2
After test was finished	19°c	11 530 kg/mm^2

Thus, taking the mean of the values before and after cooling as the norm, a reduction of 60°c increased the modulus by about 3·1%. This figure should be compared with the increase to be expected in the modulus of annealed copper over the same temperature range, given by Köster (1948) as about 1·9%. Hence it appears that there is some increase of the modulus on cooling by 60°c below room temperature, but that it is only about 10% of the original loss.

Fig. 3

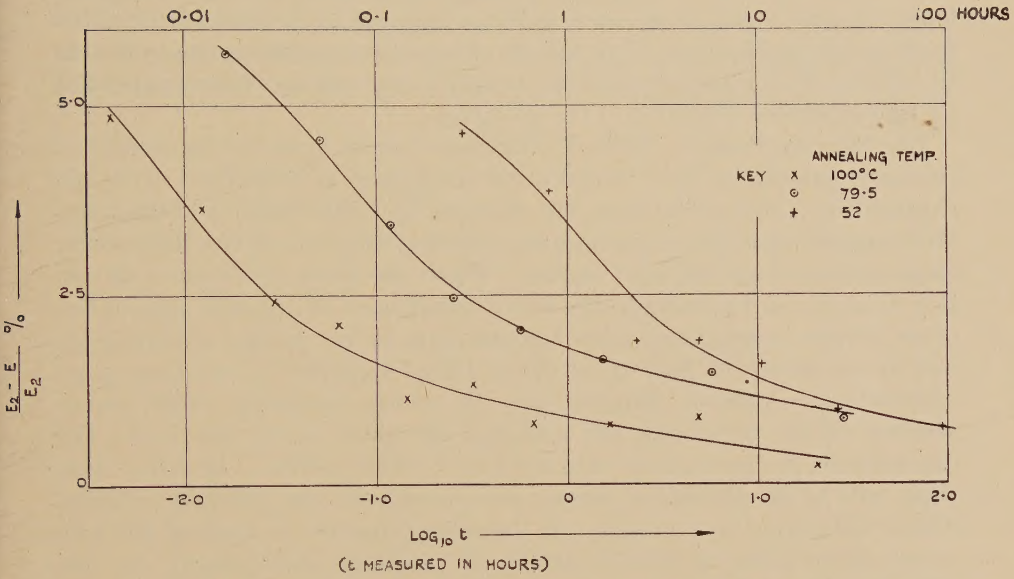

Recovery curves for spec. pure copper extended 1%.

§ 4. Discussion

Possible Causes of the Reduction in Modulus : Possible causes of the reduction and the subsequent recovery after low temperature annealing have been put forward by Zener (1948), Eshelby (1947) and Mott (1952).

Zener attributes the reduction, together with the Bauschinger effect, to the viscous nature of freshly formed slip-bands. If this is the case the effect should be very sensitive to temperature, since this usually affects the viscosity exponentially, through an activation energy. However reducing the temperature from 19°c to −41°c only increased the modulus by 10% of the original reduction. Assuming that the coefficient of viscosity increased by a similar amount, this indicates an activation energy of only about 200 cals/mole, which is far below that normally encountered in viscous flow in solids, for which the activation energy is usually in the range 20 000–40 000 cals/mole. It therefore seems most unlikely that Zener's explanation is correct.

Both the other theories involve dislocations. Eshelby (1947) suggested that dislocations lie in potential energy ' troughs ', and that these dislocations oscillate (elastically) under the application of small alternating stresses, thus increasing the macroscopic strain and apparently reducing the modulus. However Eshelby attributed the whole of the reduction to the movement of edge dislocations, while in the opinion of Mott (1952) it is the motion of the relatively more mobile screw components of dislocation loops which is responsible. It is worth noting that the evidence indicates that it is probably an elastic oscillation of the dislocations which is occurring, rather than any form of hysteresis mechanism whereby dislocations ' snap loose ' at some small stress, such as that suggested by Nowick (1951) in his work on internal friction. This follows since an increase in strain amplitude by a factor of four did not affect the modulus, nor was the recovery speeded up by continuous vibration of the specimen.

The Recovery Process : If Mott's theory is correct, then on this model the recovery caused by low temperature annealing is consistent with his explanation (1951) of the cross-slip observed by Cahn (1951) in aluminium. Mott suggests that this is a consequence of the behaviour of two dislocation loops generated on different planes. When the screw component of one loop is above and parallel to the screw component of opposite sign of the other, thermal energy may allow the two loops to join up into a single loop, half in one plane and half in the other, joined together by two short edge dislocations. Another possible way in which annealing could cause recovery is by promoting the diffusion of solute atoms to ' lock ' the dislocations, in the manner explained by Cottrell (1948). In either case there will be an activation energy associated with the recovery process, which will either be a measure of the energy barrier separating the two screw dislocations on Mott's model, or the activation energy for the diffusion of the solute in copper. For the moment let us assume that it is the former mechanism which is operative here, and examine the experimental results on this basis. In order to obtain a value for the activation energy it is necessary to make some assumptions, which are :

1. Only a given number, N, of screw dislocations lie in relatively favourable positions from which they can be moved by thermal activation.
2. The rate of movement of dislocations with a given activation energy is proportional to the number still to be moved.
3. The recovery in E at any time is proportional to the number of dislocations which have moved.
4. The activation energies are distributed in a Gaussian manner about a mean.

On the basis of these four assumptions equations are obtained in the Appendix from which both the mean activation energy, $\bar{H}$, and the standard deviation, σ, of the distribution may be determined from the experimental results. It is there shown that if the modulus after working is E_1, after time t is E and after the final prolonged low temperature anneal is E_2, then a good approximation to the relation between E and t is

$$\frac{E-E_1}{E_2-E_1}=1-\exp\left\{\frac{-t}{\tau_0}\exp\left[\frac{-\bar{H}}{RT}\right]\right\},$$

where T is the absolute temperature, R the gas constant and τ_0 a constant. A simple way of obtaining $\bar{H}$ from the experimental data is to measure the time t_1 taken to reach a given degree of recovery at an annealing temperature T_1, and to plot $\log_{10}t_1$ against $1/T_1$. Several such graphs may be obtained for different degrees of recovery, which should be a number of parallel straight lines whose slope is proportional to $\bar{H}$.

If the diffusion mechanism is the cause of recovery we should expect that the rate of diffusion of one solute element would dominate those of any of the others, so that all the dislocations would be anchored by this one element. Hence a similar plot would again yield a series of parallel straight lines with a gradient proportional to the activation energy for diffusion of the solute in copper.

Fig. 4

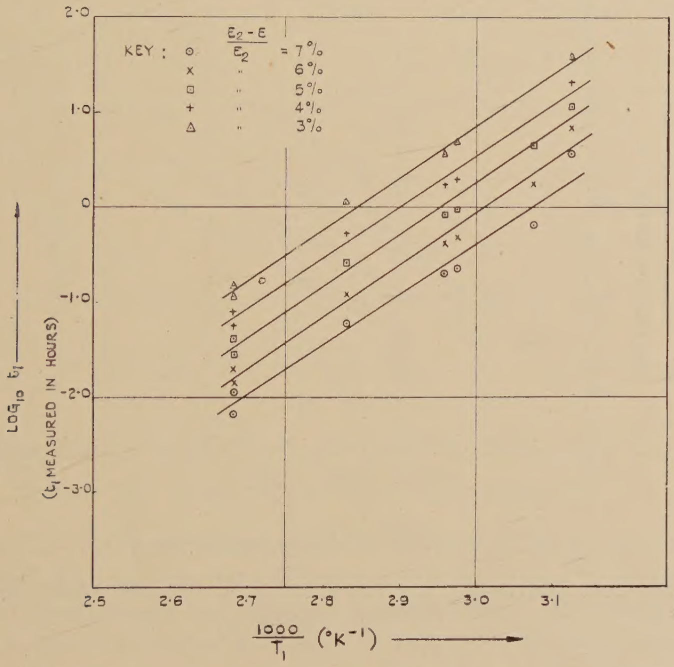

Time–temperature relation for a given amount of recovery : 1% extension. O.F.H.C. copper.

One of the main differences between the two theories is that one would expect that the distribution of activation energy would be fairly wide if it is the thermal activation of the dislocations themselves which governs recovery, while it would be fairly narrow if it is the diffusion mechanism which is operative. Thus if we can determine the standard deviation, it should help to distinguish the two.

Interpretation of Results: Figures 4–6 show the graphs of $\log_{10}t_1$ plotted against $1/T_1$ for different recovery levels for the O.F.H.C. copper bars extended 1% and 8·4%, and for the spec. pure bars extended 1%. Examination of these figures shows that the points are scattered about straight lines, although the linearity in the case of fig. 6 is doubtful, since there are only three points on each line. The lines which have been drawn to fit the points have been calculated statistically as the best regression lines, assuming that all the error lies in $\log_{10}t_1$ and none in $1/T_1$, although had the opposite assumption been made the differences in gradient would have been small.

Fig. 5

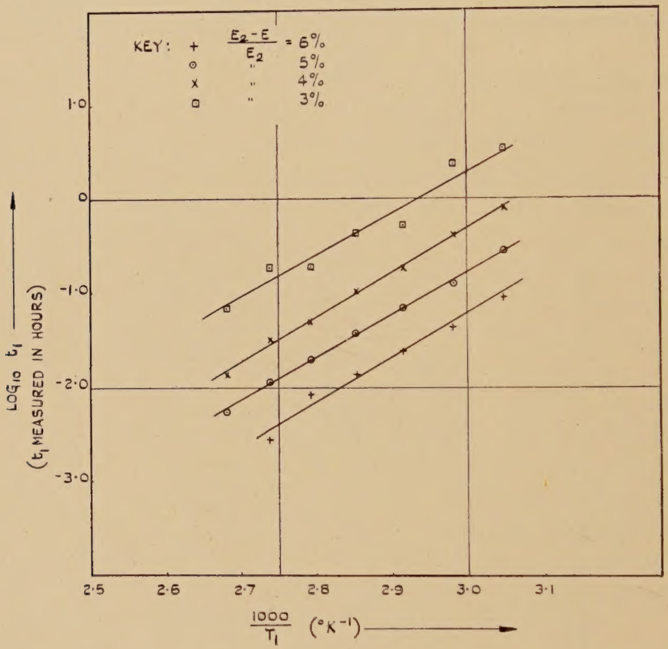

Time–temperature relation for a given amount of recovery: 8·4% extension. O.F.H.C. copper.

The standard deviation of the slope of each line was found by normal statistical methods and the 95% confidence zone found in the usual way. The mean values of these gradients (expressed as activation energies) together with these limits are given in table 1 for all the results shown in figs. 4–6, except that the 95% confidence zone for the spec. pure copper is so large, owing to the small number of results, that it is not worth quoting, and the 50% zone is given instead.

It will be seen that there is a considerable difference between the activation energies for recovery for the O.F.H.C. copper extended by 1% and by 8·4%. This suggests that the cause of recovery is more likely to be the annihilation of dislocations themselves rather than the diffusion of solute atoms, since it is unlikely that the diffusion activation energy would change so appreciably after different degrees of working. It will also be shown below that the standard deviation of the distribution is such as to confirm this view, so that it will henceforth be assumed that recovery is caused by the elimination of the mobile screw dislocations.

Fig. 6

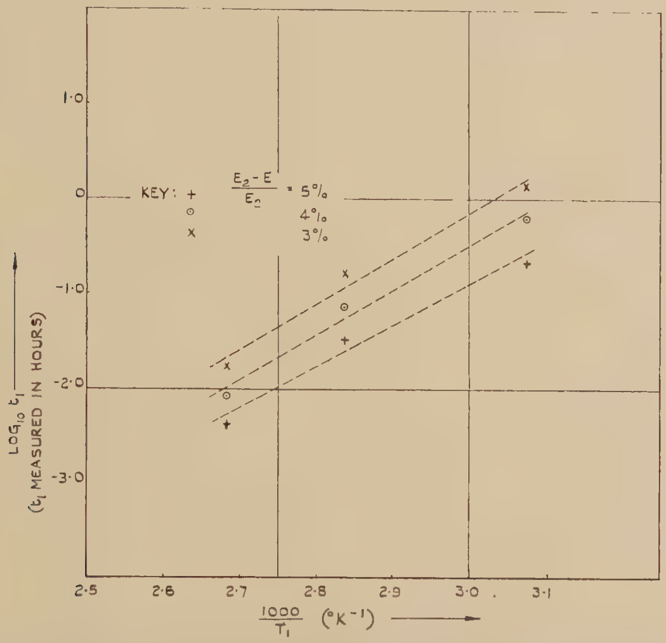

Time–temperature relation for a given amount of recovery : 1% extension. Spec. pure copper.

From table 1 a closer estimate can be made of $\overline{H}$, by taking the variation in activation energy for the different recovery levels to be random, and weighting each figure according to its reliability. It should be realized that we have not obtained a number of independent estimates of $\overline{H}$, which

Table 1. Activation Energies for Recovery

$\frac{E_2-E}{E_2}$	1% Extension O.F.H.C. Cu		8·4% Extension O.F.H.C. Cu		1% Extension Spec. Pure Cu	
	$\overline{H}$(cals/mole)	95% zone	$\overline{H}$(cals/mole)	95% zone	$\overline{H}$(cals/mole)	50% zone
7%	24 500	±21%	—	—	—	—
6%	25 300	±15%	21 500	±18·5%	—	—
5%	25 500	±13%	21 200	±4·0%	19 900	±11%
4%	24 800	±14·5%	22 000	±6·4%	21 700	±13%
3%	25 200	±7·7%	20 200	±24%	22 100	±12%

may be used to determine the probable limits within which $\overline{H}$ lies, since errors which affect one value tend to affect all. It is in fact difficult to obtain any precise limits to set on $\overline{H}$, but they should not differ very much from the closest limits given in table 1. We may therefore estimate the 95% confidence zones, in round figures to be,

1% extension O.F.H.C. Copper : 25 000 cals/mole ± 10%,

8·4% extension O.F.H.C. Copper : 21 500 cals/mole ± 5%,

while all that may be said about the spec. pure copper is that there is a 50 : 50 chance that $\overline{H}$ lies within the zone 21 000 cals/mole ± 12%.

It should be noticed that if these confidence limits are accepted, and we regard the final mean figures as though they had been derived experimentally as the slopes of lines through 7 points (as is the case with most of the lines of figs. 4 and 5), the chance that the difference between the two values of $\overline{H}$ is not statistically significant is less than 1 in 1000.

As mentioned above, the standard deviation, σ, of the distribution of activation energies may be estimated from the gradients of the experimental recovery curves, figs. 1–3, by a method given in the Appendix. It is there shown that the values of σ are :

1% extension O.F.H.C. Copper : 1800 ± 300 cals/mole,

8·4% extension O.F.H.C. Copper : 2200 ± 200 cals/mole,

the limits placed on the values being the 95% probability zones. This fairly wide distribution confirms the view that it is not the diffusion of solute elements which causes recovery.

Summing up, we conclude that the most satisfactory explanation of the drop in modulus and subsequent recovery is that suggested by Mott (1952) viz. the application of an alternating stress causes relatively mobile screw dislocations to oscillate in their potential energy troughs, giving an extra contribution to the macroscopic strain which is entirely elastic ; low temperature annealing provides sufficient thermal energy to enable suitably placed screw dislocations lying in different planes to annihilate one another in pairs. From the results obtained it appears that the mean activation energy for recovery decreases as the cold-work increases, but that the standard deviation of the energy distribution increases. There is also some evidence that this activation energy is less for the recovery of spectrographically pure copper than for O.F.H.C. copper, for the same amount of working, but this is not certain.

ACKNOWLEDGMENTS

The author is greatly indebted to Mr. S. Pearson for many helpful discussions and to Miss D. M. Seal for her advice on statistics. Acknowledgment is also made to the Chief Scientist, Ministry of Supply, and to the Controller, H.M. Stationery Office for permission to publish this paper.

REFERENCES

BEILBY, G., 1907, *Proc. Roy. Soc.* A, **79,** 463.
CAHN, R. W., 1951, *J. Inst. Met.*, **79,** 129.
COTTRELL, A. H., 1948, *Report of Conference on Strength of Solids* (Phys. Soc.), 30.
ESHELBY, J. D., 1949, *Proc. Roy. Soc.* A, **197,** 396.
FÖRSTER, F., 1937, *Z. für Metallkunde,* **29,** 109.
KAWAI, T., 1930, *Sci. Rep. Imp. Univ., Tohoku,* **19,** 209.
KÖSTER, W., 1940, *Z. für Metallkunde,* **32,** 282 ; 1948, *Ibid.*, **39,** 1.
KUNTZE, W., 1928, *Z. für Metallkunde,* **20,** 145.
MOTT, N. F., 1951, *Proc. Phys., Soc.* B, **64,** 729 ; 1952, *Phil. Mag.*, **43,** 1151.
NOWICK, A. S., 1951, *Phys. Rev.*, **80,** 249.
ZENER, C., 1948, *Elasticity and Anelasticity of Metals,* Monograph (University of Chicago Press), 144.

APPENDIX

THE RELATION BETWEEN RECOVERY AND ANNEALING TIME

The assumptions on which this relation will be derived have been given above in § 4. Now suppose that immediately after working, the number of dislocations contributing to the reduction in modulus with energies between H and $H+\delta H$ is δn. Then the number of these dislocations which have moved after time t is $\delta n\,(1-\exp\,(-t/\tau))$, where it is assumed that $\tau=\tau_0\exp\,(H/RT)$. Since the recovery in E is proportional to the total number of dislocations which have moved, irrespective of their energies, the relation between E and t is

$$\frac{E-E_1}{E_2-E_1}=\frac{1}{N}\int_0^N\left\{1-\exp\left[-\frac{t}{\tau_0}\exp\left(-\frac{H}{RT}\right)\right]\right\}dn, \quad . \quad . \quad (1)$$

where N is the total number of movable dislocations. If the activation energies are distributed according to the Gaussian law, the relation between n and H is

$$\frac{n}{N}=\frac{1}{\sigma\sqrt{(2\pi)}}\int_{\overline{H}}^{H}\exp\left[-\frac{(H-\overline{H})^2}{\sigma^2}\right]dH,$$

where $\overline{H}$ and σ are the mean and the standard deviation, respectively. For any given values of $\overline{H}$ and σ a good approximation to the solution of eqn. (1) may be made using a step-by-step calculation. The activation energy distribution is divided into equal zones, 1000 cals/mole wide, and the proportion of N having activation energies in each zone is found from tables. Then, taking H as constant in each zone, eqn. (1) is expressed as a summation of terms, each of which may be computed in terms of t, T and the parameter τ_0. This computation has been made for ten different conditions, viz. a mean activation energy of 25 000 cals/mole with five standard deviations ($\sigma=0$, 500, 1000, 2000, 3000, cals/mole), for each of two annealing temperatures ($T=323$ and 373°K). In order to test whether a zone 1000 cals/mole wide was sufficiently narrow one computation was made using zones only 500 cals/mole wide ($\sigma=1000$ cals/mole and $T=373$°K) ; no significant difference from the corresponding computation using wider zones was found. The results of the ten computations are shown graphically in figs. 7 and 8 in which $(E_2-E)/(E_2-E_1)$ is plotted against $(\log_{10}t-\log_{10}\tau_0)$.

The above method shows how to obtain recovery curves given the distribution of activation energies: the practical problem is to find the distribution given the recovery curves.

1. *Determination of $\overline{H}$.*

As a first approximation take H as constant in eqn. (1) and equal to $\overline{H}$, then

$$\frac{E-E_1}{E_2-E_1}=1-\exp\left(\frac{-t}{\tau_0}\exp\left(-\frac{\overline{H}}{RT}\right)\right).$$

Now consider two recovery curves at different annealing temperatures T_1 and T_2. Let the times taken to reach the same arbitrary level of recovery be t_1 and t_2 in the two cases. Then

$$\log_e\frac{t_1}{t_2}=\frac{\overline{H}}{R}\left(\frac{1}{T_1}-\frac{1}{T_2}\right).$$

Applying this result to the theoretical recovery curves shown in figs. 7 and 8 at different recovery levels and different standard deviations we obtain the values of $\overline{H}$ shown in table 1.

Table 1. Values of $\overline{H}$ from Theoretical Recovery Curves

$\frac{E_2-E}{E_2-E_1}$	$\overline{H}$ (cals/mole)	
	σ=2000 cals/mole	σ=3000 cals/mole
70%	24 000	23 400
60%	24 500	24 200
50%	25 000	25 000
40%	25 500	25 700
30%	26 100	26 400

Now in this particular case the true value of $\overline{H}$ is 25 000 cals/mole, so that table 1 shows that the first approximation taken above is accurate enough to give a reasonable figure for $\overline{H}$, particularly in the region of 50% recovery.

2. *Determination of σ*

The value of the standard deviation of the distribution may be obtained from measurements of the gradients of the recovery curves at their points of inflexion. It will be seen from figs. 7 and 8 that this gradient is fairly sensitive to the value of σ, while some further computations showed that it is insensitive to the value chosen for $\overline{H}$. The gradients of the experimental curves are shown in table 2, allowance being made for the fact that the first measured value of the modulus after working was not the true value of E_1.

It is clear from this table that the experimental error outweighs any differences due to different annealing temperatures, so that the results are best treated as being random variations about a mean, corresponding to a mean annealing temperature of about 75°c. Comparing this value with

Table 2. Gradients of Experimental Curves at Points of Inflexion

	1% Extension							8·4% Extension						
Annealing Temp. (°c)	47	52	63	65	80·5	100	100	55	62·5	70	77·5	85	92	100
Gradient $\frac{d(\%\text{ possible recovery})}{d\log_{10}t}$	39	24·5	32	32	30·5	35·5	31·5	26	24	27	27	30	25	28

Fig. 7

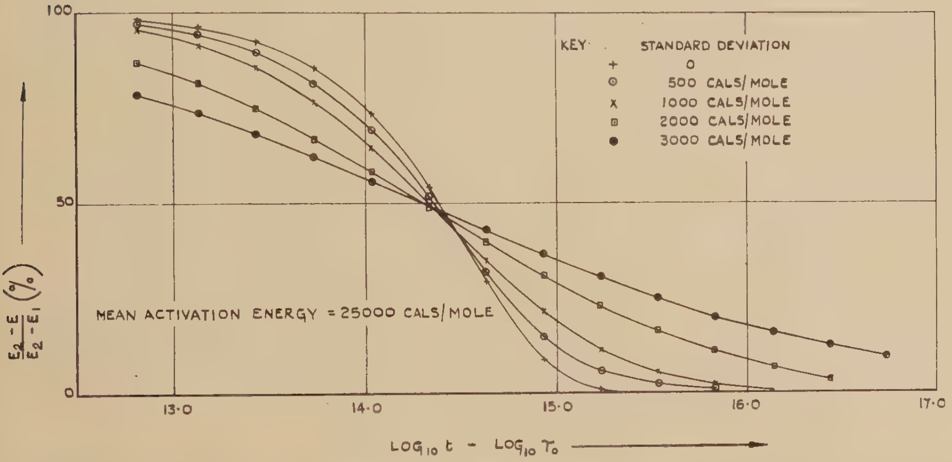

Theoretical recovery curves assuming Gaussian distribution of activation energies. Annealing temperature 100°c.

Fig. 8

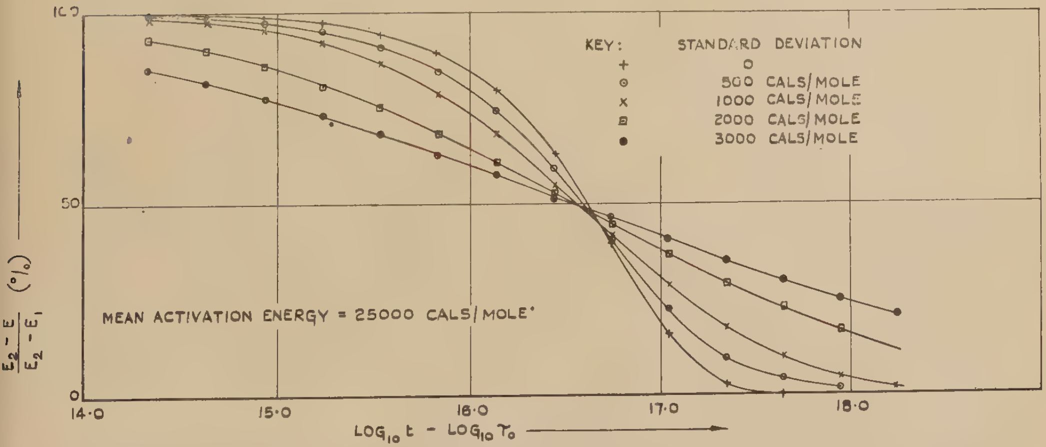

Theoretical recovery curves assuming Gaussian distribution of activation energies. Annealing temperature 50°c.

the mean of the two gradients of the theoretical curves for different values of σ, which mean is assumed to correspond roughly to an annealing temperature of 75°c, by interpolation the standard deviations of the distribution were found to be :

$$1\% \text{ extension } 1800 \pm 300 \text{ cals/mole,}$$
$$8{\cdot}4\% \text{ extension } 2200 \pm 200 \text{ cals/mole.}$$

Thus both the parameters of the distribution may be obtained, and it has been shown that one depends but little on the other.

3. *Value of* τ_0

Comparison of the experimental curves with the corresponding theoretical curves, at 50% recovery, gives the values of τ_0 as approximately 5×10^{-13} seconds for the 1% extension and 10^{-11} seconds for the 8·4% extension. It is of interest that the period of one atomic vibration for copper is about $1{\cdot}5 \times 10^{-13}$ seconds, since this will be the shortest time for a dislocation to move one atomic distance.

XLIX. *The Adsorption of Gases at High Saturations*
I: The Adsorption of Nitrogen, Argon and Oxygen

By Raymond Bowers
Institute for the Study of Metals, The University of Chicago, Chicago, Illinois*

[Received January 20, 1953]

Abstract

The adsorption of argon, nitrogen, and oxygen on an aluminium foil has been determined by a gravimetric method. The purpose of the investigation was to obtain data at high saturations for comparison with the Frenkel–Halsey–Hill equation describing multilayer adsorption. The isotherms obtained indicate that this equation is obeyed closely for the three gases. Apparent deviations in the case of argon and oxygen can be ascribed to anomalous packing in the first few atomic layers and allowance can be made for this effect. The verification is discussed in terms of the theoretical basis for the equation. Data is also given for the cross sections of the argon and oxygen molecules in the first atomic layer. It is suggested that these cross sections are considerably greater than values calculated from the corresponding bulk density. The magnitude of the standard nitrogen cross section is also discussed.

§ 1. Introduction

From a theoretical point of view, there are two regions of an adsorption isotherm which are of particular interest. These regions comprise, firstly, that at very low saturation, where the first few atomic layers are being formed, and secondly, the region at very high saturation, where the transition from multi-molecular layers to the liquid phase is taking place. Although there exists no comprehensive theory of adsorption describing the growth of the adsorbed layers over the entire pressure range, important theoretical calculations have been made which appear to be satisfactory within the two regions mentioned above. The physical difference between these two regions is best described in terms of the binding forces involved. At low saturations, the forces between adsorbed molecule and the adsorbing wall dominate the process, while near saturation, the forces between the molecules in the adsorbed layers become the most important.

The formation of the first few adsorbed layers has been described by a number of theories, of which the most successful is that of Brunauer,

---

* Communicated by the Author.

Emmet and Teller (1938); however, it is generally admitted that a number of crude approximations must be made in order to solve the equations describing the adsorption process. For example, it is assumed that the number of molecules adsorbed over a given site is independent of the numbers on adjacent sites. In other words, lateral interactions between molecules in the adsorbed layers are neglected. Furthermore, the energy of adsorption of all but the first layer is assumed to be equal to the energy of liquefaction, so that only the first layer is considered to be significantly different from the liquid.

A number of attempts have been made to introduce refinements into the B.E.T. theory (e.g. Brunauer, Deming, Deming and Teller 1940, Cassel 1944), but a satisfactory solution for the complete adsorption isotherm has not been obtained because of the mathematical difficulties encountered when a more realistic model is assumed (Hill 1952).

As a result of these difficulties, the region of high saturation is of special interest. Here the number of layers is high enough for anomalous properties of the first layer to be relatively unimportant. It is therefore possible to make predictions of the form of the isotherm without having recourse to the type of approximation necessary for any solution of the low saturation problem. Calculations for this region have been made by Frenkel (1946), Halsey (1948), Hill (1949), and McMillan and Teller (1951). They suggested that, approaching saturation, the isotherm should follow the relation

$$-\ln p/p_0=\frac{K}{\nu^3}, \quad . \quad . \quad . \quad . \quad . \quad . \quad . \quad . \quad . \quad (1)$$

where ν is the number of layers adsorbed at a pressure p, and p_0 is the saturated vapour pressure. K is a constant of proportionality determined by molecular forces, as will be discussed later. Actually, Halsey proposed a more general form

$$-\ln p/p_0=\frac{K}{\nu^s},$$

without specifying the index s explicitly.

Equation (1) has a simple physical basis. It is derived by assuming that the van der Waals forces between an adsorbed atom and the adsorbing wall fall off as the cube of the distance. The specific form of (1) results from equating the difference in the differential Gibbs free energy of the adsorbed phase and the bulk liquid, $\mu-\mu_l=RT\ln p/p_0$, to the corresponding change in potential energy due to the van der Waals forces. It is possible to allow for the influence of the interactions within the adsorbed layer as well as the attraction due to the wall. The calculation of Hill (see McMillan and Teller 1951) gives the following form for the constant of proportionality in (1):

$$K=\frac{\pi}{6}\rho_1{}^4 d_{11}{}^6 \sigma_1{}^3 \frac{\epsilon_{11}}{kT}\left(\frac{\rho_2\, d_{12}{}^6\, \epsilon_{12}}{\rho_1\, d_{11}{}^6\, \epsilon_{11}}-1\right), \quad . \quad . \quad . \quad . \quad . \quad (2)$$

where ρ is the molecular number density, d_{ij} the equilibrium distance between a pair of molecules of types i and j, ϵ_{ij} is the potential energy of such a pair at the distance d_{ij}, and σ is the effective molecular cross section. The subscripts 1 and 2 refer to the adsorbate and adsorbent respectively. McMillan and Teller have shown that this constant is approximately

$$K=\frac{\pi}{6}\frac{\epsilon_{11}}{kT}\left(\frac{\epsilon_{12}}{\epsilon_{11}}-1\right). \qquad (3)$$

It is therefore possible to correlate the magnitude of adsorption at high saturations with the molecular forces involved.

Further approximation enables us to express K in terms of the measured energies of adsorption. McMillan and Teller have shown that $\epsilon_{12}-\epsilon_{11}$ is of the order of $(E_1-E_l)/N$, where E_1 is the energy of adsorption of the first layer, E_l is the energy of liquefaction, and N is Avagadro's number. (E_1-E_l) is a quantity appearing explicitly in the equation of Brunauer, Emmet, and Teller and can be derived from the intercept of the B.E.T. plot of $p/(p_0-p)V$ against p/p_0. (V is the volume adsorbed at the pressure p.) Thus we take for our final approximation :

$$K=\frac{\pi}{6RT}(E_1-E_l). \qquad (3\,a)$$

Owing to the fundamental basis and essential simplicity of this relation, experimental tests of its validity are of particular interest. The data usually quoted as supporting these conclusions are those of Harkins and Jura (1944) who measured the adsorption of nitrogen and of water on anatase (powdered TiO_2). These data showed that eqns. (1) and (3) are followed quite closely, although Halsey (1948) deduces that an exponent of ν equal to 2·67 instead of 3 describes the data more accurately. Halsey considers this deviation from the cubic law to be important and has asserted that the empirical value of the exponent of ν in eqn. (1) "has no simple relation to the power in the expression for London forces". From the work of Drain and Morrison (1952), it appears that the exponent may even be as low as 2 for argon adsorbed on rutile.

In the case of more complicated systems, it is evident from the work of Boyd and Livingston (1942) that for adsorption of water on graphite, and propyl alcohol on anatase and barium sulphate, large deviations occur from the Frenkel-Halsey–Hill relation. This is to be expected, since the derivation of eqn. (1) is only valid for adsorbed systems with spherical fields and this simplification may not be satisfactory for complicated systems where orientation effects in the surface layer are possible. The data of Boyd and Livingston are insufficient for an exact determination of the deviation.

There are two reasons why further work on this high saturation region was desirable. In the first place, it is not easy to determine the number of adsorbed layers at high saturations using the volumetric method of previous workers, since the dead space corrections become large and deviations from the ideal gas law make them difficult to calculate. Secondly, it is desirable to observe adsorption on surfaces which are better defined than that of a fine powder such as anatase, in which capillary condensation may produce serious errors, especially near saturation. McMillan (1947) has shown that many of the deviations from the ideal B.E.T. isotherm can be explained quantitatively in terms of surface heterogeneity, thus emphasizing the importance of the character of the surface.

For these reasons a determination of the adsorption at high saturations for a number of gases has been undertaken. The measurements were carried out using nitrogen, argon, and oxygen as adsorbate gases and aluminium foil of low roughness factor as an adsorbent. Measurements have also been made with helium and these results will be described in the next paper (Bowers 1953). Due to the unique properties of helium at low temperatures, its adsorption is of interest for reasons beyond those being considered in this paper.

The adsorption was determined gravimetrically, using a microbalance similar to that described by Gulbransen (1944) and more recently by Rhodin (1950). The principle of the method is simply that of determining the increase in weight of the specimen as adsorbed layers form on it. This method has the important advantage that at high saturations there are no corrections to be applied to the observed weight of the adsorbed layer. Furthermore, it is possible to use a relatively small specimen with a small roughness factor for this determination.

§ 2. METHOD

The microbalance used in this determination was very similar in design to that described by Rhodin (1950), having in particular the same symmetrical construction in order to avoid buoyancy corrections. The apparatus was primarily designed for experiments on helium adsorption at liquid helium temperatures, but by filling the liquid helium dewars with liquid argon, nitrogen, or oxygen, the specimen and counterweight could readily be maintained at various temperatures between 77 and 90°K, determined by the boiling points of the respective gases. The arrangement is shown schematically in fig. 1. The specimen of aluminium foil and the aluminium counterweight, balanced to 10^{-5} g, are supported from the arm of the balance by Kovar wires of 0·002 in. diameter. They are suspended inside tubes of $\frac{1}{2}$ in. diameter which lead into two separate dewar vessels as shown in fig. 1.

The specimen of aluminium foil was wound into a loose coil; it had a geometrical area of 306 cm^2 and weighed $\frac{1}{2}$ gram. The counterweight was cylindrical and had a surface area of 2 cm^2. Thus the adsorption measured refers to the difference in area between specimen and counterweight equal to 304 cm^2. The specimen was degassed initially at 350°C for 12 hours, the pressure in the specimen chamber being 2×10^{-6} mm of mercury. This was done with the specimen in its final position in the cryostat and subsequent contamination was avoided by keeping the chamber evacuated to 2×10^{-6} mm between experiments. Presumably, there is a layer of chemisorbed oxygen on the aluminium, which is not removed in the degassing.

Elaborate shock mounting was used in order to prevent vibration reaching the balance system. Much of the complexity in the apparatus is necessary only for the adsorption work with liquid helium ; accordingly, the details of the microbalance and associated cryogenic equipment will not be described here. There is one aspect of the arrangement which differs from similar apparatus of other workers. When working with nitrogen, argon, and oxygen, it was found desirable to place these liquids not only in the dewars represented in fig. 1, but also in dewars which enclosed the ones shown. These outer dewars are essential for providing nitrogen temperature shielding of the inner dewars when liquid helium is being used, but their use with the other gases results in a quiescent liquid in the inner vessels and this reduces spurious movement of the balance. The pumping

Fig. 1

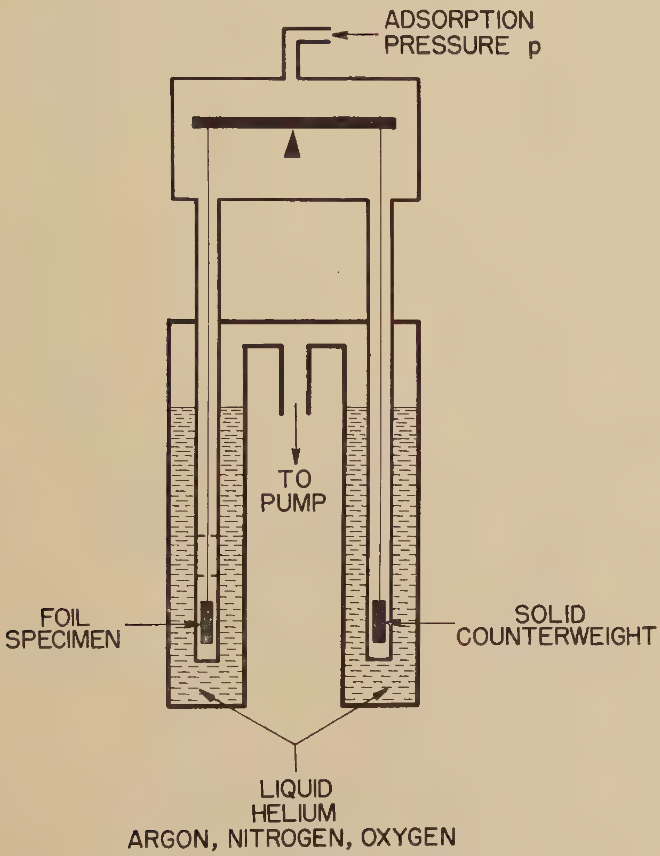

Schematic diagram of apparatus.

tube shown in fig. 1 is only used with helium, since delayed boiling in the other liquefied gases renders precise temperature control impossible during pumping.

Fig. 2

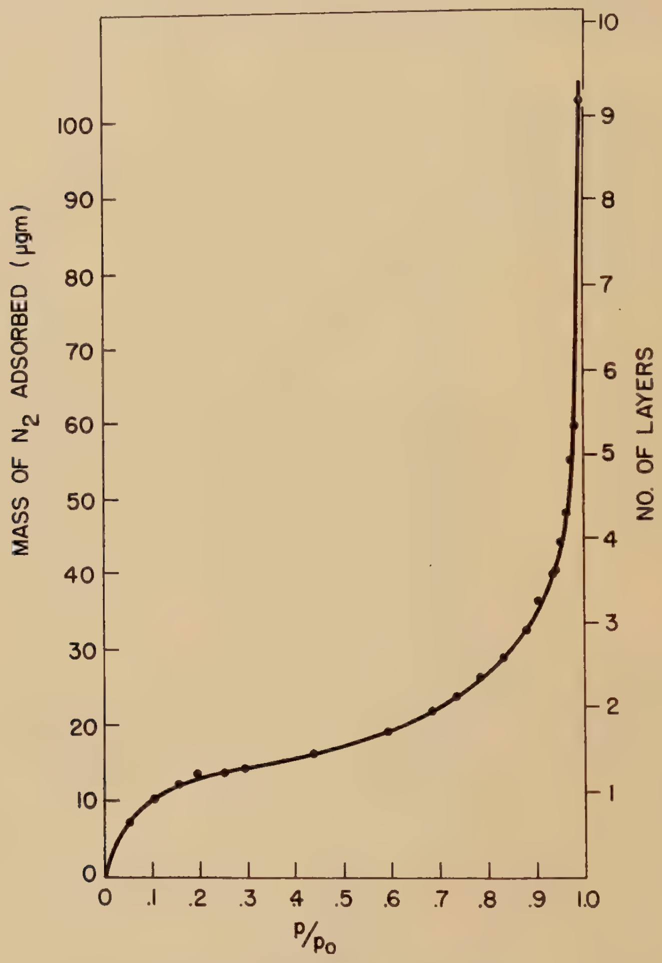

Nitrogen isotherm at 77·4°K.

§ 3. Results

Adsorption of Nitrogen

In fig. 2 is shown an isotherm for nitrogen at 77·4°K and in fig. 3 the corresponding B.E.T. plot (Brunauer, Emmet, and Teller 1938) which indicates a satisfactory agreement between theory and experiment between 5 and 30% saturation. The effective area of the foil determined from this B.E.T. diagram was 388 cm^2 as compared with the geometrical area of 304 cm^2. This implies a surface roughness factor of 1·3. In the calculation of the surface area, the cross section of the nitrogen molecule was taken to be 16·2 Å^2 (Emmet 1948, Harkins 1952, p. 227). Thus the specimen of aluminium foil could be considered relatively smooth from the point of view of adsorption, since this roughness factor is small. From the

Fig. 3

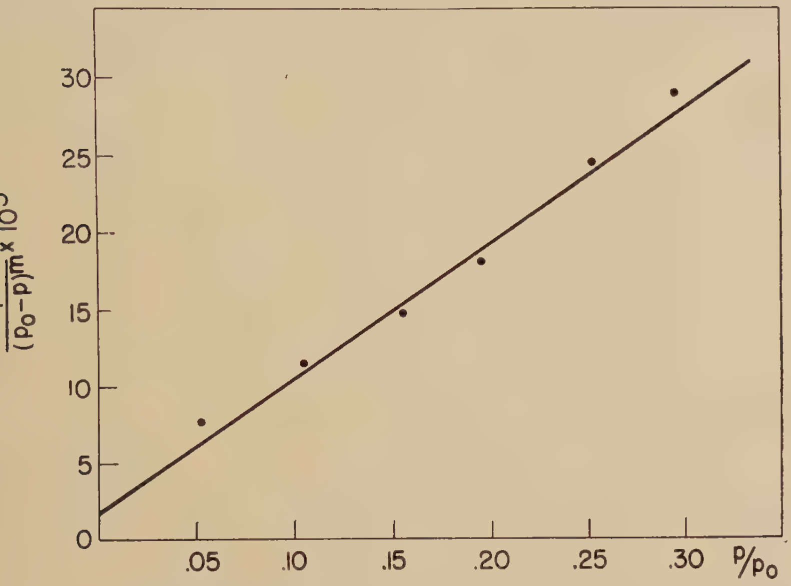

The B.E.T. plot for nitrogen at 77·4°K. (In this figure, *m* is the mass adsorbed in μg.)

Fig. 4

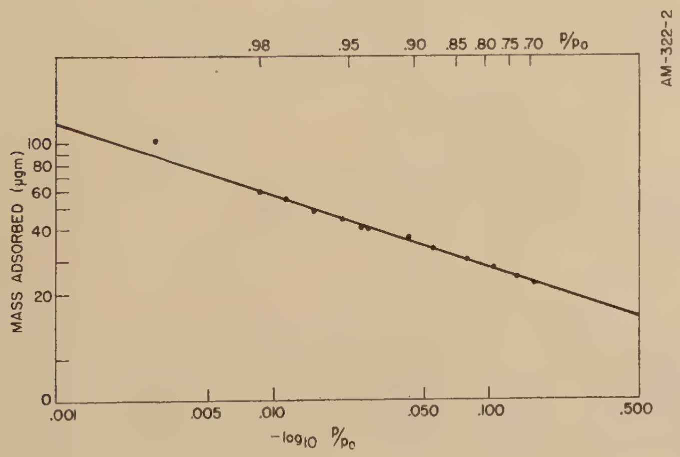

B.E.T. plot it was calculated that a completed monolayer on the specimen weighed $11{\cdot}1 \times 10^{-6}$ g ; the number of layers could therefore be determined to a precision of at least one-tenth of a layer.

We shall now turn to an analysis of these data. In fig. 4 we show a graph of loglog p/p_0 against log (mass adsorbed). This graph should be a straight line, the slope giving the exponent of ν in the Frenkel–Halsey–Hill relation, assuming the number of layers is proportional to the mass adsorbed. The slope of this straight line was found to be 3·0 as predicted by Frenkel and Hill. One notices that there is one point, corresponding to 99·3% saturation, which lies above the line, suggesting that in this very high saturation region the number of layers is increasing at a more rapid rate than given by the cubic relation. However, since the isotherm is extremely steep in this region, one cannot say with certainty that this deviation does not arise from experimental error. Nevertheless, it does seem possible that at the highest saturations the number of layers is indeed increasing faster than the cubic law would require. It is difficult to specify the exact meaning of such an increase, because even though the roughness factor of the aluminium foil is small, some form of capillary condensation may be influencing the total weight of the specimen so near the saturation point. It is probably significant that one can see this tendency to a more rapid growth in the number of layers at a lower saturation, of the order of 96%, in the data of Harkins and Jura on anatase, where capillary condensation is more likely to occur. Apart from capillary effects, the influence of surface tension and gravity on the adsorbed film may have to be reconsidered at these high coverages.

In fig. 5 we have plotted log p/p_0 against $1/\nu^3$ in order to determine K, the constant of proportionality in eqn. (1). The agreement between experiment and theory is most striking when plotted in this manner. The value of the constant K for nitrogen was found to be 3·10.

We may compare the empirical value with the approximate eqn. (3 *a*). Substituting $E_1-E_l=800$ cal/mole (Brunauer 1945, p. 157) in this equation, we obtain $K\simeq 2{\cdot}7$ at 77°K. This is very close to the observed value of 3·1 mentioned above. This degree of agreement may be fortuitous, since an order of magnitude is all that McMillan and Teller claim for their method of estimating K.

Summing up the results for nitrogen, it seems that the Frenkel–Halsey–Hill relation is followed very closely; the proportionality between $\log p/p_0$ and $1/\nu^3$ is established and the constant K has the correct order of magnitude.

The Adsorption of Oxygen

The adsorption of oxygen has been measured at 77·4°K and 89·7°K. The two isotherms were found to be similar in character, and in fig. 6 we show the data for 77·4°K. Adsorption and desorption points are shown in this figure. There is no evidence of significant hysteresis in the data. This is to be expected, since hysteresis in adsorption is usually ascribed to cracks and pores in the surface of the adsorbent (Zsigmondy 1911, McBain 1935).

The B.E.T. plot was found to be a straight line between 5% and 25% saturation. The weight of the first layer was found to be 10·1 μg at 77·4°K and 9·05 μg at 89·7°K. Assuming the area for adsorption is 388 cm^2, as determined from the nitrogen isotherm, these values imply a cross section for the oxygen molecule in the first layer which is greater than that calculated from the bulk liquid density (Brunauer 1945, p. 287). The area per molecule in the first layer was found to be 20·3 Å^2 at 77·4°K and 22·7 Å^2 at 89·7°K as compared with a value of 14·2 Å^2 calculated from the bulk liquid density at 89°K. The existence of anomalous densities in the first few layers is well known in the adsorption of gases (Beebe, Beckwith, and Honig 1945, Davis, DeWitt, and Emmet 1947, Emmet 1948), although the values for the cross sections found in this experiment for oxygen seem higher than those of other workers.

Fig. 5

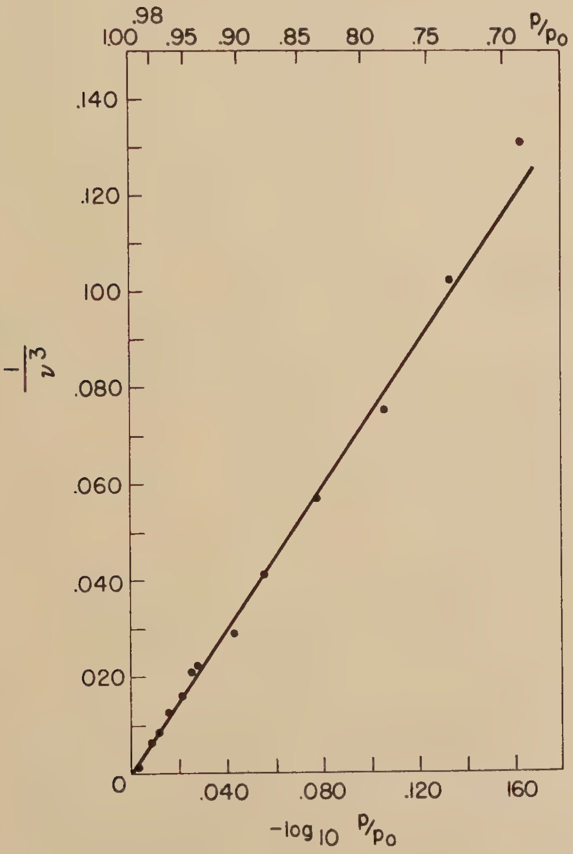

The existence of the anomalous first layer introduces a further problem in the comparison of our results with the Frenkel–Halsey–Hill equation. We must allow for the varying density of the layers in computing ν, the number of layers, from our measured values of the mass adsorbed. In the case of nitrogen, previous work has shown that the first layer is not anomalous, so that it has become a standard gas for area determinations (Harkins and Jura 1944); this means that we could take the number of layers as proportional to the mass adsorbed. It is instructive to see how the variation in layer density affects the evaluation of our data, because

Fig. 6

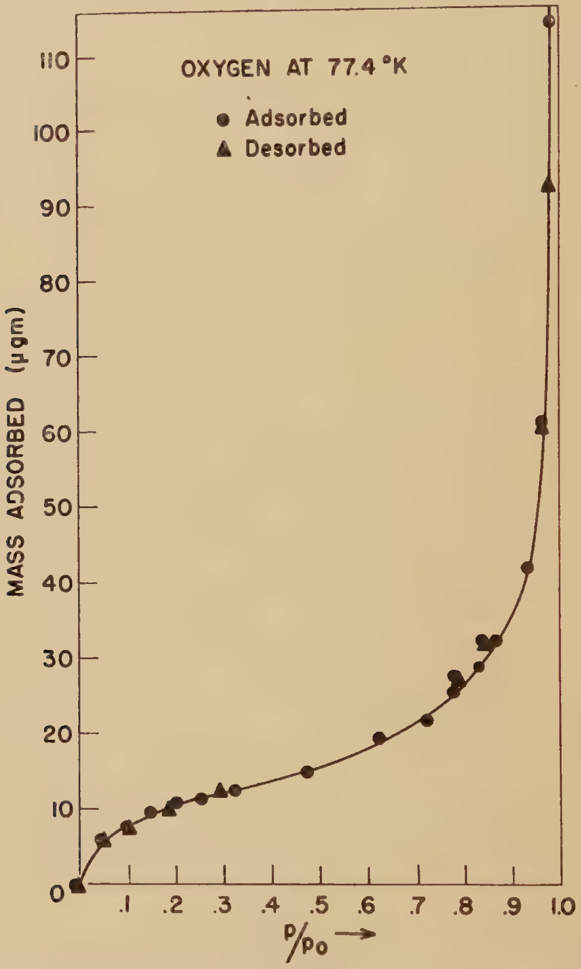

Oxygen isotherm.

this factor may be responsible for apparent deviations from the Frenkel–Halsey–Hill relation.

In fig. 7 we show a graph of log ν against loglog p/p_0 for data obtained at 89·7°K. In computing the points for curve **I**, we have assumed that all the layers have the same density as the first layer. The inverse slope of this line (which should equal the exponent of ν in eqn. (1)) was found to be 2·78. The points on curve II have been computed, assuming that only the first layer has the anomalous density determined from the B.E.T. plot, while all the rest have the bulk liquid density. The inverse slope of this line is 3·34. It is quite clear that the assumptions underlying the computation of these two curves are unrealistic ; neither can be accepted physically. However, the errors involved are in opposite directions and the real physical picture must lie between the two assumptions. The situation in the adsorbed film must involve a gradual change from the low density of the first layer to the liquid density in the outermost layers. It is interesting to see that one assumption yields an exponent slightly greater than 3, while the second yields one which is slightly less than 3. Since a realistic distribution of density would give a line in between the two shown in fig. 7, an exponent of 3 cannot be far wrong.

Fig. 7

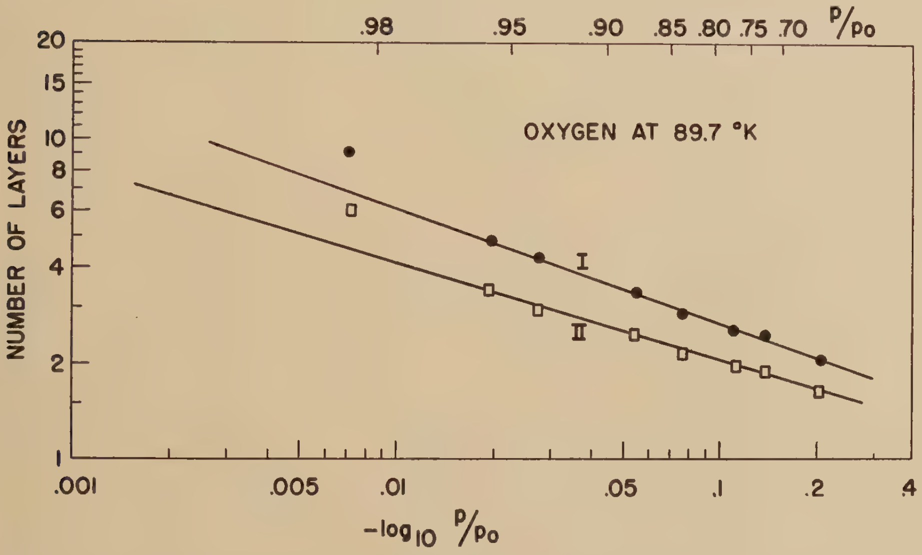

The value of K computed from the experimental results is 4·5 for points on curve I and 2·7 for those on curve II. These values have the correct order of magnitude as calculated from eqn. (3a). At the highest saturations, greater than about 98%, the number of layers again appear to be greater than expected from the cubic law.

The isotherm obtained at 77·4°K for oxygen presents features which are very similar to the 89·7°K isotherm. Plotting the results as for curves I and II of fig. 7, we obtain inverse slopes of 2·7 and 3·1 respectively. The corresponding values for K are 6·4 and 2·9. (In comparing these values for K, it should be remembered that K determines the cube of the number of layers ; hence the evaluation of K is subject to 3 times the errors in the basic isotherm.)

Thus the results for oxygen exhibit two features. They indicate the existence of a packing in the first adsorbed layer which is significantly less than that calculated from the bulk density. They also indicate that if this anomalous packing is taken into account in a realistic manner, the isotherm at high saturation is described by eqn. (1).

The Adsorption of Argon

Isotherms for argon have been determined at 77·4°K and 87·5°K. At the saturation vapour pressure, argon is solid at 77·4°K and liquid at 87·5°K. The isotherm at 77·4°K is therefore the only one involving solid layers which we have investigated.

Fig. 8

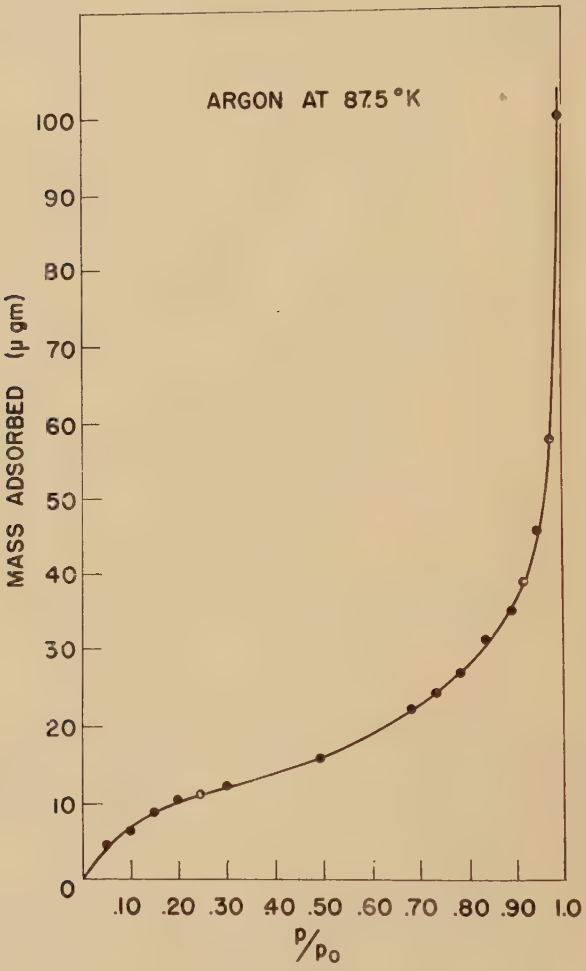

Argon Isotherm.

The data for 87·5°K are shown in fig. 8. This isotherm exhibits features which are similar to the oxygen isotherms. The weight of the first layers was calculated to be 10·3 μg. This implies a cross section at the argon atom in the first layer equal to 24·8 Å^2, as compared with a value of 14·3 Å^2

calculated from the bulk liquid density. This disparity is even greater than that observed for oxygen ; it is similar in magnitude to that observed by Beebe, Beckwith, and Honig (1945) for the krypton monolayer. Thus in analyzing the data at high saturations we are faced with the same situation presented by the oxygen results because of the anomalous first layer. In fig. 9 we show a graph of log ν plotted against loglog p/p_0, computing ν in the same way as for fig. 7. The assumption of a uniform layer density equal to that in the first layer (curve I) gives a value of 2·78 for the exponent of ν in eqn. (1). The assumption of a layer density given by the bulk liquid density in all but the first layer (curve II) gives 3·13 for this exponent. Again we may assume that the real physical situation is

Fig. 9

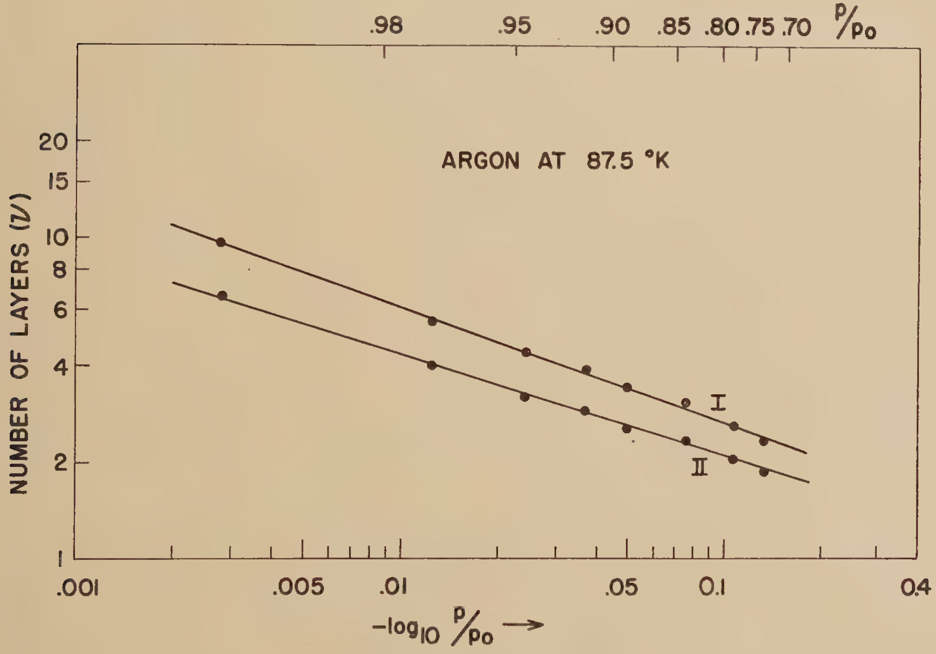

one involving the gradual change throughout the first few layers from the anomalous first layer packing to that calculated from bulk liquid density. Such a physical model would lead to a curve between I and II of fig. 9 and at the highest saturations would be approximately a straight line whose inverse slope must be close to 3·0.

In fig. 10 we show the data plotted on the form of $1/\nu^3$ against $-\log p/p_0$; ν was calculated as for curve II in fig. 9. The purpose of this plot is merely to show how closely the highest saturation data is represented by the cubic law in spite of the fact that an exponent of 3·12 should provide the best general fit. It emphasizes the question of whether we should consider small deviations from the power 3 to be significant, as has been done by Halsey (1948).

The value of K was found to be 4·7 for the points on curve II of fig. 9 and 2·2 for the points on curve I. These values are of the correct order as calculated from eqn. (3 *a*).

The isotherm for argon at 77·4°K is shown in fig. 11. The value taken for p_0 is that appropriate to *the solid phase* at 77·4°K. Considerable difficulty was encountered when measuring the adsorption at high saturations in this

Fig. 10

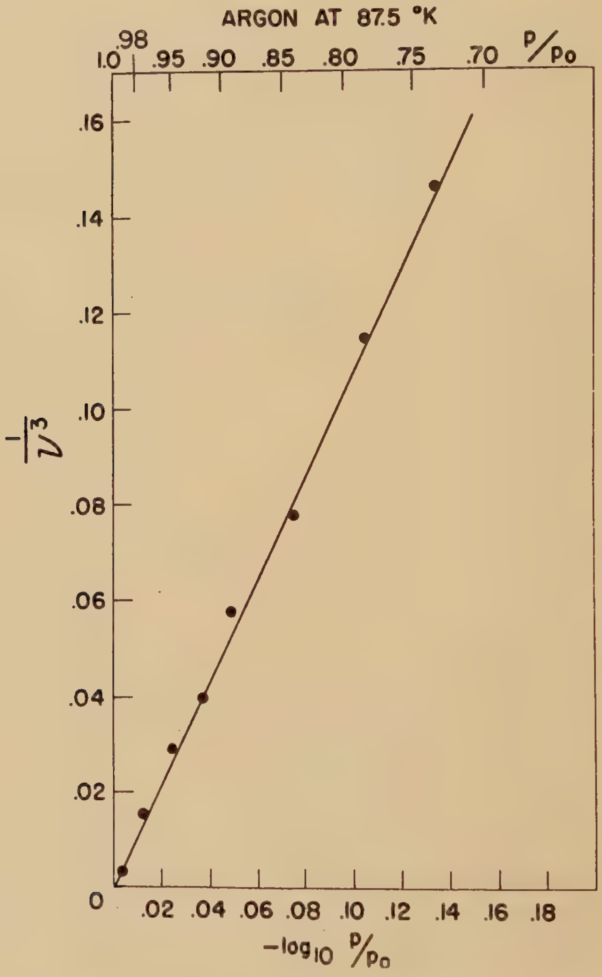

case. It is not certain that equilibrium was finally attained; heat transfer between the specimen and the gas seemed to be very slow. The isotherm has two interesting aspects. Firstly, the cross section of the argon atom in the first layer is again greater than one can calculate from the density of solid argon; the figures are 17·9 Å^2 and 12·9 Å^2, respectively. Secondly, the isotherm appears to meet the $p/p_0 = 1$ axis at a finite value in the region of 3·5 layers. The adsorption at high saturations of solid layers is little understood, but the latter effect has been observed before with other gases, for example, carbon dioxide (Brunauer and Emmet 1937) and krypton (Beebe, Beckwith, and Honig 1945). As the result of this effect, the data at the high saturations cannot be represented by a power law similar to eqn. (1).

Frequently the isotherm for solid layers is plotted with a p_0 appropriate to the supercooled liquid (David, DeWitt, and Emmet 1947) which is larger than the solid value for a given temperature. In the case of argon at 77°K, the difference between the two saturated values is 15% (Clark, *et al.* 1951). However, if the data are plotted with respect to this liquid p_0, the highest saturation obtained experimentally is 85%, so that the data are insufficient for a test of eqn. (1).

Fig. 11

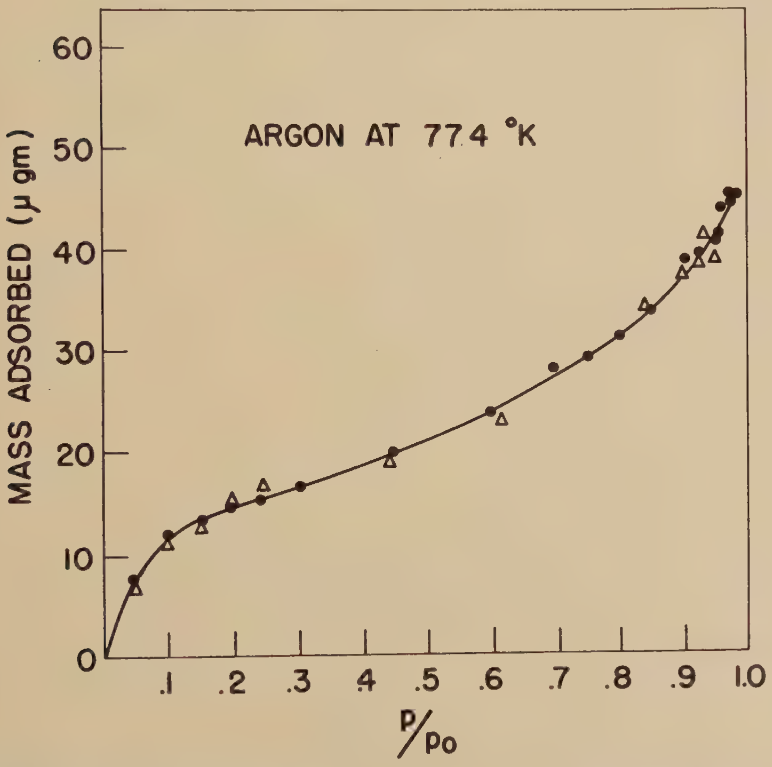

Argon Isotherm. The two symbols represent separate determinations.

§ 4. Discussion

The results presented in this paper suggest that eqn. (1) is accurate in describing the adsorption of nitrogen, oxygen, and argon at the highest saturations and at temperatures where the layers can be considered to be ‘ liquid ’. The apparent deviation in the case of oxygen and argon may be ascribed to anomalous structure of the first few layers. The only serious deviations appear in the region of 99% saturation ; however, it is difficult to determine the isotherm precisely so close to saturation.

The relation verified is based particularly on the following assumptions : (*a*) The van der Waals forces involved vary as $1/r^3$ (London 1930) ; (*b*) The distance of an adsorbed molecule in the outer layer from the wall may be taken proportional to the number of layers.

For the interaction of a neutral molecule with the metallic wall, calculations of Lennard-Jones (1932), Bardeen (1940), and Margenau and Pollard (1941) all yield a $1/r^3$ dependence for the forces involved. They differ only in calculations of the size of the force. Until the K of eqn. (1) can be estimated more precisely than by eqn. (3*a*), we are not able to make a comparison between our data and the calculations mentioned. Prosen and Sachs (1942) have made a direct quantum mechanical calculation of the interaction between a neutral molecule and a metallic wall, using perturbation theory. They propose that the potential energy varies as $\log r/r^2$ when electron degeneracy is taken into account. Of course, the interaction between neutral molecules and the non-conducting adsorbed film still varies as $1/r^3$. The introduction of this potential into an equation similar to (1) would lead to deviations from the cubic law if its influence were significant compared with interactions between adsorbate molecules. However, it is almost certain that the treatment of Prosen and Sachs is not valid for the distances from the wall found in multilayer adsorption and should only be applied to limited aspects of monolayer adsorption. It breaks down at short distances where the wave functions of neutral atom and metallic electrons overlap and also at large distances where the electron coulomb interactions cannot be properly treated. Thus assumption (*a*) seems justified.

Halsey (1948) has criticized assumption (*b*). He points out that one should not take the distance of an adsorbed molecule in the outer layer as proportional to the number of layers, because the actual distance involved is not continuously varying, but is a step function with values which are appropriate to integral numbers of layers. However, this view is based on a rather idealized picture of the adsorbed layers and the validity of the criticism may be less when we consider the statistical nature of what we call ‘ the number of layers ’. The verification of eqn. (1) for the simple systems described in this paper indicates that assumption (*b*) does not introduce serious error.

In the course of this work it has been necessary to determine the density of the first adsorbed layers for nitrogen, oxygen, and argon on the specimen of aluminium. Unfortunately, the values we give for the cross sections of argon and oxygen are relative to the nitrogen cross section. If the nitrogen first layer is normal, as appears to be the case from other workers (Harkins and Jura 1944), then the first layers of oxygen and argon are significantly less dense than the outer layers calculated from the appropriate bulk density. The differences in density we obtain are larger than the comparable values of other workers (Emmet 1948). Considering the work of Beebe, Beckwith, and Honig (1945) on krypton, which yielded a disparity of similar magnitude, it is clear that the first layer packing of the isotherm is not adequately understood.

With regard to the nitrogen first layer, Davis, DeWitt, and Emmet (1947) state the following : " . . . it is well to keep in mind the present status of area determination by nitrogen and to ask particularly whether or not it is possible that the cross sectional area assigned to the nitrogen molecule may be too low. The most convincing answer to this question will be obtained when and if someone measures the surface area of a metal foil or ribbon using nitrogen as an adsorbate. Only if one then obtains too low a roughness factor for such surfaces, will one be able to conclude with certainty that the usual value of 16·2 Å^2 per molecule is too small. The experiment of Harkins and Jura (1944) is not absolutely conclusive." The value of 1·3 for the roughness factor of the aluminium foil determined in the present investigation seems reasonable and lends support to the assumption of the normal 16·2 Å^2 for nitrogen.

ACKNOWLEDGMENTS

Grateful acknowledgment is due to Professors E. A. Long and L. Meyer for their constant advice and encouragement. My thanks are also due to Dr. J. R. Arnold, of the Institute for Nuclear Studies, for his helpful interest.

REFERENCES

BARDEEN, J., 1940, *Phys. Rev.*, **58,** 727.
BEEBE, R. A., BECKWITH, J. B., and HONIG, J. M., 1945, *J. Amer. Chem. Soc.*, **67,** 1554.
BOWERS, R., 1953, *Phil. Mag.*, **44,** 485.
BOYD, G. E., and LIVINGSTON, H. K., 1942, *J. Amer. Chem. Soc.*, **64,** 2383.
BRUNAUER, S., 1945, *The Adsorption of Gases and Vapours* (Oxford : University Press).
BRUNAUER, S., DEMING, L. S., DEMING, W. E., and TELLER, E., 1940, *J. Amer. Chem. Soc.*, **62,** 1723.
BRUNAUER, S., and EMMET, P. H., 1937, *J. Amer. Chem. Soc.*, **59,** 2682.
BRUNAUER, S., EMMET, P. H., and TELLER, E., 1938, *J. Amer. Chem. Soc.*, **60,** 309.
CASSEL, H. M., 1944, *J. Phys. Chem.*, **48,** 195.
CLARK, A. M., DIN, F., ROBB, J., MICHAELS, A., WASSENAAR, T., and ZWIETERLING, T. N., 1951, *Physica*, **17,** 876.
DAVIS, R. T., DEWITT, T. W., and EMMET, P. H., 1947, *J. Amer. Chem. Soc.*, **51,** 1237.
DRAIN, L. E., and MORRISON, J. A., 1952, *Trans. Faraday Soc.*, **48,** 840.
EMMET, P. H., 1948, *Advances in Catalysis*, Vol. I (New York : Academic Press).
FRENKEL, J., 1946, *Kinetic Theory of Liquids* (Oxford : University Press), p. 332.
GULBRANSEN, E. A., 1944, *Rev. Sci. Instrum.*, **15,** 201.
HALSEY, G. D., 1948, *J. Chem. Phys.*, **16,** 931.

HARKINS, W. D., 1952, *The Physical Chemistry of Surface Films* (New York : Reinhold Publishing Corp.).

HARKINS, W. D., and JURA, G., 1944, *J. Amer. Chem. Soc.*, **66,** 1362, 1366.

HILL, T. L., 1946, *J. Chem. Phys.*, **14,** 263, 441 ; 1947, *Ibid.*, **15,** 767 ; 1949, *Ibid.*, **17,** 580, 668 ; 1952, *Advances in Catalysis*, Vol. IV (New York : Academic Press), p. 225.

LENNARD-JONES, J. E., 1932, *Trans. Faraday Soc.*, **28,** 333.

MARGENAU, H., and POLLARD, W. G., 1941, *Phys. Rev.*, **60,** 128.

MCBAIN, J. W., 1935, *J. Amer. Chem. Soc.*, **57,** 699.

MCMILLAN, W. G., 1947, *J. Chem. Phys.*, **15,** 390.

MCMILLAN, W. G., and TELLER, E., 1951, *J. Chem. Phys.*, **19,** 25.

PROSEN, E. J. R., and SACHS, R. G., 1942, *Phys. Rev.*, **61,** 65.

RHODIN, T. N., 1950, *J. Amer. Chem. Soc.*, **72,** 4343.

ZSIGMONDY, R., 1911, *Zeit. anorg. Chem.*, **71,** 356.

L. *The Adsorption of Gases at High Saturations*
II: The Thickness of the Unsaturated Helium Film

By Raymond Bowers
Institute for the Study of Metals, The University of Chicago, Chicago, Illinois*

[Received January 20, 1953]

Abstract

The adsorption of helium on an aluminium foil has been measured between 1·8°K and 4·2°K. The principal interest was in the form of an isotherm close to saturation. The maximum thickness observed for the adsorbed layer at the highest saturations (greater than 99·9%) was twenty atomic layers below the λ-point and ten layers above the λ-point. These values for the unsaturated film are compared with existing data for the thickness of the saturated helium II film. The data are also compared with the Frenkel–Halsey–Hill equation for multilayer adsorption and the calculations of Band on the adsorption of a Bose–Einstein gas.

§ 1. Introduction

It is well known that when any solid surface is in contact with liquid helium II or its vapour, a thick film is formed which possesses unique transport properties (Daunt and Mendelssohn 1939). Estimates of the thickness of the film above the liquid vary from 50 to 150 atoms. Recently attention has been drawn to the fact that even in the comparatively thin adsorbed layers, characteristic of pressures below the saturated vapour pressure, superfluidity is observed when the temperature is reduced below 2·19°K. Long and Meyer (1950) showed that this peculiar mobility could be observed whenever the number of layers exceeded the first statistical layer. More recently, considerable work has been done on the magnitude of the mobility to be found in these thin layers (Bowers, Brewer and Mendelssohn 1951, Long and Meyer 1952 a, b). In these experiments one measures the mass transfer directly or its contribution to the heat flow through the film. These total flows involve a product of the linear velocity of the flow and the thickness of the film, as well as ρ_n/ρ_s (the relative concentration of normal and superfluid components in the flowing film). One of the striking features of the data available is that the total superflow, even at 95% saturation, is still very much smaller (less than 10%) than that in the saturated film. It is of considerable interest to determine whether this is merely a consequence of the much smaller film thickness involved in the unsaturated case, or whether the other factors determining the flow are also different in the two cases.

---

* Communicated by the Author.

In order to separate the variation of the velocity and ρ_n/ρ_s from the measured transport property, it is necessary to know the variation of the thickness of this film with pressure. Essentially, this requires an accurate determination of the adsorption isotherm. There is available a considerable amount of data on the isotherm up to about 90% saturation (e.g., Keesom and Schweers 1941, Frederikse and Gorter 1950, Schaeffer, Smith and Wendell 1949, Strauss 1952) and, on the whole, the agreement between the results of different workers appears to be satisfactory. However, much less is known about the form of the isotherm at the highest saturation. The isotherms determined by Kistemaker (1947) and Long and Meyer (1949) are the only ones which give measured points close to saturation. Long and Meyer found that the thickness of the film is of the order of 7 to 8 layers at 90% saturation, as observed by the earlier workers. However, with helium II, the adsorption at saturations higher than 90% was found to be anomalously high, the isotherm rising very rapidly close to saturation to a measured value of 160 atomic layers. This effect was not observed above the λ-point. In Kistemaker's original paper, he calculated about 30 layers for a similar limit, but a re-evaluation of his data (Frederikse 1950) indicates a film several times thicker than the 30 layers stated. The observation by Long and Meyer and by Kistemaker of a very thick film close to, but definitely below, the saturation pressure is of considerable importance, since it has direct bearing on the problem of whether the thick helium II film is formed from the vapour, or whether contact with the liquid is necessary for its formation (Mendelssohn 1946). If we assume that they are observing the formation of the thick helium II film, normally characteristic of saturation conditions, there is a large disparity between their values and the most recent direct determinations of the thickness of the saturated film (Burge and Jackson 1951, Henshaw and Jackson 1951). The latter workers have obtained thicknesses which are less than a third of the 160 atoms recorded by Long and Meyer.

The form of the helium isotherm at high saturation is of interest from another point of view. One may ask whether the Frenkel–Halsey–Hill relation, described in the preceding paper (Bowers 1953), is valid for helium adsorption. This law was actually derived on a classical basis, using the $1/r^3$ van der Waals force. If the cubic law is found to be valid, it would mean that quantum phenomena influence the magnitude of the forces involved, but not their dependence on the effective distance. On the other hand, quantum effects such as Bose–Einstein degeneracy, might dominate the picture to such a degree that the simple cubic law is no longer valid. The influence of the gravitational field on the Bose–Einstein condensation is also a factor that may influence the adsorption considerably (Lamb and Nordsieck 1941, Becker 1950, Liebfried 1950, Halpern 1952 a, b). Calculations on the influence of degeneracy on helium adsorption have been made by Temperley (1949) and Band (1951).

This paper describes a determination of the helium isotherm by a gravimetric method. The work has been undertaken for the following reasons :

(1) To investigate the high saturation region in greater detail in order to obtain data which are sufficient for a test of the cubic law.

(2) To investigate the disparity between the values reported by Kistemaker and by Long and Meyer for the thickness of the film and the comparable values due to Jackson and co-workers.

(3) To provide a basis for a gravimetric determination of the thickness of the helium II film under saturated conditions.

Fig. 1

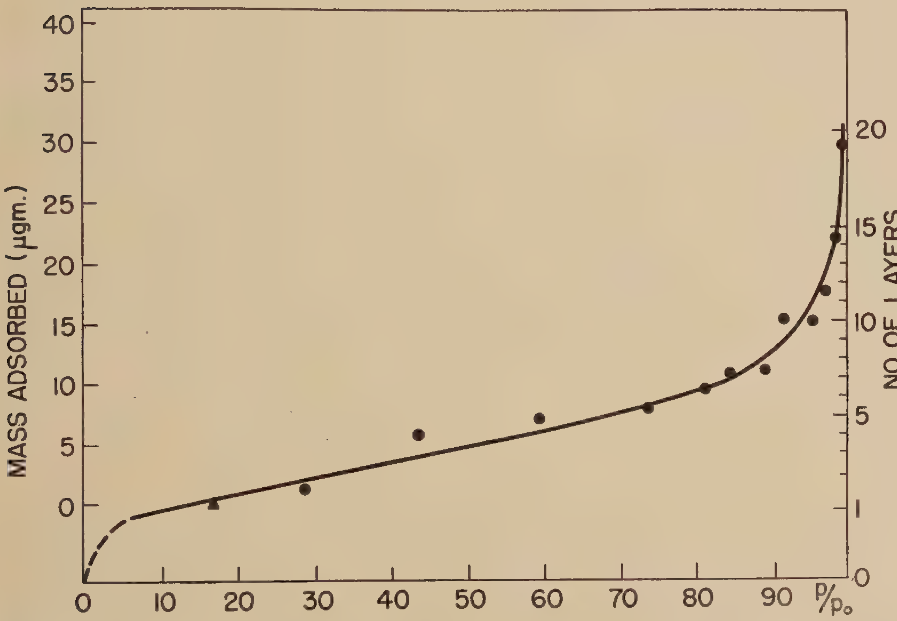

Helium isotherm at 1·829°K. The symbol ▲ denotes the arbitrary starting point mentioned in the text.

§ 2. Method

The apparatus and specimen used in this experiment were the same as used for the nitrogen, oxygen, and argon work described in the preceding paper. The microbalance and associated low temperature system will be described in detail elsewhere.

The two helium baths (see fig. 1, preceding paper) were pumped through a common pumping tube, keeping the same temperature in both. Furthermore, care was taken to keep the helium levels in these two dewars at the same height. The vapour pressure of the helium in the dewars is the p_0 of the isotherm ; the value of p is the pressure in the tubes containing the specimen and counterweight. The specimen and counterweight space could be evacuated to 5×10^{-7} mm Hg when liquid helium was in the dewars. During a determination of the isotherm, the vapour pressure p_0 in the helium dewars was held constant to 0·1 mm of oil (octoil-S). The pressure inside the specimen chamber was changed by adding purified helium gas and, as in the earlier experiments, the deflection of the balance beam was observed as the adsorbed layers increase the weight of the specimen. Two radiation shields, with orifices of 1 mm, were mounted above the specimen. Both shields were in good thermal contact with the outer helium bath.

In spite of the elaborate shock mounting of the apparatus, a slight residual disturbance was noticeable when the helium was being pumped. This presented a difficulty only when a zero reading was being taken with the specimen space evacuated; the presence of even a small amount of gas in the specimen space provided enough damping of the balance for complete stability. Accordingly, all the isotherms below 4·2°K are measured from an arbitrary starting-point at about 15% saturation, and in computing the total number of adsorbed layers, it is necessary to allow for the gas already adsorbed at this initial saturation. Such a correction can be made quite accurately, using the data of other workers, because at 15% saturation we are in the region of the completed monolayer where the isotherm has a small slope. Since no difficulty of a similar nature was encountered when using liquid nitrogen, oxygen, and argon at their boiling points, the disturbance presumably originated in the pumping system. A zero reading was obtained for helium at 4·2°K.

§ 3. RESULTS

Isotherms have been determined at the following temperatures: 1·644, 1·829, 2·050, 2·132, 3·012, 4·198°K. In fig. 1 is shown an isotherm for helium II determined at 1·829°K. The left-hand ordinate gives the mass of helium adsorbed, while the right-hand ordinate gives the equivalent number of statistical layers. For layers other than the first two, the weight of the layer is calculated assuming a normal liquid density, taking the effective area of the specimen as 388 cm^2 as determined by the nitrogen isotherm described in the preceding paper. We allow for the fact that the density in the first and second layers is significantly higher than successive layers by the following method: we have assumed that the density in the first layer is 3·6 times that for liquid packing (Schaeffer, Smith and Wendell 1949, Long and Meyer 1949, Gorter and Frederikse 1950, Strauss 1952), while the second layer is arbitrarily taken to be half as dense as the first. It can be seen that the right-hand ordinate in fig. 1 has a scale which allows for these closely-packed layers.

In fig. 2 we have a similar isotherm at 2·132°K, including in this curve some values for the coverage obtained by desorption from 99·25% saturation. It can be seen that there is no significant hysteresis, as was the case for oxygen with the same specimen (see preceding paper, Bowers 1953).

As a final example of a measured isotherm, we show in fig. 3 the data for 4·197°K. Two isotherms have been obtained above the λ-point, at 3·02°K and 4·20°K. It is much more difficult to obtain accurate isotherms in the helium I range. The bubbling of the liquid helium I and the simultaneous difficulty in controlling temperature make the balance less stable. Furthermore, the total number of layers found above the λ-point is considerably less than the number observed below the λ-point for the same saturation. The maximum number of layers observed above the λ-point was ten at 99·91% saturation, for the 4·2° isotherm.*

Fig. 2

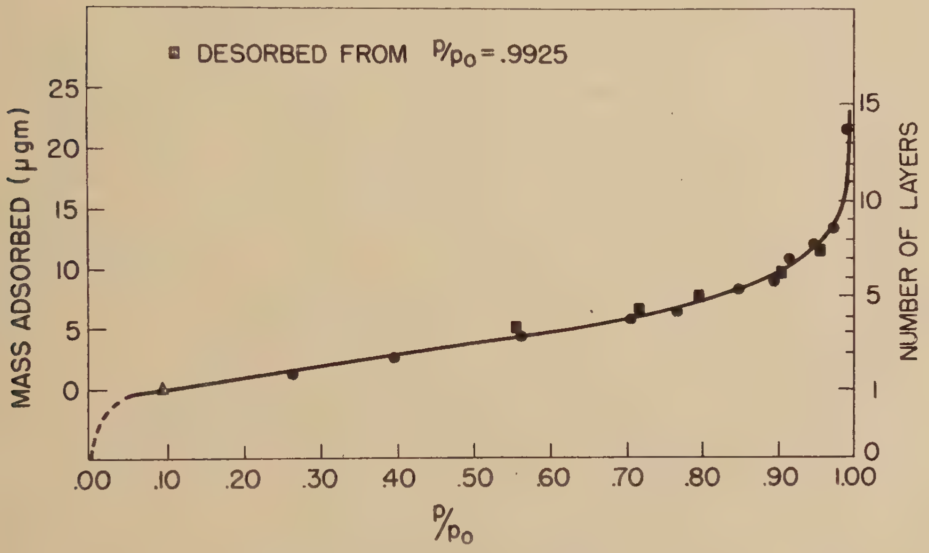

Helium isotherm at 2·132°K.

§ 4. Discussion

The results presented above will be considered from two points of view. First we shall consider their relation to the formation of a very thick film at saturation and, secondly, we shall consider to what extent the adsorption at high saturation is compatible with a law of the type proposed by Frenkel, Halsey, and Hill outlined in the introduction to the preceding paper. With regard to the formation of a thick film at saturation in helium II, it can be seen that there is no sign of a 160-layer film even at saturations as high as 99·92%. However, the isotherm is very steep in this region and it is difficult to put a definite upper limit on the number of layers which one could obtain, but in no case were films thicker than 20 atoms observed. Furthermore, it may be said provisionally that we have not been able to obtain films thicker than 40 or 50 layers even with the bulk liquid helium II present, providing the specimen is in contact with the vapour alone *as opposed to being in direct contact with the liquid* (see

---

* See recent paper Jackson, L. C., and Henshaw, D. G., 1953, *Phil. Mag.*, **44**, 14.

Mendelssohn 1946). (Work on the film associated with the bulk liquid is still in progress and requires further clarification.)

These results seem to contradict those of Kistemaker and of Long and Meyer, which yielded a film about 160 atoms thick near saturation. Our results are in better agreement with those of Jackson and co-workers. One explanation of the disparity with the results of Long and Meyer may be found in capillary condensation, since they used tightly-packed rouge as an adsorbent. However, the fact that Long and Meyer did not find a similar thick film above the λ-point is evidence against capillary condensation.

Fig. 3

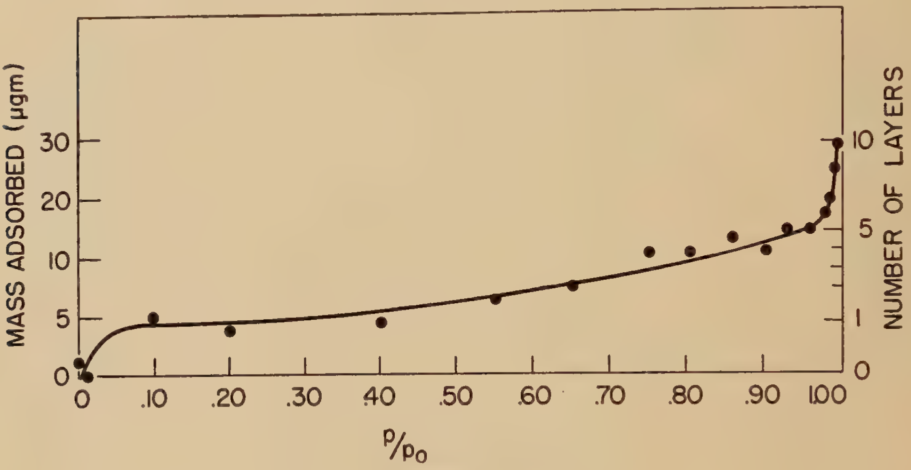

Helium isotherm at 4·197°K.

There is another possible explanation for the disparity involving the dependence of the helium II film thickness on the height above the bulk liquid. It is well known that the thickness of the film varies rapidly with the height above the bulk liquid level for heights less than a few millimeters (Burge and Jackson 1951). Any bulk liquid introduced into a tightly-packed powder, such as the rouge, would be dispersed throughout the rouge by the large surface tension forces in the very small channels, and if we imagine a helium II film being formed from this dispersed liquid, it is clear that the film on the grains will have a thickness characteristic of a ‘ height ’ of the order of the grain size. Since this effective height is extremely small, we should expect the thickness to be considerably greater than the value obtained in experiments such as those of Burge and Jackson, where a height of order of the centimetres is involved. Thus, even if a correction could be made for the presence of bulk liquid in an adsorption experiment at saturation, it seems reasonable to expect a film thickness for the fine powder which is greater than that obtained in other determinations. This is, of course, largely an academic point, since such a correction for the presence of bulk liquid is almost impossible to make.

None of the arguments presented above can be used in order to explain the disparity between our values and those of Kistemaker. He measured the adsorption of helium in a glass system designed so as to virtually eliminate the possibility of capillary condensation. At the present time no reasonable explanation of this disparity presents itself. The thickness of the film very near saturation should be extremely sensitive to the temperature of the specimen with respect to its surroundings and the disparity may indicate that the temperature of the specimen was higher in our case. This is mentioned because it is definitely easier to shield the specimen in the volumetric methods of Kistemaker and of Long and Meyer than in the present investigation. However, considering the radiation shields used in the present work, this mechanism for the disparity remains unlikely.

We have already mentioned in the introduction to this paper, the fact that the total superflow observed in these adsorbed layers is very much smaller than that in the saturated film. Our isotherms and those of previous workers indicate that this is largely due to the smaller thickness of the adsorbed layers as compared with the film at saturation. However, there is a spread of about 50 to 150 atoms in the existing values for the thickness of the saturated film, so that it is not possible to analyse this aspect of the isotherms in any detail. If the saturated film is 50 atoms thick, the reduced thickness of the adsorbed film at 95% saturation would result in a direct reduction of superflow to about 20% of its value in the saturated film ; a saturated film 100 atoms thick would make this figure 10%.

Leaving the question of the relation to the bulk liquid film, we shall now consider the over-all magnitude of the adsorption observed. Our data are in general agreement with the previous work of Gorter and Frederikse (1950), Kistemaker (1947), Long and Meyer (1949) (except as mentioned above), and Strauss (1953). Generally speaking, helium forms a larger number of layers above about 70% saturation than one finds with other gases (cf. preceding paper, Bowers 1953) when the temperature is below the λ-point.

In order to compare our data with the equation of Frenkel–Halsey–Hill (eqn. (1) of the preceding paper) we have plotted in fig. 4 a graph of log p/p_0 against $1/\nu^3$ for three different temperatures. As in the previous notation, ν is the number of layers. It is clear that the data illustrated can be described by the relation :

$$-\ln \frac{p}{p_0} = \frac{K}{\nu^3},$$

where K varies with temperature, and this seems to be true of all the isotherms obtained. The very striking way in which the data at 3·02°K fit on a straight line is to some extent accidental, since this degree of agreement exceeds the experimental precision for isotherms above the λ-point. However, taking errors above the λ-point into account, it seems as though the relation is consistent with the data between 1·8°K and 4·2°K. The variation of the constant of proportionality K with $1/T$ is shown in fig. 5. It must be remembered that the value of K determines the cube of the number of layers, hence its determination is subject to three times the errors inherent in the original measurement of the isotherm. The variation of K in the helium II region from 60 at 1·64°K to 24 at 2·13°K involves only a difference of 35% in a number of layers. Hence the points in fig. 5 should be taken to illustrate the definite rise in K in going through the λ-point, but they are not accurate enough to give the exact functional dependence of K on temperature. (In fig. 5 a straight line has been drawn through the helium I region because this is the variation predicted by theory.)

Fig. 4

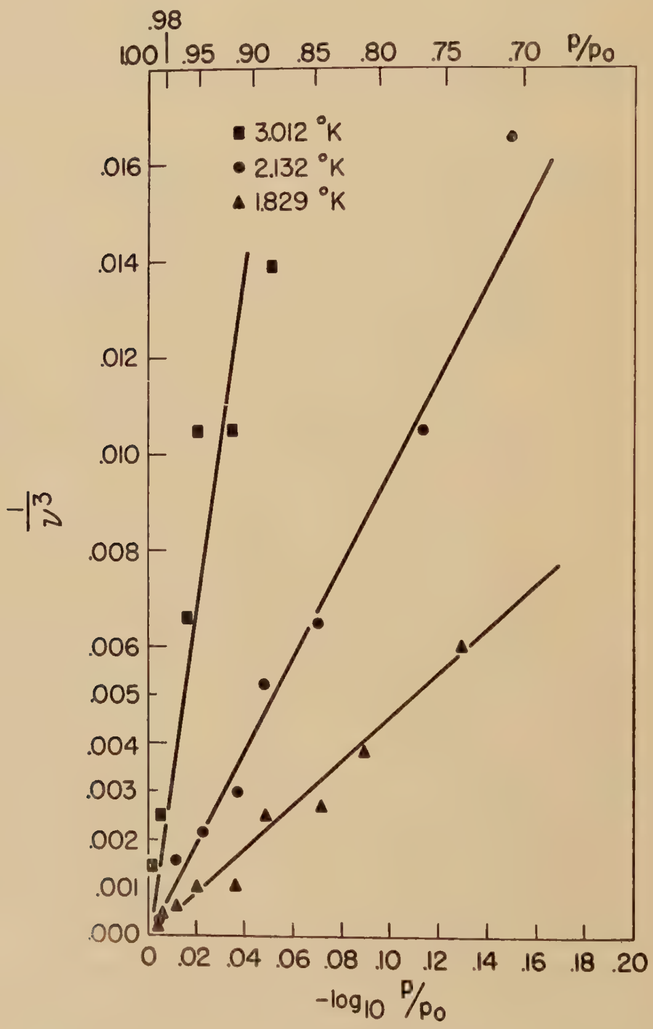

In the preceding paper, estimates of K have been made using the approximation :

$$K=\frac{\pi}{6RT}(E_1-E_l),$$

where E_1 is the energy of adsorption in the first layer and E_l is the energy of liquefaction. A difficulty arises in the application of this formula to helium adsorption because E_1-E_l varies considerably with coverage throughout the first layer (Keesom and Schweers 1941). If we obtain E_1-E_l from the B.E.T. plot, as in the preceding paper, we obtain a value appropriate to the completed first layer which has an anomalously high density. The B.E.T. plot of Schaeffer, Smith, and Wendell (1945) yields about 25 cal/mole for E_1-E_l. However, the data of Keesom and Schweers (1941) show that E_1-E_l is at least 80 cal/mole at the lowest coverages and one could justify taking even higher values on the basis of the anomalous high density of the completed first layer. Taking $E_1-E_l=25$ cal/mole, we obtain $K\simeq3$, while an assumption of 80 cal/mole yields $K\simeq10$. It is important to emphasize that these values for K represent no more than a guess. Firstly, the value taken for E_1-E_l is arbitrary. Secondly, on more fundamental grounds, we cannot expect a formula derived classically to explain helium II adsorption which is probably influenced considerably by the Bose–Einstein degeneracy. Apart from statistics, we have allowed for the anomalous first layer in computing the total number of layers by assigning a particular high density to this layer, but we have not considered

Fig. 5

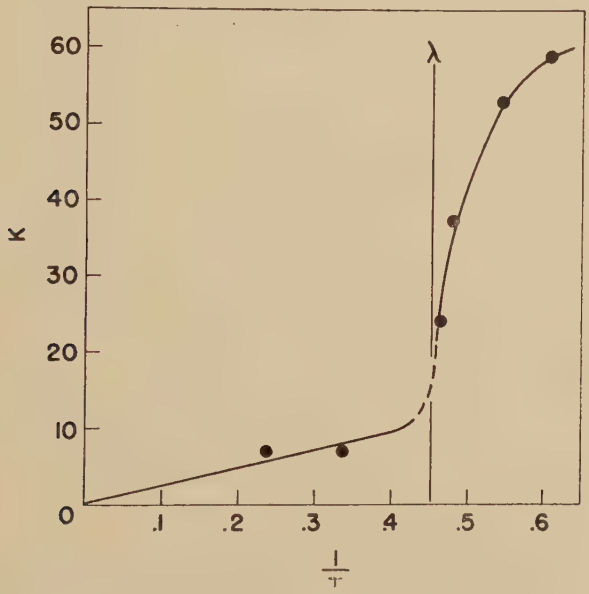

The variation of K with $1/T$.

the possibility of a cooperative effect between the first and subsequent layers which would render the treatment of Hill and Frenkel inapplicable.

The experimental data are best described by a $K \simeq 7$ in the helium I region ; this is not too far from the estimates made above. In the helium II region it is clear that the experimental K is considerably larger than the estimates. The data show that K is not proportional to $1/T$, but this is not surprising because of the λ-transition. Summing up the observations, it is found that the Frenkel–Halsey–Hill equation describes the variation of the number of layers with pressure quite well for a given temperature ; the variation with temperature is complicated by the λ-transition which invalidates the application of their formula.

Fig. 6

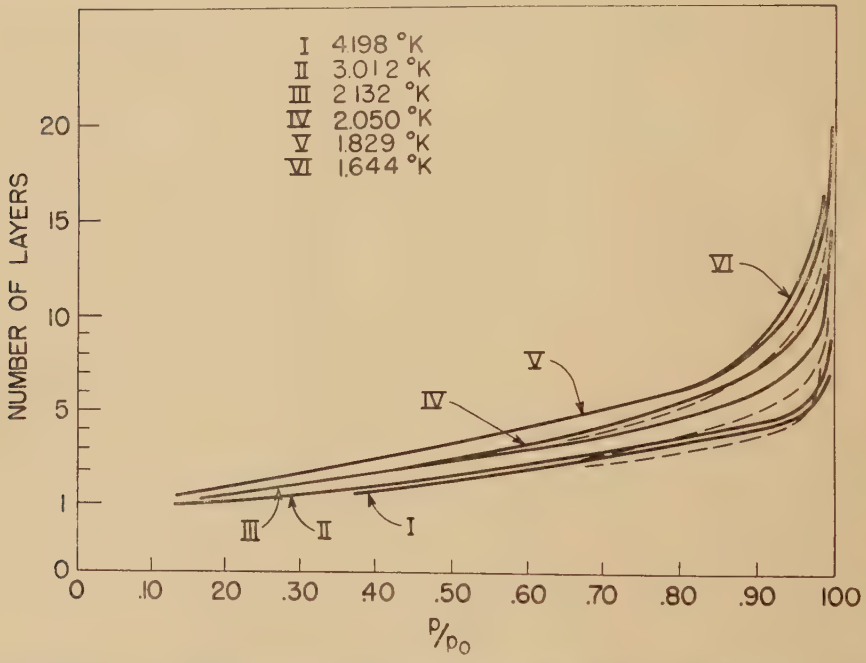

The solid lines are the isotherms determined in the present investigation. The broken lines represent the calculations of Band with $n=2$, $2{\cdot}5$ and 3 ; the highest broken line refers to $n=2$ and the lowest to $n=3$.

Recently Band (1951) has provided another method for the comparison of our results with theory. He has calculated the form of an isotherm for a degenerate Bose–Einstein system, taking various powers in the force between the adsorbate gas and the solid adsorbent. In fig. 6 we compare his predictions with our data. In this figure are shown six isotherms and three calculated curves of Band. The various dotted lines correspond to $n=2$, $2{\cdot}5$, and 3, where n is the exponent in the attractive field potential proportional to $1/r^n$. It appears that the curve with $n=2$ fits the data most successfully. Band's formula implies that the isotherm is independent of temperature for a fixed value of n and clearly this is an approximation in the case of helium.

It is difficult at the present time to choose between the equation of Frenkel–Halsey–Hill and the equation of Band as representing the most reasonable picture of helium adsorption. The agreement with the data in the case of the former suggests that a binding potential energy proportional to the inverse cube of the distance is applicable to helium at low temperatures, but the magnitude of these forces may be very different in the helium II region from that which one could calculate classically. On the other hand the description given by Band, although based on the important degeneracy, has one feature which is difficult to understand physically. As mentioned above, the best fit between his formula and the helium II data is given when a binding potential between the adsorbate gas molecule and the combined wall and helium film varies as the inverse square of the distance involved. It is not easy to see the significance of such a law of force (see discussion in preceding paper, Bowers 1953). Such a formulation may be compared with the calculation of Bijl, de Boer, and Michels (1941) on the influence of zero-point energy in a thick film of helium. However, this calculation has been criticized by Mott (1949) because their potential term in $1/r^2$, which results from the zero-point energy, would not exist if lateral interactions in the film were taken into account. Temperley (1949) has also calculated quantum-mechanically the binding energy of a gas molecule with a wall and adsorbed layer. He considered the approximation of a very thick adsorbed layer. This calculation yields an energy with terms in $1/r^2$ and $1/r^4$. However, the term in $1/r^2$ is very much smaller than the term in $1/r^4$, so that this cannot be considered an interpretation of the Band formula.

The influence of the zero point energy is obviously important in calculating the magnitude of the adsorption of helium, but one can see from the large change in K in the region of the λ-point that zero-point energy alone cannot explain the disparity between a classical treatment of the problem, such as that of Frenkel and Hill, and the observed isotherms. It would be interesting to see if one could calculate its influence on K ; no calculation exists at the present time on this point.

§ 5. CONCLUSION

The isotherms obtained with helium possess the following features: first, there appears to be no evidence with helium II for a film greater than about 20 atoms thick below the saturation pressure. Secondly, the over-all magnitude appears to be best described by a relation derived from a van der Waals force varying as the inverse cube of distance. The results can also be described reasonably successfully by Band's formula for the adsorption of a degenerate Bose–Einstein system. In this case it is necessary to assume that the force of interaction between a gas molecule and the wall varies as the inverse square of the distance.

ACKNOWLEDGMENTS

I wish to thank Professors E. A. Long and L. Meyer for their continued interest in this work. Many aspects of this investigation have originated in their suggestions.

REFERENCES

BAND, W., 1951, *J. Chem. Phys.*, **19,** 435.
BECKER, R., 1950, *Z. Physik*, **128,** 120.
BIJL, A., DE BOER, J., and MICHELS, A., 1941, *Physica*, **8,** 655.
BOWERS, R., 1953, *Phil. Mag.*, **44,** 467.
BOWERS, R., BREWER, D. F., and MENDELSSOHN, K., 1951, *Phil. Mag.*, **42,** 1445.
BURGE, E. J., and JACKSON, L. C., 1951, *Proc. Roy. Soc.* A, **205,** 270.
DAUNT, J. G., and MENDELSSOHN, K., 1939, *Proc. Roy. Soc.* A, **170,** 423.
FREDERIKSE, H. P. R., 1949, *Physica*, **15,** 860 ; 1950, *Thesis*, Leiden, p. 60.
GORTER, C. J., and FREDERIKSE, H. P. R., 1950, *Physica*, **16,** 403.
HALPERN, O., 1952 a, *Phys. Rev.*, **86,** 126 ; 1952 b, *Ibid.*, **87,** 520.
HENSHAW, D. G., and JACKSON, L. C., 1951, *Proc. Int. Conf. on Low Temp.*, Oxford, p. 65.
KEESOM, W. H., and SCHWEERS, J., 1941, *Physica*, **8,** 1020, 1032.
KISTEMAKER, J., 1947, *Physica*, **13,** 81.
LAMB, W., and NORDSIECK, A., 1941, *Phys. Rev.*, **59,** 677.
LIEBFRIED, G., 1950, *Z. Physik*, **128,** 133.
LONG, E. A., and MEYER, L., 1949, *Phys. Rev.*, **76,** 440 ; 1950, *Ibid.*, **79,** 1031 ; 1952 a, *Ibid.*, **85,** 1030 ; 1952 b, *Ibid.*, **87,** 153 ; 1953, *Advances in Physics*, **2,** 1.
MENDELSSOHN, K., 1946, *Proc. Int. Conf. on Low Temp.*, Cambridge, p. 41.
MOTT, N. F., 1949, *Phil. Mag,*. **40,** 61.
SCHAEFFER, W. D., SMITH, W. R., and WENDELL, C. B., 1949, *J. Amer. Chem. Soc.*, **71,** 863.
STRAUSS, A. J., 1952, *Thesis*, Chicago (reviewed in Long and Meyer, 1953).
TEMPERLEY, H. N. V., 1949, *Proc. Roy. Soc.* A, **198,** 438.

LI. *On the 'Heating' Resulting from the Absorption of Gamma-Rays at Extremely Low Temperatures*

By R. L. Platzman
Purdue University, U.S.A.*

[Received January 22, 1953]

Abstract

The various mechanisms for the conversion of absorbed γ-ray energy to heat are surveyed. It is shown that in dielectric crystals electronic excitation of the constituent molecular groups, followed by dissociation and recombination, and ionization followed by recombination, are to a large extent responsible for the energy dissipation. The partial inhibition, at low temperatures, of the final conversion to heat is discussed, with particular reference to the γ-ray heating method in low temperature calorimetry.

In research at temperatures below about 1°K, a major problem is the conversion of readily measured ' magnetic temperatures ' to true thermodynamic temperatures (Cooke 1949). In one essential stage of this conversion, namely, the experimental determination of heat capacities on the ' magnetic temperature scale ', it is necessary to add heat to a sample at an ascertainable rate. One feasible way of accomplishing this is exposure of the sample to a beam of gamma-rays (Kurti and Simon 1938). It appears to be tacitly assumed in the literature (Kurti and Simon 1938) that the energy so absorbed by the sample ultimately manifests itself entirely, or principally, in the form of heat. This note draws attention to the fact that such an assumption is unjustified.

It is necessary first to trace the course of the absorbed energy through various stages of its dissipation. When a material is exposed to gamma-rays (or x-rays), those photons which are absorbed produce swiftly moving electrons (Compton recoil electrons, photoelectrons, electron pairs), virtually all of which have kinetic energy very great compared to the binding energies of valence electrons in the material. Thus, at this ' first stage ', the absorbed energy is still in a form which may be thought of as having high thermodynamic potential. The fast electrons interact with the medium and are gradually decelerated and ultimately captured (in the course of deceleration other (secondary, etc.) electrons may be ejected, these being similar in effect to primary electrons). The energy loss of all such electrons, as long as their energy exceeds the lowest electronic excitation potential of the medium, has the character that *electronically* excited and ionized atoms and molecules are predominantly produced. Some energy is transferred from the moving electrons to vibrational modes of the lattice, but this process is highly improbable

---

* Communicated by Professor F. E. Simon, F.R.S.

(Platzman 1952), except for the slow electrons for which it is the only possibility ; hence the fraction of originally absorbed energy so transferred must be small, certainly less than 15% and perhaps not in excess of a few per cent. Thus the ' direct ' production of heat is comparatively unimportant. Most of the heat follows later from the electronic excitation and ionization, i.e. the absorbed energy, in being degraded from electron kinetic energy to heat, passes, for the most part, through the intermediate form of atomic or molecular *potential* energy. At this ' second stage ' of dissipation, then, most of the energy has retained an essentially high thermodynamic potential.

It will now be argued that at the conclusion of a third and ' final stage ', a substantial fraction of the energy originally absorbed will persist in forms other than heat and will, indeed, at extremely low temperatures, be stable with respect to transformation into heat.

The ionized atoms and molecules are, in most solid substances at ordinary temperatures, quickly neutralized through various types of recombination. The mechanisms here are perhaps not understood in all detail, but one does know that the recombination energy is usually converted to heat more or less directly (often through the agency of internal conversion ; see below). At extremely low temperatures, however, the recombination is likely to be inhibited and much of the recombination energy stored in the substances (as free energy), for the ejected electrons may be trapped at remote sites, the energy released in the act of trapping being dissipated to heat but the remainder of the recombination energy being preserved because of the smallness of the mobility of the trapped electrons. (The ionization energy is partially stored in some crystals even at room temperatures ; consider the case of colour centres.)

The fate of excited molecules is next considered. (Only electronic excitation energy is treated ; some vibrational excitation almost always accompanies both electronic excitation and ionization (Franck–Condon principle), but this relatively small quantity of energy is quickly dissipated to heat.) If the excited system were an isolated atom it would radiate the excitation energy, but the case of an atom coupled to other atoms in a lattice, or of a polyatomic molecule, is entirely different. Here radiation is comparatively improbable and may in general be disregarded (although in exceptional cases it may occur with high yield ; consider cathodoluminescent or scintillant materials). Instead, the two most likely consequences of electronic excitation are dissociation (including predissociation) and *internal conversion* (Teller 1937, Franck and Sponer 1948). The latter process, very common in polyatomic molecules, results in a direct conversion of the excitation energy to molecular vibrational energy (and thence quickly to heat). The former, however, results in molecular fragments (which will always have some kinetic energy, this being quickly dissipated to heat) having considerable chemical free energy. Such fragments may, in rare cases be stable, or they may react chemically with other molecules in the vicinity, or, most commonly in *condensed* phases, they may recombine. This recombination, because it may be followed by internal conversion, therefore expedites ultimate dissipation of the excitation energy to heat. It is important to appreciate, however, that such recombination almost invariably has some activation energy, and that this activation energy is such that at temperatures below 1°K the recombination is completely inhibited. Consequently, that portion of the absorbed energy which is utilized to dissociate molecules is for the most part lost as far as heating is concerned. In experiments at extremely low temperatures the working substance is a paramagnetic crystal (e.g. various alums) and in almost all cases it contains polyatomic groups such as NH_4, SO_4, and H_2O which have great probabilities for dissociation if electronically excited. Indeed, ionization of such molecular groups is also commonly followed by dissociation.

It may be mentioned that in these crystals virtually no energy is transferred directly from the moving electrons to the energy levels of the paramagnetic ions which must ultimately acquire the thermal energy at very low temperatures. Only *after* the absorbed energy is dissipated to molecular and lattice oscillation does energy transfer to the ions occur.

Quantitative information bearing on these complex phenomena is at the present time insufficient for the calculation of the fraction of absorbed energy which is stored and thus unconverted to heat, but an estimate for very low temperatures ranges from about 20 to 70%. The result of irradiation by alpha-particles would be approximately the same, although there is a possibility of slightly greater efficiency of conversion because of high transient 'temperatures' in the vicinity of the alpha-particle path. The conversion efficiency could be measured approximately by repeating the Kurti–Simon experiment, and at the same time computing the energy absorption by means of an absolute determination of the intensity of the radioactive source and the various absorption coefficients. It would, of course, be expected to differ for different substances. (It would not, in general, be 100% even at normal temperatures, and for certain substances would apparently *exceed* 100%.)

The possible consequences of these considerations in interpretations of experiments at extremely low temperatures will not be analysed here. It may be mentioned, however, that the method of Kürti and Simon (1938) is to a first approximation protected from error by the fortunate fact that the heat absorbed from the gamma-ray beam is not calculated from the intensity of the source, but, rather, is deduced indirectly, and in such a way that the only assumption regarding heating is that the heat added per unit time be independent of time, and of temperature. However, the possibility that this heating, in view of the mechanisms discussed above, may not be strictly independent of temperature in the range from 0·01° to 1°K, might merit examination. (There exists ample evidence of non-linearity with time, and dependence on previous treatment, in the case of alkali halide crystals irradiated at room temperatures (Estermann, Leivo and Stern 1949).) It should also be borne in mind that the sample is altered chemically by the irradiation, paramagnetic atoms and radicals being a common product; moreover, if repeated experiments are performed on a sample without permitting its temperature to rise greatly in intermediate stages, this decomposition is cumulative.

REFERENCES

COOKE, A. H., 1949, *Proc. Phys. Soc.* A, **62,** 269.

ESTERMANN, I., LEIVO, W. J., and STERN, O., 1949, *Phys. Rev.*, **75,** 627.

FRANCK, J., and SPONER, H., 1948, *Contribution à l'Etude de la Structure Moléculaire* (Liège: Desoer), p. 169.

KURTI, N., and SIMON, F., 1938, *Phil. Mag.*, **26,** 840.

PLATZMAN, R. L., 1952, *Symposium on Radiobiology* (J. J. Nickson, ed.) (New York: Wiley), Chap. 9.

TELLER, E., 1937, *J. Phys. Chem.*, **41,** 109.

LII. *On the Use of γ-Rays in Low Temperature Calorimetry*

By N. KURTI and F. E. SIMON
Clarendon Laboratory, Oxford*

[Received January 22, 1953]

ABSTRACT

The effects due to delayed heat evolution that might accompany γ-ray absorption in crystals are discussed. It is concluded that, at least in the experimental conditions and with the substances employed so far, γ-ray heating is a reliable method for use in calorimetry in the ' magnetic ' temperature region.

THE foregoing paper by Professor Platzman (1953) on the mechanism of γ-ray absorption in dielectric crystals and its bearing on low temperature calorimetry offers a good opportunity of stating briefly the essential features and some practical aspects of the γ-ray heating method that has been used extensively in the Clarendon Laboratory, and, in some experiments, at the Laboratoire du Grand Eléctroaimant, in Bellevue, Paris (Kurti and Simon 1935, 1938 a, Kurti, Lainé and Simon 1937, Cooke 1949, Bleaney 1950). Such a survey is particularly desirable since some doubts have been expressed about the reliability of the method (de Klerk, Steenland and Gorter 1948, 1949).

When calorimetric experiments below 1°K (in the temperature range obtainable by adiabatic demagnetization) were first begun it was realized that conventional heating methods were unsuitable below about 0·1°K because of the poor thermal contact and thermal conductivity at these temperatures. Heating by absorption of radioactive radiations appeared to be a suitable alternative (Simon 1935, Kurti and Simon 1935) because this would give uniform heat generation throughout the specimen provided that the attenuation of the radiation intensity across the specimen was small enough. This condition could be easily satisfied for γ-rays of, say, 1 MEV, with specimens of about 1 cm thickness and a suitable geometrical arrangement of the γ-ray sources. For instance, if the sources have to be disposed rather close to the specimen so as to get the required heat input, variation of intensity across the specimen can be considerably reduced by rotating the sources round the cryostat (e.g. Hull 1947).

Two possible shortcomings of γ-ray heating have had to be considered. One was the difficulty of obtaining an absolute value for the heat generated ; this was overcome by calibration in a temperature range in which the thermal properties of the specimen were known from other experiments. The other and more serious difficulty was the possibility of an incomplete conversion of absorbed γ-rays into thermal energy or, more precisely, of the existence of a finite relaxation time for this energy transfer to the system of electron spins. It was realized, of course, that with our method of determining the absolute value of the rate of heat input no error could be caused by this so long as the relaxation time was either very short or very long compared with the appropriate phase of the experiment. But for intermediate relaxation times the error might have been considerable. However, no indications of such relaxation times have been found in the numerous experiments with γ-ray heating.

---

* Communicated by the Authors.

Let us first consider the case of a relaxation time comparable with a heating period during a specific heat measurement. This would show itself by a delay in the temperature rise at the beginning of the period and a delay in the establishment of a steady drift rate after the heating period. No such time effects were usually observed and, on the few occasions when they did occur they were found to be due to inhomogeneous heating by γ-rays (Hunt 1952). It is of course very important to arrange the γ-ray-sources in such a way as to produce a uniform incident intensity over the whole specimen. Failing this, considerable temperature differences may be established in the specimen ; their equalization results in time effects. The absence of time-effects shows that, at least for the substances used by us, the relaxation time for the γ-ray conversion is either less than half a minute or more than about five minutes.

Next we have to consider the possibility of a relaxation time of between five minutes and the duration of a calorimetric run (the time taken to cover the entire temperature range, from about 0·01° K to 1° K), that is, of the order of a few hours. In this case, the effective rate of heat evolution would be a function of time and would, in particular, depend on previous history. One would, for example, get a different value for the specific heat at a given temperature according to whether one measured it on a 'virgin' specimen, i.e. not exposed to γ-rays in the preceding hour or so, or whether this particular determination had been preceded by γ-ray heating. Since no discrepancies of this type were found in our experiments relaxation times of this order may also be ruled out.

There is also the possibility, as Professor Platzman points out, of a temperature-dependent relaxation time, very long in the lowest temperature range and rather short in the neighbourhood of 1°. If this were the case, one would either observe effects similar to those mentioned in the previous paragraph, or, if the relaxation time changed sharply with temperature an actual heat evolution when a relaxation time of a few minutes is reached. The absence of such effects seems to rule out this possibility as well.

When de Klerk, Steenland and Gorter (1948, 1949) expressed doubts about the reliability of γ-ray heating, they did so in order to account for a discrepancy between their specific heat values for chromium potassium alum below 0·1° K, and some of our preliminary results quoted by Hebb and Purcell (1937). Now, our early experiments were carried out on cylindrical samples for which no T^* scale can be defined (Kurti and Simon 1938 b) and the discrepancy between these two sets of results was therefore not significant. We nevertheless thought it worth while to carry out some new experiments on chromium potassium alum (Daniels and Kurti 1953) and although these showed none of the time effects or anomalies mentioned above the results differed considerably from those of de Klerk, Steenland and Gorter (1949). This discrepancy is still unaccounted for and perhaps the most effective way of clearing it up would be to carry out successive experiments on the same specimens in the two laboratories. The use of chromium methylammine alum for such comparative experiments might even be more favourable as this salt has none of the undesirable properties of the potassium alum (Bleaney 1950).

Finally, Professor Platzman mentions the chemical changes that are produced in the specimen by irradiation. This effect might indeed be serious when high γ-ray intensities are used. In the calorimetric experiments we are concerned with, the rate of heat input is seldom higher than 10 ergs/g/sec, and one can estimate that even continuous heating for five hours would produce electronic excitation at the worst in only about 1 in 10^6 of the polyatomic groups contained in the usual paramagnetic crystals.

In conclusion it may be said that Professor Platzman's detailed analysis is of great help in the assessing of the various possible errors that could be associated with γ-ray heating. And, although present results show no effects that can be attributed to delayed heat evolution, experiments specifically designed for the purpose may well provide quantitative data on the mechanism of γ-ray absorption in dielectric crystals.

REFERENCES

BLEANEY, B., 1950, *Proc. Roy. Soc.* A, **204,** 216.
COOKE, A. H., 1949, *Proc. Phys. Soc.* A, **62,** 269.
DANIELS, J. M., and KURTI, N., 1953, to be published.
DE KLERK, D., STEENLAND, M. J., and GORTER, C. J., 1948, *Nature, Lond.*, **161,** 678 ; 1949, *Physica*, **15,** 649.
HEBB, H. M., and PURCELL, E. M., 1937, *J. Chem. Phys.*, **5,** 338.
HULL, R. A., 1947, *Report of Cambridge Conference on Low Temperatures*, p. 72.
HUNT, B., 1952, *Thesis*, Oxford.
KURTI, N., and SIMON, F. E., 1935, *Proc. Roy. Soc.* A, **152,** 21 ; 1938 a, *Phil. Mag.*, **26,** 840 ; 1938 b, *Ibid.*, **26,** 849.
PLATZMAN, R. L., 1953, *Phil. Mag.*, **44,** 497.
SIMON, F. E., 1935, *Nature, Lond.*, **135,** 763.

LIII. *The Propagation of Very Low Frequency Radio Waves to Great Distances*

By K. G. Budden
The Cavendish Laboratory, Cambridge*

[Received February 2, 1953]

Summary

In discussing the propagation of very low frequency radio waves to great distances, it is convenient to treat the space between the earth and the ionosphere as a wave-guide. This treatment is applied to some experimental measurements made by Dr. Weekes on signals of frequency 16 kc/s, over a range of distances from 340 km to 3640 km from the sender. It is shown that the measurements can be explained in terms of the four least attenuated wave-guide modes. If the earth's magnetic field is neglected, and the ionosphere is assumed to be a sharply bounded homogeneous, ionized medium, then it is shown that the height of the boundary is 69·1±0·5 km.

§1. Introduction

In the theoretical discussion of the propagation of very low frequency radio waves to great distances, it is often convenient to treat the space between the earth and the ionosphere as a wave-guide, and to consider the propagation in terms of a number of wave-guide modes. This was essentially the method followed in many well known theoretical papers, for example, Watson (1919), Eckersley (1932), Bremmer (1949).

In the present paper the wave-guide treatment is applied to some recent experimental measurements made by Dr. Weekes, in which a receiver in an aeroplane was used to measure the strength of the signal from the sender GBR at Rugby (frequency 16 kc/s), over a range of distances from 340 km to 3640 km from the sender. It is shown that this treatment provides a simple interpretation of the results, and enables an estimate to be made of the height of reflection, and of some of the properties of the ionosphere.

§2. Previous Theoretical Work

In two previous papers (Budden 1951 a, 1952), hereinafter referred to as I and II, the application of the wave-guide method to the propagation of a radio atmospheric was discussed, and it was shown that some of the experimental results (Gardner 1950, Bowe 1951) were conveniently interpreted by this method. In both I and II the ionosphere was assumed to be a sharply bounded homogeneous medium. In Paper I the

---

* Communicated by the Author.

relation between the wave-guide treatment and the alternative treatment in terms of successively reflected waves was discussed. It was shown that at short distances from the transmitter, the received signal is most conveniently considered as composed of a ground wave and a few reflected waves, but at great distances this picture becomes complicated because it is then necessary to include a large number of rays successively reflected at the ground and the ionosphere. If, however, the signal at a great distance is analysed into wave-guide modes, usually only a small number of modes of low order need be included because the higher order modes are heavily attenuated. In Paper II the full mathematical theory was given, and the effect of the earth's magnetic field on the wave-guide modes was discussed. It was found to have little effect on the general form of the results, and in the present paper it is neglected.

In Papers I and II the electro-magnetic field in a wave-guide mode was thought of as composed of two component plane waves, with their wave normals inclined at a (complex) angle θ to the vertical. One component wave is converted into the other by reflection at the ground or at the ionosphere. After a part of a wave front has undergone two reflections, it is parallel to its original direction, and the phases and amplitudes of the original and of the twice reflected wave must be the same. This implies that only certain discrete values of θ are possible.

The changes of phase and amplitude of a wave can be represented as changes of a single complex quantity which is the complex amplitude of the wave. This changes both when the wave traverses a given path and when it is reflected at a surface. The earth's surface is assumed to be a perfect reflector so that the only changes of complex amplitude arising from reflection occur at the ionosphere, which is assumed to have a (complex) reflection coefficient R. The wave front of a twice reflected component wave coincides with its original position after travelling a distance $2h \cos\theta$, where h is the width of the wave-guide (height of the ionosphere). This introduces a difference of (complex) phase $2hp(\cos\theta)/c$ between the original and the twice reflected wave, where p is the angular wave frequency and c is the velocity of light. The corresponding change of the complex amplitude is $\exp\{-2ihp(\cos\theta)/c\}$ and the product of this with R gives the total change of complex amplitude arising both from reflection and from the path traversed. This product must be unity for a self consistent mode and hence

$$R \exp\{-2ihp(\cos\theta)/c\} = \exp(2\pi in), \quad . \quad . \quad . \quad . \quad (1)$$

where n is an integer, and is the phase difference measured in cycles between the original and the twice reflected wave. The reflection coefficient R is a function of the angle θ. The integer n may be positive, negative or zero, and determines the order of the mode. Equation (1) must be modified if allowance is made for the earth's curvature. This modification is given in detail in Paper II and is used in § 5 of the present paper.

The value of the reflection coefficient R depends on the model adopted for the ionosphere. The model to be used in this paper is the same as that in Paper I, in which the ionosphere was assumed to be a homogeneous, sharply bounded, ionized medium containing N electrons per unit volume, making, on the average ν collisions per unit time. The effect of the earth's magnetic field is neglected. At the level where very low frequency waves are reflected, ν is of the order 10^7 sec^{-1}, and it is therefore assumed that $\nu \gg p$. Then if μ is the (complex) refractive index of the medium

$$\mu^2=1-ip_r/p \qquad (2)$$

where $p_r=4\pi Ne^2/\epsilon_0 m\nu$,

e=charge on the electron,

m=mass of the electron,

ϵ_0=electric permittivity of free space

and the reflection coefficient R is given by

$$R=\{\mu^2 \cos\theta-\surd(\mu^2-\sin^2\theta)\}/\{\mu^2 \cos\theta+\surd(\mu^2-\sin^2\theta)\}. \qquad (3)$$

A combination of (1) and (3) gives the equation

$$\{\mu^2 \cos\theta-\surd(\mu^2-\sin^2\theta)\}/\{\mu^2 \cos\theta+\surd(\mu^2-\sin^2\theta)\}$$
$$=\exp\{2ihp\,(\cos\theta)/c+2\pi in\}, \qquad (4)$$

from which θ may be determined.

The amplitude of the signal in a single wave-guide mode is given by an expression containing a Bessel function, but provided the distance from the transmitter to the receiver is greater than one or two wavelengths it is permissible to use the asymptotic form for the Bessel function, and the signal at the ground is then proportional to

$$\rho^{-1/2}(\sin\theta)^{1/2}\exp\{-ip\rho\,(\sin\theta)/c\} \qquad (5)$$

(see Paper I, Appendix A), where ρ is distance measured horizontally from the transmitter.

§ 3. COMPOSITE WAVE-GUIDE MODES

In the specific examples discussed in Paper I, it was found that the modes of orders 0 and -1 had very similar characteristics so that the fields in these two modes were practically indistinguishable even at great distances from the source. In the same way the characteristics of the modes of orders $+1$ and -2 were similar. This result applies also to the calculations of the present paper, and it is therefore convenient to treat the two modes of orders 0 and -1 together as a single composite mode, which will be called 'mode A'. The field in this composite mode is given by (5) where $\sin\theta$ has an effective value $\sin\theta_A$. It is shown in § 6 that $\sin\theta_A$ is given with sufficient accuracy by the average of the values of $\sin\theta$ for the modes of orders 0 and -1. Similarly, the modes of orders $+1$ and -2 are treated together as a composite 'mode B'. This has an effective value of $\sin\theta$, denoted by $\sin\theta_B$, which is a suitably weighted average of the values of $\sin\theta$ for the modes of orders -2 and $+1$.

§4. Analysis of the Experimental Results

The study of the reflection of radio waves from the ionosphere by measurements of the signal at varying distances from the sender was first applied to very low frequency waves by Hollingworth (1926), and was used extensively by Best, Ratcliffe and Wilkes (1936), Budden, Ratcliffe and Wilkes (1939), and Weekes (1950). These observers made nearly all their measurements within a few hundred kilometres of the sender, and were concerned with the field resulting from the interaction of the ground wave and one predominant reflected wave. The e.m.f. of the ground wave is inversely proportional to the distance ρ from the sender, and they therefore found it convenient to display their results by plotting the product 'signal strength $\times \rho$' against ρ. By this method the field of an unattenuated ground wave alone would be plotted as a horizontal line, and the departures from this line could be ascribed to the interaction of a reflected wave with the ground wave.

At great distances from the sender the field must be that of the least attenuated wave-guide modes, as explained in Paper I. The expression (5) shows that the amplitude in one composite mode is inversely proportional to $\sqrt{\rho}$. This suggests that the product 'signal strength $\times \sqrt{\rho}$' be plotted against ρ. For one composite mode the result should be a smooth curve showing an exponential attenuation arising from the imaginary part of $\sin\theta$ in the exponential term of (5). Any departures from this smooth curve can be ascribed to the interaction of more than one composite mode.

In fig. 1 this method of plotting is applied to some results obtained by Dr. Weekes from measurements made in an aeroplane which flew from England to Cairo and back in June and July 1950. The field strength from the sender GBR (16 kc/s) was measured continuously during the flight. Inspection of the curve suggests that there are two predominant wave-guide modes which interact to give an interference pattern. This suggestion is strongly supported by the fact that the spacing of the maxima and minima of the pattern is roughly constant, as it should be if the signal was produced by the interaction of two waves propagated radially outwards with constant but different phase velocities. The results displayed in fig. 1 were analysed on the assumption that the two composite modes A and B mentioned in the last section combine to give the observed signal.

With this assumption it is possible to obtain three numerical quantities from the results shown in fig. 1. These are:

(i) The difference of the reciprocals of the phase velocities V_A and V_B for the modes A and B. This gives a value for $\mathscr{R}(\sin\theta_A)-\mathscr{R}(\sin\theta_B)$, where the symbol $\mathscr{R}$ denotes 'real part of'.

(ii) The attenuation constant of mode A. This gives $\mathscr{I}(\sin\theta_A)$ where $\mathscr{I}$ denotes 'imaginary part of'.

(iii) The attenuation constant of mode B. This gives $\mathscr{I}(\sin\theta_B)$.

The relation (i) was found as follows. Successive maxima and minima in fig. 1 correspond to increments of π radians in the phase difference between the two modes A and B. The positions of the maxima and minima were therefore plotted as abscissae with ordinates increasing in steps of π radians. The resulting graph is a fairly good straight line, and its slope in radians per unit distance is easily shown to be equal to $p(1/V_A-1/V_B)$. Now from (5) $1/V_A=\mathscr{R}(\sin\theta_A)/c$; $1/V_B=\mathscr{R}(\sin\theta_B)/c$, so that the slope of the line is equal to $\{\mathscr{R}(\sin\theta_A)-\mathscr{R}(\sin\theta_B)\}/c$. It was found that $\mathscr{R}(\sin\theta_A)-\mathscr{R}(\sin\theta_B)=0{\cdot}0181\pm0{\cdot}0003$ (standard error estimated roughly by inspection of the graph).

Fig. 1

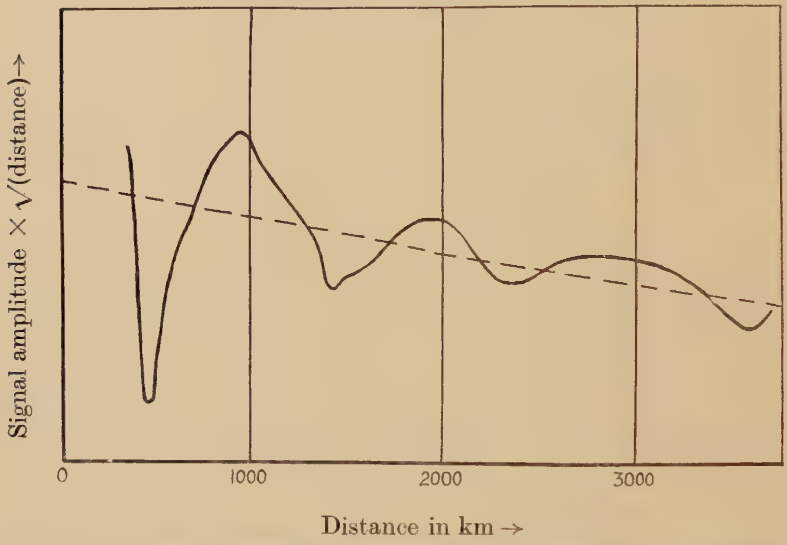

The product 'signal strength × square root of distance' is plotted against 'distance' for the signal from the sender GBR (16 kc/s) during the day-time in June and July, 1950.

The attenuation constant of mode A ((ii) above), was found by smoothing the curve of fig. 1, to eliminate the effect of mode B. Let E_1, E_3, be the ordinates of two adjacent maxima (or minima) in fig. 1, and let E_2 be the ordinate of the intervening minimum (or maximum). Let $E_A=\frac{1}{4}(E_1+E_3+2E_2)$. Then E_A was taken as the smoothed ordinate for the distance corresponding to E_2. This is a somewhat crude method of smoothing, but the accuracy of the experimental data is not high enough to justify a more elaborate method. $\log_e E_A$ was plotted against distance, and a straight line drawn through the points. The slope, χ_A, was taken as the attenuation constant of mode A. From (5) it is clear that $\chi_A=\mathscr{I}(\sin\theta_A)p/c$. It was found that $\mathscr{I}(\sin\theta_A)=0{\cdot}00048\pm0{\cdot}00003$ (rough estimate of standard error). Using this value of $\mathscr{I}(\sin\theta_A)$, the quantity ‘signal amplitude $\times\sqrt{\rho}$’ in mode A alone was found, and is shown as a dotted curve in fig. 1.

The departures of the maxima and minima from the dotted curve in fig. 1 give an indication of the quantity $E_B=$ ‘signal amplitude $\times\sqrt{\rho}$’, for mode B alone. $\text{Log}_e\, E_B$ was plotted against distance, but the resulting points were so widely scattered that only a very rough estimate of the attenuation constant χ_B of mode B could be made. χ_B can also be estimated, when χ_A is known, by comparing the signal amplitudes in modes A and B at the same distance from the transmitter, because the theory shows that the two modes should have approximately equal amplitudes when $\rho=0$. This method also gave only very approximate values of χ_B, but the two estimates were consistent. It was found that $\mathscr{I}(\sin\theta_B)$ probably lies within the range 0·002 to 0·003.

§ 5. Summary of the Theory of Wave-Guide Modes

It is now desirable to find a model for the ionosphere, in which composite modes A and B would be propagated with the characteristics found in the last section. It was explained in § 2 and in Papers I and II that some progress with the theory is possible, if the ionosphere is assumed to be a homogeneous sharply bounded medium, and it will be shown that this assumption leads to a consistent explanation of the results.

First, eqns. (1) to (4) were solved to give the characteristics of the simple modes of orders -2, -1, 0 and $+1$. It is convenient to put:

$$p/p_r=u\ ;\ hp_r/c=\beta\ ;\ R=\mathrm{e}^{2i\alpha}\ ;\ \cos\theta=C. \qquad (6)$$

Then eqns. (2) and (3) give

$$\mathrm{e}^{2i\alpha}=\{(u-i)C-\sqrt{(u^2C^2-iu)}\}/\{(u-i)C+\sqrt{(u^2C^2-iu)}\}. \qquad (7)$$

If the earth is assumed to be flat, eqn. (1) gives

$$\alpha-n\pi=\beta uC. \qquad (8)$$

If the curvature of the earth is allowed for, and K denotes its effective value, then it was shown in Paper II (*loc. cit.* eqn. (61)) that provided $hK\ll 1$:

$$\alpha-n\pi=\beta uC-\tfrac{1}{2}Kh\beta u/C. \qquad (9)$$

(7) and (9) are two equations which determine C for given values of β, u and n. They were solved with the aid of the EDSAC calculating machine in the Mathematical Laboratory of the University of Cambridge. Details of the method are given in the next section.

§ 6. Method of Calculation

Equation (9) is a quadratic for C and the required solution is

$$C=(\alpha-n\pi)/2\beta u+\{(\alpha-n\pi)^2+2Kh\beta^2u^2\}^{1/2}/2\beta u. \qquad (10)$$

Values were first chosen for β, u and n. A trial value of α was then taken, and (10) used to find C. This was put into (7) to give a new trial value of α. The process was then repeated, and was found to converge. The EDSAC programme was so arranged that the machine compared two successive values of α, and when the difference had become less than a specified quantity, the calculation was stopped, and the values of u, β, n, α, C and $\sin\theta$ were recorded. The calculation was then repeated with a new value of u. From the results it was possible to tabulate $\mathscr{R}(\sin\theta)$ and $\mathscr{I}(\sin\theta)$ for a series of values of u, β, and n.

Let θ_0, θ_{-1}, be the calculated values of θ for the modes of orders 0 and -1 respectively. Then the signal in the composite mode A is proportional to

$$2S_{\mathrm{A}}=\rho^{-1/2}\{(\sin\theta_0)^{1/2}\exp(-ip\rho\sin\theta_0/C)$$
$$+(\sin\theta_{-1})^{1/2}\exp(-ip\rho\sin\theta_{-1}/C)\}. \quad . \quad . \quad . \quad (11)$$

Let $$\sin\theta_0+\sin\theta_{-1}=2\sin\theta_{\mathrm{A}}\,;\ \sin\theta_0-\sin\theta_{-1}=2\Delta_{\mathrm{A}}, \quad . \quad . \quad (12)$$

where Δ_{A} is small. Then approximately from (11)

$$S_{\mathrm{A}}=\rho^{-1/2}(\sin\theta_{\mathrm{A}})^{1/2}\exp(-ip\rho\sin\theta_{\mathrm{A}}/C)[\cos(p\rho\Delta_{\mathrm{A}}/C)$$
$$-\tfrac{1}{2}i\Delta_{\mathrm{A}}(\sin\theta_{\mathrm{A}})^{-1}\sin(p\rho\Delta_{\mathrm{A}}/C)]. \quad . \quad . \quad . \quad . \quad . \quad . \quad . \quad (13)$$

From the numerical results for the largest value of ρ used, it is found that

$$|\cos(p\rho\Delta_{\mathrm{A}}/C)|\approx 0{\cdot}97\,;\ \arg\{\cos(p\rho\Delta_{\mathrm{A}}/C)\}\approx 50'$$

and $$|\tfrac{1}{2}\Delta_{\mathrm{A}}(\sin\theta_{\mathrm{A}})^{-1}\sin(p\rho\Delta_{\mathrm{A}}/C)|\approx 0{\cdot}00024.$$

The second term in the square bracket of (13) was therefore neglected, and the first was set equal to 1.

For the composite mode B a more complicated process was necessary, because the difference of the attenuations of the modes of order $+1$ and -2 was appreciable, and at 3640 km from the source the amplitude of the mode of order -2 was only about one-half that of the mode of order $+1$. The signal in the composite mode B is proportional to

$$2S_{\mathrm{B}}=\rho^{1/2}\{(\sin\theta_{+1})^{1/2}\exp(-ip\sin\theta_{+1}\rho/C)$$
$$+(\sin\theta_{-2})^{1/2}\exp(-ip\sin\theta_{-2}\rho/C)\}. \quad . \quad . \quad . \quad (14)$$

The factors $(\sin\theta_{+1})^{1/2}$ and $(\sin\theta_{-2})^{1/2}$ were both sufficiently close to unity to treat them as equal. It was only in the exponentials that small differences between $\sin\theta_{+1}$ and $\sin\theta_{-2}$ were important. Let

$$\exp(-ip\sin\theta_{+1}\rho/C)+\exp(-ip\sin\theta_{-2}\rho/C)=\exp(-ip\sin\theta_{\mathrm{B}}\rho/C). \quad . \quad . \quad (15)$$

Sin θ_{B} could be calculated from (15) for each value of ρ but it was found sufficiently accurate to take

$$2\sin\theta_{\mathrm{B}}=a\sin\theta_{+1}+b\sin\theta_{-2}, \quad . \quad . \quad . \quad . \quad . \quad . \quad (16)$$

where $a+b=2$, and a and b are constant weighting factors, which were calculated from (15) and (16) for $\rho=2000$ km. This is the value of ρ about half way between the extreme values shown in fig. 1. The resulting error in phase for the largest value of ρ used was then about 20°, and an error of only 67 km in assessing the position of the last minimum in fig. 1 would give a similar error in phase.

For a given value of β, $\mathscr{R}(\sin\theta_A)-\mathscr{R}(\sin\theta_B)$ was plotted against u, and the value u_0 of u was found which made the ordinate equal to the experimental value 0·0181. For this value of u, $\mathscr{I}(\sin\theta_A)$ was then found. The process was repeated for other values of β, and the results are shown in fig. 2. The experimental value of $\mathscr{I}(\sin\theta_A)$ was 0·00048, and it is clear from fig. 2 that this is given by $\beta=10$. In this way it was possible to find the values of β and u which fitted the experimental results best. The appropriate value of u_0 was found to be $2{\cdot}35\pm0{\cdot}02$, and since $p=2\pi\times16$ rad. sec^{-1} this gives $p_r=4{\cdot}28\times10^4$ rad. sec^{-1}. With these values, the second relation in (11) shows that $h=69{\cdot}1\pm0{\cdot}5$ km. For the above values of β and u, the value of $\mathscr{I}(\sin\theta_B)$ was found to be 0·0027, which is within the range indicated by the experiments.

Fig. 2

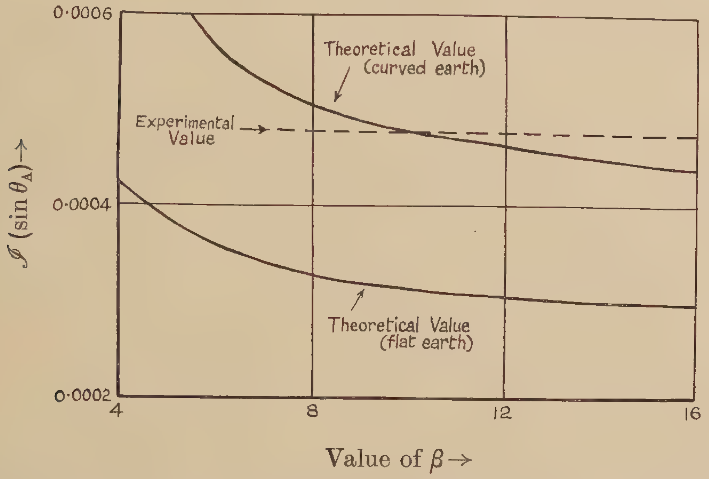

Determination of β from experimental results. The experiments show that $\mathscr{I}(\sin\theta_A)=0{\cdot}00048$.

§ 7. DISCUSSION OF RESULTS

It is natural to ask whether the results of the previous section would be appreciably altered if the curvature of the earth were not allowed for. Some calculations were made in which the earth was assumed to be flat, and the results are shown in the lower curve in fig. 2. This is seen to be consistently below the experimental value for $\mathscr{I}(\sin\theta_A)$, and no reasonable values of β and u could be found which would fit the experimental results. It is therefore essential to include the effects of the earth's curvature.

The value $69{\cdot}1\pm0{\cdot}5$ km found for h, the height of the ionosphere, depends only on the experimental value of $\mathscr{R}(\sin\theta_A)-\mathscr{R}(\sin\theta_B)$ and not on $\mathscr{I}(\sin\theta_A)$. This is because the product βu_0 proves to be independent of β for a range of values of β around 10. $\mathscr{R}(\sin\theta_A)-\mathscr{R}(\sin\theta_B)$

is the most accurately determined of the three numerical quantities deduced from the measurements, and hence h is given within narrow limits. It is interesting to compare this value with that given by Bracewell *et al.* (1951) who deduced a height of 74 km from measurements made on summer days at steep angles of incidence. Since the component waves in the wave-guide modes impinge at nearly grazing incidence on the ionosphere, the two values obtained for the height of reflection would not be expected to agree exactly.

In § 2 an expression for p_r was given which shows that it is proportional to the ratio of the electron density N to the collision frequency ν. The best estimate of ν at a height of 70 km seems to lie between 1×10^7 and 3×10^7 sec^{-1}. Then, using the value of p_r given in the last section, it is found that N lies between 135 and 400 cm^{-3}.

It is of interest to find how far the fields of the wave-guide modes penetrate into the homogeneous medium which is assumed for the ionosphere. The upgoing component wave of a mode is incident on the ionosphere at a (complex) angle θ, and gives rise to a transmitted wave in the medium with its wave normal at a (complex) angle ϕ to the vertical. The vertical variation of the field in the medium is thus given by $\exp \{ip\,(t-\cos\phi\,.\,\mu z/c)\}$ where t is time, and z is height. The amplitude in the medium is therefore proportional to $\exp\{-p\,|\mathscr{I}(\mu\cos\phi)|\,z/c\}$. It falls to half value in a vertical distance $\lambda\,(\ln 2)/2\pi\mathscr{I}(\mu\cos\phi)$, where λ is the wavelength in free space. The value of this distance was about 4·7 km for all the four modes of orders -2, -1, 0 and $+1$. Thus it is probable that only a thin region of the ionosphere plays an effective part in the propagation of low frequency waves to great distances.

Figure 1 shows clearly that the oscillations of the curve at small distances from the transmitter are less smooth and regular than at greater distances. This could be explained by the presence of modes of higher order. These would be more heavily attenuated than the composite modes A and B, and so would cease to have appreciable amplitude at greater distances.

§ 8. CONCLUSION

The propagation of very low frequency radio waves (16 kc/s) to distances between about 400 km and 4000 km can be adequately explained in terms of wave-guide modes, and to account for most of the experimental results only two composite modes (four simple modes) need be considered. If it is assumed that the wave-guide is bounded by a perfectly conducting ground, and an ionosphere which is a sharply bounded homogeneous ionized medium, then good agreement with the experimental results can be obtained, and estimates can be made of the height of the ionosphere, and of the electron density in it. It is found that the height is $69 \cdot 1 \pm 0 \cdot 5$ km and if the collision frequency is taken to be between 1×10^7 and 3×10^7 sec^{-1} at that height then the electron density is between 135 and 400 cm^{-3}.

ACKNOWLEDGMENTS

This work forms part of a programme of radio research at the Cavendish Laboratory. I am much indebted to Dr. Weekes for allowing me to use his experimental results, and to the Director and staff of the Mathematical Laboratory, University of Cambridge, for permitting me to use the EDSAC calculating machine.

REFERENCES

BEST, J. E., RATCLIFFE, J. A., and WILKES, M. V., 1936, *Proc. Roy. Soc.* A, **156,** 614.
BOWE, P. W. A., 1951, *Phil. Mag.*, **42,** 121.
BRACEWELL, R. N., BUDDEN, K. G., RATCLIFFE, J. A., STRAKER, T. W., and WEEKES, K., 1951, *Proc. Instn., Elec. Eng.*, **98,** III, 221.
BREMMER, H., 1949, *Terrestrial Radio Waves* (Elsevier Pbl. Co.).
BUDDEN, K. G., 1951 a, *Phil. Mag.*, **42,** 1 ; 1951 b, *Ibid.*, **42,** 833 ; 1952, *Ibid.*, **43,** 1179.
BUDDEN, K. G., RATCLIFFE, J. A., and WILKES, M. V., 1939, *Proc. Roy. Soc.* A. **171,** 188.
ECKERSLEY, T. L., 1932, *Proc. Roy. Soc.* A, **136,** 499.
GARDNER, F. F., 1950, *Phil. Mag.*, **41,** 1259.
HOLLINGWORTH, J., 1926, *J. Instn., Elec. Eng.*, **64,** 579.
WATSON, G. N., 1919, *Proc. Roy. Soc.* A, **95,** 83, 546.
WEEKES, K., 1950, *Proc. Instn., Elec. Eng.*, **97,** III, 100.

LIV. *Observations on Slip Found in a Diamond*

By S. Tolansky and M. Omar
Royal Holloway College (University of London), Egham, Surrey*

[Received February 17, 1953]

Abstract

Interferometric and optical studies on a twinned diamond reveal the presence of true crystallographic slip on two opposite faces of the twin. Slip occurs parallel to a (111) plane, in both cases, making thus an angle of $70\frac{1}{2}°$ with the surface. An internal optical opacity is found associated with the slip. The two faces on either side of one slip line are not parallel but inclined at the very small angle of 10^{-5} radian.

§ 1. Introduction

It is doubtful whether earlier observers have been able fully to substantiate the existence of slip in diamond. Williams (1932) has suggested that certain features appearing on some microphotographs of diamond might be attributable to slip, but the evidence is somewhat tenuous. Since diamond cleaves only effectively on the (111) octahedron plane, it might be anticipated that if slip were to be found, then it should occur parallel to this natural cleavage plane.

During an extensive interferometric study of growth features on the surfaces of many diamonds, we have found on one crystal, a contact twin (i.e. ‘ macle ’) loaned to us by Dr. Grenville-Wells, decisive evidence of crystallographic slip which we have studied quantitatively by interferometric and light profile methods (Tolansky 1952 a, b). Slip regions have been found on both the major (111) faces of the twin and it has been established also that the slip plane is indeed parallel to (111).

To study this crystal use has been made of a number of optical techniques. The surface had on it some high projecting regions and since it has long been established that multiple beam interferometry requires close approach to the two surfaces involved, a special micro-flat technique was developed, in which the flat used was the small tip of a truncated cone, which could be brought into close approach with the desired region. This technique is being described elsewhere. Again, high magnification multiple beam interferometry was desirable in some regions and we reproduce later an interferogram taken at × 2000, using for this the thin film technique we have already described (Tolansky and Omar 1952) elsewhere.

---

*Communicated by the Authors.

§ 2. OBSERVATIONS

(*a*) *Slip on the First Face*

On the one side of the crystal the slip appears as a straight line, cutting right through all the growth features, some 15 mm long, running right across the surface. Part of this is shown in fig. 1, Plate 29 (× 30). The series of parallel lines KL are growth sheet fronts, and at 60° to these lies XY the slip line. The topography of this region is rendered clear by fig. 2, Plate 29 (× 100) which is a multiple beam interferogram. Here MN is a growth sheet step, parallel to the group of steps KL and once more XY is the slip direction. From the fringes one can readily evaluate the topography, a simplified diagram being shown schematically in fig. 7. The Fizeau fringes of fig. 2, Plate 29 are ambiguous as to step directions and these have been clarified by using fringes of equal chromatic order (Tolansky 1945). With these fringes it is confirmed that in fact the level differences A–B and C–D are identical in the neighbourhood of the cross over.

Fig. 7

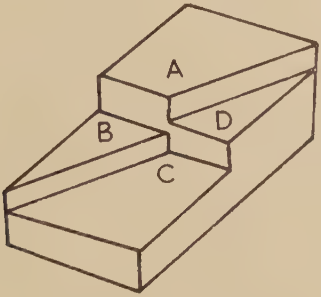

An examination of the slip step over the entire length of the crystal reveals the existence of a slight slope. The step increases regularly from the left to the right. Thus at the extreme left-hand side the slip is only 480 A. At a point 2 mm to the right it has increased to 680 A, and at 8 mm to the right to 1280 A. This corresponds to a slope between the slipped regions with the very small angle of 10^{-5} radian, i.e. merely 2 seconds of arc. Although small, this value is precise and has been confirmed by measurements on intermediate positions between ends. If this slip were to be taken as due to a dislocation the angle would imply a displacement of one atomic lattice in 10^5 lattices, to account for the slope. However, it should be pointed out that the slip does not run to zero at one end of the crystal, the minimum step of 480 A clearly corresponding to a slip of some hundreds of lattices.

Examination of the crystal in transmission with polarized light reveals a general distribution of strain other than in the slip region. Near the slip region itself and undoubtedly closely associated with it is a peculiar opacity. This is shown in fig. 4, Plate 29 (× 90). Examination with an intense light source shows that the opaque region is sharply defined by the slip edge and then falls off somewhat, the final edge (lower) tailing away in a fuzzy manner. Inside the opaque region are some faintly transparent interference fringe regions. The difference in sharpness at the edges of the opaque region is clearly shown in the picture.

It will be shown later that the slip makes a large angle with the surface. This being so, high magnification experiments were undertaken to see whether the slip step discontinuity was sharp. To do this a silvered thin film technique (Tolansky and Omar 1952) was used. The crystal was silvered for multiple beam interferometry. A very thin film of Canada balsam was drawn over the slip boundary by means of a dilute solution of xylol. This dried rapidly and was then silvered. Multiple beam fringes are then formed in the thin film, the optical step being, of course, magnified by the ratio of the refractive index of the film to that of air. We have already demonstrated that high lateral magnification multiple beam fringes are obtainable by this procedure, fig. 3, Plate 29 shows the fringes across the slip step at × 2000. When the high lateral magnification is taken into account, it will be recognized that the fringe definition is exceptionally good.

Apart from the fact that such a picture permits accurate determination of the step, with an error of but a few angstrom units, the picture establishes that the step is discontinuous, sharply so. Now evidence will be produced later that the slip steps found on both faces have an undercut angle of $70\frac{1}{2}°$ and there is every reason to believe, that the same will always be true. The sharp discontinuity observed is then only what can be expected if indeed the slip step undercuts, and is thus far a satisfactory observation.

It is to be noticed that the slip line is exactly at 60° to the growth direction and is thus parallel to an edge of the (111) face.

(*b*) *Slip on the Second Face*

Because of the twinned nature of the crystal the slip cannot be expected to penetrate from one side to the other and indeed this is the case, for the line XY does not appear on the opposite face of the flat stone. However an independent slip line does appear on the second face, this being inclined at 60° to the direction of XY. This second slip line also traverses right across the crystal and in doing so very clearly reveals a feature of some considerable interest. For the second face has on it a number of high growth plateaus, as well as deep triangular depressions (familiar features on (111) faces). The slip in question runs across some of these and in doing so becomes quite clearly displaced. It is from these displacements that the angle of undercutting can be determined, as shown in fig. 8. Suppose we have a growth step P. If this be cut by a slip plane normal to the surfaces then the cut lines in the upper and lower growth regions, when viewed from above, are colinear. If the cutting slip plane has an angle to the surface, then the two lines will appear displaced, as in fact shown schematically in fig. 8. If the growth sheet step height be known, and is reasonably large, the measured displacement in the slip line permits the angle of undercut to be calculated. Furthermore the direction of displacement determines the direction of undercut. An example of a measurement made this way is shown by fig. 5, Plate 29. Here the slip traverses a growth trigon. The discontinuity in the slip line as it passes over the growth step PQ, for example, is readily seen. This step height PQ measured by the light profile is large, i.e. 90 μ. The lateral displacement of the slip line measured in fig. 5, Plate 29 (× 30) is 32 μ. From a simple calculation it follows that the angle of undercut is $70\frac{1}{2}°$. This is precisely the angle made by adjoining (111) faces on diamond. We have therefore established that the slip line is not only parallel to a (111) edge, but indeed the whole slip plane is parallel to a (111) plane, i.e. to a cleavage plane.

Fig. 8

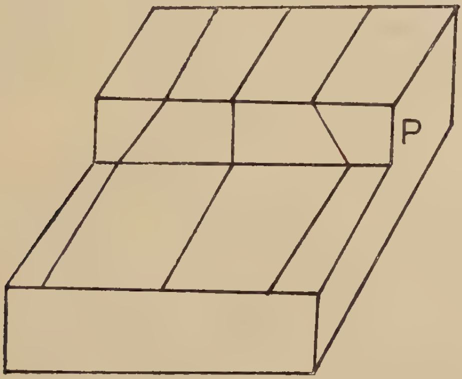

This interesting and exact geometrical deduction has only been made possible because of the occurrence of one very large discontinuity (90 μ) over which the slip traverses on the second face. Only in one position does the other slip line on the first face also pass over a relatively large discontinuity, and it is striking that from this face also it has been established to have an angle of $70\frac{1}{2}°$, exactly as in the case of the second face. The light profile picture over this part is shown in fig. 6, Plate 29 (× 90) in which the growth discontinuity is 31·5 μ and the slip line shift 11 μ. In fig. 6, the slip line is that which runs in the north-east to south-west direction crossing the group of parallel growth steps, the discontinuity appearing markedly in the last step. The optical light profile, which also shows the discontinuity at this step, is the vertical line having on it a short horizontal cross, some 1 cm from the top of the picture. The slip on the second face has also associated with it an internal opacity. Furthermore the second-face slip dose not penetrate the two twins but, as in the first case, ends within the body of the crystal.

(*c*) *A Possible Explanation of the Opacity*

Now that it is established that the slip plane is making an angle of $70\frac{1}{2}°$ with the surface it is quite possible to explain the opacity on the following lines. If the slip has developed partly into a crack, then an air film in the crack would totally reflect the incident light at the interface of diamond-air. The incident light would make an angle of $70\frac{1}{2}°$ with the perpendicular to the slip plane which is greater than the critical angle of diamond ($24\frac{1}{2}°$). As either part of the macle is 1·5 mm thick and the opacity at its maximum as estimated in different parts is $\frac{1}{3}$ mm, the crack, on this assumption, could only have penetrated to no more than two-thirds of the thickness of either part. If this interpretation of the opacity is correct it is reasonable to assume that the crack might have a finite width at its mouth where it emerges on the crystal face. Although the formation of such a small wedge crack might lead to the appearance of a small inter-facial angle between the two parts on either side of the crack, no such very small inter-facial angle has been detected. It is clear that the observed step cannot be accounted for by postulating such a mechanism for this suggested alternative would lead not to fringe steps but to fringes showing an angle kink. The fringes would appear continuous but change abrupt direction at the crack and would not, as are observed, be violently out of step.

It is emphasized that the observed angle of 10^{-5} radian referred to above applies to the fact that the slip is emerging out of the surface with a slightly increased step height as one traverses along the length of the ledge.

Thus it may be concluded that

(*a*) the occurrence of crystallographic slip on diamond has been demonstrated on two faces of a twin,

(*b*) the slips takes place on (111) planes, which are the planes of easy cleavage,

(*c*) the two faces on either side of one slip are inclined at the slight angle of 10^{-5} radian,

(*d*) the slips have associated with them regions opaque to transmitted light,

(*e*) the slip appears on both sides of a twinned macle, but in neither case does the slip penetrate to the opposite side.

REFERENCES

TOLANSKY, S., 1945, *Phil. Mag.*, **36,** 225; 1952 a, *Nature, Lond.*, **169,** 445; 1952 *b*, *Zeitschrift für Elektrochemie*, **56,** 263.

TOLANSKY, S., and OMAR, M., 1952, *Nature, Lond.*, **170,** 81.

WILLIAMS, A. F., 1932, *The Genesis of Diamond* (London).

LV. *A Surface Contribution to the Debye Specific Heat**

By R. Stratton†
University of Manchester‡

[Received February 24, 1953]

Abstract

The vibrations of a bounded lattice are identified with those of an elastic medium (isotropic, arbitrary elastic constants) having stress free surfaces. The densities of the representative points in wave number space for the four possible types of vibration are estimated. These estimates are carried one step further than the usual (Debye) method by including terms proportional to the surface. Summing over the densities, the total number of excited modes and the intrinsic energy of the lattice vibrations are obtained in the usual manner. From these we calculate surface terms for the Debye temperature and specific heat and for the free energy of the lattice vibrations.

§ 1. Introduction

The specific heat of a solid has been calculated (Debye 1912) by replacing the thermal vibrations of the lattice with elastic waves in a continuous and isotropic elastic medium of the same volume. For a large volume, arbitrary surface conditions are selected and the total number of modes $M(\omega_m)$ having a frequency ($\nu_m = \omega_m/2\pi$) calculated. ω_m is then determined by equating $M(\omega_m)$ to the total number of degrees of freedom of the lattice points (ions, atoms or molecules), i.e. $3NV$, where N is the number of lattice points per unit volume and V is the lattice volume. If, however, the ratio of surface area to volume becomes large, natural surface conditions should be used thus affecting the value of ω_m which becomes surface dependent. The natural condition appropriate for a continuous medium will be a stress free surface.

The intrinsic energy, which corresponds to the sum of the average energy of the vibrations over the $M(W_m)$ modes, thus contains a surface term from which a surface term in the specific heat and a temperature dependent surface free energy can be calculated.

The calculation has been carried out by Brager and Schuchowitzky (1946, referred to as B) for the case of an incompressible medium. This gives a great simplification since only transverse waves can occur. They considered the two-dimensional vibrations of a parallel plate (normal to the plane of the plate) of infinite extent but finite thickness and then extended the solution to three-dimensional waves. Their treatment is however in need of correction since they pay no special attention to waves with a zero wave number component in the direction of the thickness of the plate and carry out the extension to the three-dimensional case incorrectly.

---

* This paper is part of a thesis submitted to the University of Manchester in support of an application for the degree of Doctor of Philosophy.

† Now at Metropolitan-Vickers Electrical Co. Ltd., Trafford Park, Manchester.

‡ Communicated by L. Rosenfeld.

Besides investigating the effect of these corrections, it seems desirable to extend the calculation to the case of arbitrary compressibility, thus including longitudinal waves. This not only gives a better insight into the present problem, but consideration of the longitudinal waves is required for the calculation of the electron-lattice interaction in a finite plate. This last problem arises in the discussion of the surface energy of a super-conducting specimen to which we hope to return in a future paper.

Our calculation is based on the representation of the possible modes of vibration, for the various types that are found to occur, by points in wave number planes. The densities of these points are then estimated and the total number of modes obtained by summing over the densities. Having determined the Debye frequency we can calculate the intrinsic energy, again using the density of modes.

In § 2 we consider two-dimensional waves first as they are simpler to interpret and occur as special cases of the three-dimensional waves subsequently treated in § 3. The evaluation of the surface terms for the specific heat and free energy of the lattice depends only on the final result of § 3 which expresses the total number of excited modes of vibration in terms of the maximum frequency and elastic parameters.

§ 2. THE TWO-DIMENSIONAL CASE

We consider a parallel plate of infinite extent but finite thickness which fills the space between $z=+L_z$ and $z=-L_z$ of a rectangular co-ordinate system. Solving the elastic stress–strain equations, we can express the displacement in the (x, z) plane as (cf. Lamb 1917)

$$u=(u_x, u_z)=\left[\left(\frac{\partial\phi}{\partial x}+\frac{\partial\psi}{\partial z}\right), \left(\frac{\partial\phi}{\partial z}-\frac{\partial\psi}{\partial x}\right)\right], \quad . \quad . \quad . \quad (1)$$

where the potential functions ϕ and ψ are given by

$$\left.\begin{aligned}\phi&=-2i^S\mathscr{P}_l\cos q_{lz}z\exp[i(q_x x-\omega t)]\\ \psi&=2^S\mathscr{P}_t\sin q_{tz}z\exp[i(q_x x-\omega t)]\end{aligned}\right\}\text{ symmetrical waves} \quad . \quad (2)$$

or

$$\left.\begin{aligned}\phi&=2^A\mathscr{P}_l\sin q_{lz}z\exp[i(q_x x-\omega t)]\\ \psi&=-2i^A\mathscr{P}_t\cos q_{tz}z\exp[i(q_x x-\omega t)]\end{aligned}\right\}\text{ antisymmetrical waves} \quad (3)$$

with respect to the xy plane.

The wave number components satisfy the relationships

$$\left.\begin{aligned}q_{lz}^2+q_x^2&=q_l^2\equiv\omega^2/c_l^2\equiv\omega^2\rho_0/(\lambda+2\mu)\\ q_{tz}^2+q_x^2&=q_t^2\equiv\omega^2/c_t^2\equiv\omega^2\rho_0/\mu.\end{aligned}\right\} \quad . \quad . \quad . \quad . \quad (4)$$

Here ω is the angular frequency of the elastic waves whose velocity (c_l—longitudinal, c_t—transverse) is given in terms of the usual elastic constants (μ and λ) and the density ρ_0 of the material. The form of the constant coefficients will be shown to be convenient in later work.

In the x direction we take the usual periodic boundary conditions with periodicity $2L_x(L_x \gg L_z)$ so that

$$q_x=\frac{n_x\pi}{L_x}; \quad (n_x=\ldots.-3,-2,-1,0,1,2,3,\ldots.), \quad . \quad . \quad (5)$$

while the surfaces $z=\pm L_z$ must be stress free. The latter condition gives the spectrum of the waves; namely

$$\frac{\tan Q_{tz}}{\tan Q_{lz}}=\frac{4(1+K)\alpha(1+2K-\alpha^2K)}{(1+2K+\alpha^2)^2}=-g_K(\alpha), \quad . \quad . \quad . \quad . \quad (6)$$

for the symmetric and

$$\frac{\tan Q_{tz}}{\tan Q_{lz}}=-\frac{1}{g_K(\alpha)}, \quad . \quad . \quad . \quad . \quad . \quad . \quad . \quad . \quad (7)$$

for the antisymmetric waves. Here we have introduced the quantities

$$Q_{tz}=q_{tz}L_z; \quad Q_{lz}=q_{lz}L_z; \quad \alpha=Q_{tz}/Q_{lz}; \quad K=\mu/\lambda, \quad . \quad . \quad . \quad (8)$$

where K can be expressed in terms of Poisson's ratio

$$K=\mu/\lambda=(1/2\sigma)-1. \quad . \quad . \quad . \quad . \quad . \quad . \quad . \quad (9)$$

Further from eqns. (4)

$$Q_x{}^2=[KQ_{tz}{}^2-(1+2K)Q_{lz}{}^2]/(1+K), \quad . \quad . \quad . \quad . \quad (10)$$

$$W^2=[Q_{tz}{}^2-Q_{lz}{}^2]K(1+2K)/\rho_0(1+K), \quad . \quad . \quad . \quad . \quad (11)$$

where

$$Q_x=q_xL_z \quad \text{and} \quad W=\omega L_z. \quad . \quad . \quad . \quad . \quad . \quad . \quad (12)$$

For any pair of solutions Q_{tz} and Q_{lz} satisfying (6) or (7) the ratio of the coefficients will be given by

$$\frac{({}^{S}_{A}\mathscr{P}_l)^2}{({}^{S}_{A}\mathscr{P}_t)^2}=-\alpha\,\frac{\sin 2Q_{tz}}{\sin 2Q_{lz}}. \quad . \quad . \quad . \quad . \quad . \quad . \quad (13)$$

There are three possible types of wave motion:

(1) ‘ Pure Rayleigh Waves ’

$$q_x{}^2>q_t{}^2 \ \therefore \ q_{lz} \text{ and } q_{tz} \text{ are imaginary.}$$

(2) ‘ Mixed Waves ’

$$q_t{}^2>q_x{}^2>q_l{}^2 \ \therefore \ q_{lz} \text{ is imaginary and } q_{tz} \text{ is real.}$$

(3) ‘ Pure Bulk Waves ’

$$q_l{}^2>q_x{}^2 \ \therefore \ q_{lz} \text{ and } q_{tz} \text{ are real.}$$

From the displacement function it will be seen that waves of type (1) are confined to the surface of the plate, those of type (2) consist of the superposition of a longitudinal surface wave and a transverse bulk wave, whose amplitude is constant over the volume of the plate, while those of type (3) consist of the superposition of longitudinal and transverse bulk waves. We now discuss the frequency spectrum for the three types and determine the number of modes of vibration having a frequency less than a fixed maximum frequency (the Debye frequency).

2.1. *Pure Rayleigh Waves*

Introducing the real quantities

$$Q'^{2}_{tz}=-Q_{tz}^{2} \quad \text{and} \quad Q'^{2}_{lz}=-Q_{lz}^{2}, \qquad . \quad . \quad . \quad . \quad (14)$$

so that $\alpha=Q_{tz}/Q_{lz}=Q'_{tz}/Q'_{lz}$ (taking the positive square root), the spectrum for symmetrical waves becomes

$$\frac{\tanh Q'_{tz}}{\tanh Q'_{lz}}=\frac{\tanh \alpha Q'_{lz}}{\tanh Q'_{lz}}=-g_K(\alpha). \qquad . \quad . \quad . \quad . \quad (15)$$

First of all there exists a solution of (15) as $Q'_{lz}\rightarrow\infty$, namely the real, positive solution of the cubic

$$g_K(\alpha)+1=0, \qquad . \quad . \quad . \quad . \quad . \quad . \quad . \quad . \quad . \quad . \quad (16)$$

say $\alpha_0(K)$. (There is a factor $(\alpha-1)$ for all K which corresponds to zero frequency.) It can be easily shown that

$$\alpha_0(0)\leqslant\alpha_0(K)\leqslant\alpha_0(\infty)$$

$[\alpha_0(0)=0{\cdot}2956,\ \alpha_0(\infty)=0{\cdot}6181]$.

$\alpha_0(K)$ increasing monotonically from one extreme to the other.

Turning again to eqn. (15) we consider the solution for $\alpha\rightarrow 0$. This is

$$\frac{Q'_{lz}}{\tanh Q'_{lz}}=\frac{4(1+K)}{1+2K}; \quad \alpha=0 \quad \text{i.e. } Q'_{tz}=0, \qquad . \quad . \quad . \quad (17)$$

which is approximately $Q'_{lz}\approx 4(1+K)/(1+2K)$. Finally, for large Q'_{lz} the asymptotic solution is

$$Q'_{tz}\sim Q'_{lz}\left[\alpha_0+\frac{2}{g'_K(\alpha_0)}\exp\left(-2\alpha_0 Q'_{lz}\right)\right], \qquad . \quad . \quad . \quad (18)$$

$[g'_K(\alpha_0)$ is always negative$]$. If we now exhibit the solutions of (15) as a curve in the Q'_{tz}, Q'_{lz} plane the possible frequencies will be given by the intersections between it and the family of hyperbola defined by eqns. (10) and (5). From (11), the maximum frequency ω_m corresponds to a maximum Q'_{lz} while (10) gives the range of q_x in terms of that of Q'_{lz}. Thus the total number of modes is

$$M_R{}^S(\omega_m)=2\Delta q_x\frac{L_x}{\pi}=\frac{Aq_{mt}}{2\pi L_z}\left[\left(\frac{1+2K-K\alpha^2}{1+K}\right)^{1/2}\left(\frac{1+K}{(1+2K)(1-\alpha^2)}\right)^{1/2}\right.$$
$$\left.-\frac{1}{q_{mt}L_z}\left(\frac{1+2K}{1+K}\right)^{1/2}\frac{4(1+K)}{1+2K}\right], \qquad . \quad . \quad . \quad . \quad (19)$$

where $q_{mt}=\omega_m/c_t$ is the maximum transverse wave number and $A=4L_xL_z$. The factor 2 occurs since Q_x can have negative and positive values.

Now $M_R{}^S$ is proportional to A/L_z, i.e. the surface area (for two-dimensional motion A represents the volume and A/L_z the surface area, if we consider unit thickness in the y direction). Thus we can neglect the second term in the bracket which corresponds to the non-zero value of Q'_{lz} given by (17).

$$M_R^S(\omega_m)=\frac{A}{2\pi L_z}Y_0 q_{mt}; \quad Y_0^2=\frac{1-\alpha_0^2K/(1+2K)}{1-\alpha_0^2}. \quad . \quad . \quad (20)$$

A similar argument applied to the antisymmetric waves, where the only difference is the lower limits of the q_x range, gives

$$M_R^A(\omega_m)=M_R^S(\omega_m),$$

so that

$$M_R(\omega_m)=M_R^A(\omega_m)+M_R^S(\omega_m)=\frac{A}{\pi L_z}Y_0 q_{mt}. \quad . \quad . \quad . \quad (21)$$

2.2. *Mixed Waves*

Since q_{lz} is imaginary we introduce $\alpha'=i\alpha$ so that the spectrum for symmetrical waves becomes

$$\frac{\tan Q_{tz}}{\tanh Q'_{lz}}=-ig_K(-i\alpha')\equiv\psi_K(\alpha'), \quad . \quad . \quad . \quad . \quad . \quad (22)$$

where

$$\psi_K(\alpha')=\frac{4(1+K)\alpha'(1+2K+K\alpha'^2)}{(1+2K-\alpha'^2)^2}. \quad . \quad . \quad . \quad . \quad (23)$$

For large Q'_{lz} the solution of (22) is

$$Q_{tz}=n_{tz}\pi/2+\delta; \quad \delta=\tan^{-1}\psi(\alpha') \quad \left[0\leqslant\delta\leqslant\frac{\pi}{2}\right], \quad . \quad . \quad (24)$$

$$n_{tz}=0,\ 2,\ 4,\ 6,\ 8\ \ldots.$$

The possible frequencies will be given by the intersections of the curves represented by eqn. (24) and the ellipses represented by eqn. (10) with $Q'^2_{lz}=-Q^2_{lz}$. The total number of modes will be the number of intersections, inside the quarter circle given by eqn. (11) with $\omega=\omega_m$. The radius of this circle is

$$P_m=W_m\left[\frac{\rho_0(1+K)}{K(1+2K)}\right]^{1/2}. \quad . \quad . \quad . \quad . \quad . \quad . \quad . \quad (25)$$

To calculate the density (ρ) of the representative points we consider the intersections A, B, A′, B′, for consecutive values of n_{tz} and n_x (cf. fig. 1). The density will be given by the reciprocal of the area ABB′A′. In calculating this area we can neglect the curvature of AB since it introduces higher order approximations.

$$\text{Area A'B'BA}\approx\text{AB}\,.\,\text{EF}=-\text{DC}\,.\,\text{GF}. \quad . \quad . \quad . \quad . \quad (26)$$

Now

$$\text{DC}=\left(\frac{\partial Q_{tz}}{\partial n_{tz}}\right)_{q_x}2 \quad \text{and} \quad \text{FG}=\left(\frac{\partial Q'_{lz}}{\partial q_x}\right)_{Q_{tz}}\frac{\pi}{L_x}. \quad . \quad . \quad . \quad . \quad (27)$$

Substituting into eqn. (26) the density is given by (factor 2 to account for positive and negative q_x)

$$\rho=-\frac{2}{\text{DC, FG}}=\frac{L_x}{\pi}\left(\frac{\partial n_{tz}}{\partial Q_{tz}}\right)_{Q_x}\left(\frac{\partial q_x}{\partial Q'_{lz}}\right)_{Q_{tz}}. \quad . \quad . \quad . \quad (28)$$

Evaluating the derivatives ((24) and (10))

$$\rho = \frac{A}{2\pi^2 L_z^{\,2}} \frac{1+2K}{K^{1/2}(1+K)^{1/2}} \left[\alpha'^2 + \frac{1+2K}{K}\right]^{-1/2} \left[1 - \frac{\delta'}{Q'_{lz}}\left\{1 + \frac{K\alpha'^2}{1+2K}\right\}\right]. \quad . \quad . \quad . \quad (29)$$

The total number of modes is thus

$$M_M{}^S(\omega_m) = \int_0^{\pi/2}\int_0^{P_m} \rho q \, dq \, d\phi + Z_0 \quad . \quad . \quad . \quad . \quad (30)$$

where we have introduced the polar co-ordinates

$$q^2 = Q_{tz}{}^2 + Q'_{lz}{}^2 \, ; \ \tan\phi = Q_{tz}/Q'_{lz} = \alpha' \quad . \quad . \quad . \quad . \quad (31)$$

and Z_0 is the correction for modes with $n_{tz}=0$ which are included in the integral only with weight $\frac{1}{2}$, i.e.

$$Z_0 = \frac{\pi}{2}\int_0^{P_m} (\rho)_{q_{tz}-0} \, dQ'_{lz} = \frac{L_x q_{mt}}{\pi}. \quad . \quad . \quad . \quad . \quad . \quad . \quad (32)$$

(This term is omitted in B.)

Fig. 1

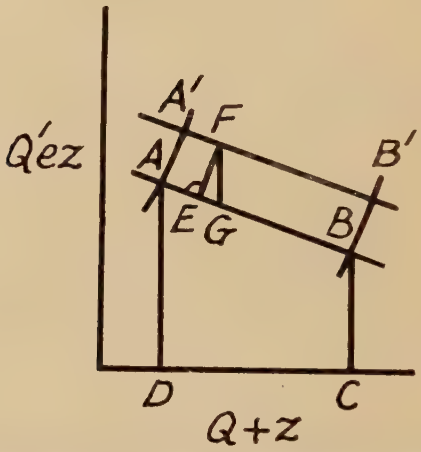

Neighbouring representative points for consecutive values of n_{tz} and n_x.

Substituting into (30) for ρ

$$M_M{}^S(\omega_m) = \frac{A}{2\pi^2}\left[\frac{q^2{}_{mt}}{2}\tan^{-1}\left(\frac{1+K}{K}\right)^{1/2} + \frac{q_{mt}}{L_z}\left(\frac{\pi}{2} - \pi I_2(K)\right)\right] \quad . \quad . \quad (33)$$

where

$$I_2(K) = \frac{1}{\pi}\left(\frac{K}{1+K}\right)^{1/2}\int_0^{\pi/2}\frac{\delta'_K(\tan\phi)}{\cos\phi}\left(\frac{2K+1}{K} + \tan^2\phi\right)d\phi. \quad . \quad . \quad (34)$$

The value of the integral $I_2(0)$ can be deduced from a similar integral given in B.

$$I_2(0) \approx 0{\cdot}2 \times \frac{4}{\pi} \approx 0{\cdot}25. \quad . \quad . \quad . \quad . \quad . \quad . \quad (35)$$

We have not evaluated the integral for any other value of K since it does not occur in the more important three-dimensional case.

The spectrum for antisymmetric waves becomes

$$\tan Q_{tz}/\tanh Q'_{lz}=-1/\psi(\alpha') \quad . \quad . \quad . \quad . \quad . \quad . \quad (36)$$

so that again for large Q'_{lz}

$$Q'_{tz}=n_{tz}\pi/2+\delta\,; \quad \delta=\tan^{-1}\psi\,(\alpha') \quad [0<\delta<\pi/2] \quad . \quad . \quad . \quad (37)$$

and $n_{tz}=1, 3, 5, 7, \ldots$.

Proceeding as for the symmetric case the density of representative points is the same so that the only difference is the absence of the zero wave number correction

$$\therefore\ M_M{}^A(\omega_m)=\frac{A}{2\pi^2}\left[\frac{q_{mt}{}^2}{2}\tan^{-1}\left(\frac{1+K}{K}\right)^{1/2}+\frac{q_{mt}\pi}{L_z}I_2(K)\right] \quad . \quad . \quad . \quad (38)$$

and adding

$$\begin{aligned} M_M(\omega_m)&=M_M{}^A(\omega_m)+M_M{}^S(\omega_m)\\ &=\frac{A}{\pi^2}\left[\frac{q_{mt}{}^2}{2}\tan^{-1}\left(\frac{1+K}{K}\right)^{1/2}+\frac{q_{mt}\pi}{L_z}\left(\frac{1}{4}-I_2(K)\right)\right]. \quad . \quad . \quad (39)\end{aligned}$$

The approximation $\tanh Q'_{lz}\approx 1$, which has been used throughout, implies $Q_{lz}\gg 1$. This is satisfied except for a narrow region of area P_m near the Q'_{lz} axis. The value of ρ given by (29) tends to zero with Q'_{lz} whereas the actual value is of order $A/L_z{}^2$. Thus the relative number of states not satisfying the condition is of order $P_mA/L_z{}^2M(\omega_m)\approx O(1/q_{mt}L_z)$. Since the approximate solutions are themselves used to calculate a surface effect (i.e. δ occurs only in the surface terms) the approximation is justified.

2.3. *Pure Bulk Waves*

The formal solution of (6) may be written in the two ways

$$Q_{tz}=n_{tz}\pi-\delta_t{}^S\,; \quad \delta_t{}^S=\tan^{-1}[g\tan Q_{lz}] \quad . \quad . \quad . \quad . \quad . \quad (40)$$

or

$$Q_{lz}=n_{lz}\pi-\delta_l{}^S\,; \quad \delta_l{}^S=\tan^{-1}[(1/g)\tan Q_{tz}] \quad . \quad . \quad . \quad (41)$$

where the n are non-negative integers and $0<\delta_{t,\,l}<\pi$. This case differs essentially from the one previously treated due to the fact that the δ contain rapidly varying trigonometric functions.

We first of all consider the representative points in the Q_{tz}, Q_{lz} plane. The solutions of (6) giving the relation between Q_{tz} and Q_{lz} are represented by the curved lines passing through the checkered pattern of fig. 2. For real values of Q_x (cf. (10))

$$\alpha^2\geqslant(1+2K)/K\ \therefore\ g_K(\alpha)\geqslant 0.$$

Thus there are no solutions inside the shaded squares. The representative points are given by the intersections of these curves with the family of hyperbola (10). The total number of modes will be the number of representative points inside the figure formed by the straight lines $\alpha=0$ and $\alpha=(1+2K)^{1/2}/K^{1/2}$, and the rectangular hyperbola defined by (11) with $W=W_m$.

Proceeding as for type 2, the density of representative points can be expressed in the two forms

$$\rho_1{}^S = -\frac{L_x}{\pi}\left(\frac{\partial n_{tz}}{\partial Q_{tz}}\right)_{Q_x}\left(\frac{\partial q_x}{\partial Q_{lz}}\right)_{Q_{tz}} \quad . \quad . \quad . \quad . \quad . \quad (42)$$

or

$$\rho_2{}^S = \frac{L_x}{\pi}\left(\frac{\partial n_{lz}}{\partial Q_{lz}}\right)_{Q_x}\left(\frac{\partial q_x}{\partial Q_{tz}}\right)_{Q_{lz}} \quad . \quad . \quad . \quad . \quad . \quad . \quad (43)$$

depending on whether we project AB of fig. 1 onto the Q_{tz} or Q_{lz} axis.

Fig. 2

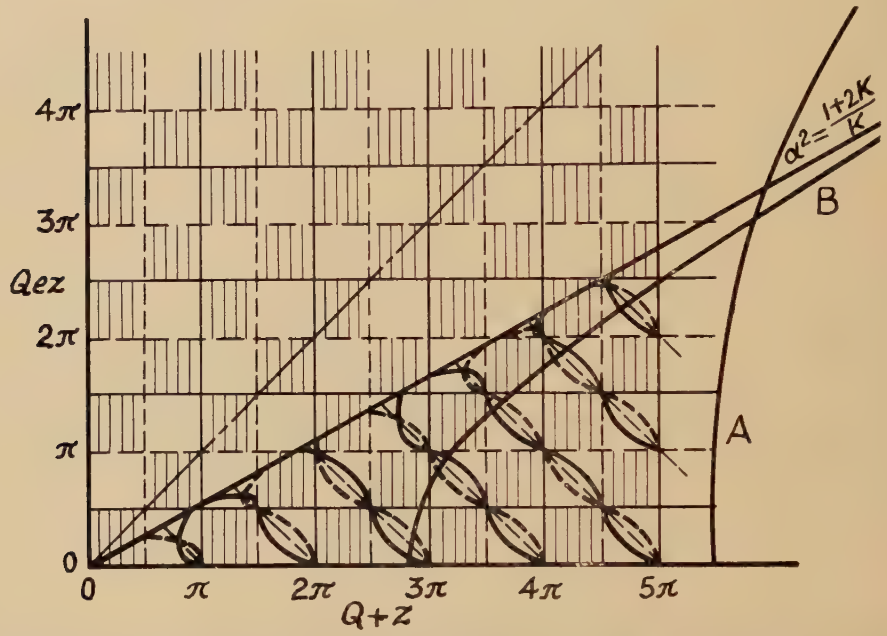

B is one of the family of hyperbola defined by (10). The curved lines passing through the blank squares of the checkered pattern represent solutions of (6) for symmetric (full lines) and (7) for antisymmetric waves (dotted lines) respectively. The intersections of B with these curves are representative points for waves of type 3. A is the bounding rectangular hyperbola given by (11) corresponding to the maximum frequency.

Considering $\rho_1{}^S$ first and substituting from (40)

$$\rho_1{}^S = \frac{A}{4\pi^2 L_z{}^2}\left(\frac{K}{1+K}\right)^{1/2}\left(\frac{1+2K}{K\alpha}\right)\left(1-\frac{1+2K}{K\alpha^2}\right)^{-1/2}\left[1+\left(\frac{\partial \delta_t{}^S}{\partial Q_{tz}}\right)_{Q_x}\right] \quad . \quad . \quad (44)$$

The derivative is not a surface term since $\delta_t{}^S$ contains tan Q_{lz}, in fact it can be expressed as

$$\left(\frac{\partial \delta_t{}^S}{\partial Q_{tz}}\right) = \frac{1}{L_z} m(\alpha)\frac{q_{tz}}{q_t^2}\sin 2Q_{tz} - \frac{q_l^2}{q_t^2}\alpha\frac{\sin 2Q_{tz}}{\sin 2Q_{lz}} \quad . \quad . \quad . \quad (45)$$

where $$m(\alpha) = \frac{1-\alpha^2}{2\alpha^2} \cdot \frac{(1+2K)^2-3\alpha^2(1+3K+2K^2)+\alpha^4 K}{(1+K)(1+2K+\alpha^2)}.$$

The former is a surface and the latter a bulk term.

Similarly, for antisymmetric vibrations

$$\rho_1{}^A = \frac{A}{4\pi^2 L_z{}^2}\left(\frac{K}{1+K}\right)^{1/2}\left(\frac{1+2K}{K\alpha}\right)\left(1-\frac{1+2K}{K\alpha^2}\right)^{-1/2}\left[1+\left(\frac{\partial\delta_t{}^A}{\partial Q_{tz}}\right)_{Q_x}\right] \quad . \quad (46)$$

where

$$\left(\frac{\partial\delta_t{}^A}{\partial Q_{tz}}\right)_{Q_x} = -\frac{1}{L_z} m(\alpha)\frac{q_{tz}}{q_t^2}\sin 2Q_{tz} - \frac{q_l^2}{q_t^2}\alpha\frac{\sin 2Q_{tz}}{\sin 2Q_{lz}}. \quad . \quad . \quad (47)$$

The surface term of the total density $\rho_1 = \rho_1{}^A + \rho_1{}^S$ thus disappears and

$$\rho_1 = \frac{A}{2\pi^2 L_z{}^2}\left(\frac{K}{1+K}\right)^{1/2}\left(\frac{1+2K}{K\alpha}\right)\left(1-\frac{1+2K}{K\alpha^2}\right)^{-1/2}\left[1-\frac{q_l^2}{q_t^2}\alpha\frac{\sin 2Q_{tz}}{\sin 2Q_{lz}}\right]. \quad (48)$$

Using the alternative definition of density (43) involving δ_l instead of δ_t gives

$$\rho_2 = \frac{A}{2\pi^2 L_z{}^2}\left(\frac{K}{1+K}\right)^{1/2}\left(1-\frac{1+2K}{K\alpha^2}\right)^{-1/2}\left(1-\frac{q_t^2}{q_l^2}\frac{1}{\alpha}\frac{\sin 2Q_{lz}}{\sin 2Q_{tz}}\right). \quad . \quad . \quad (49)$$

Although the two values of ρ are formally different, they give the same result when integrations over the Q_{tz}, Q_{lz} plane are carried out. This is due to the fact, that when integrating over one of the small squares of area $\pi^2/4$ in fig. 2 the variation of the algebraic terms is negligible compared to that of the trigonometric terms. Using (6)

$$\int_{n\pi}^{(n+1/2)\pi}\frac{\sin 2Q_{tz}}{\sin 2Q_{lz}}dQ_{lz} = -\int_{n\pi}^{(n+1/2)\pi}\frac{g\sec^2 Q_{lz}}{1+g^2\tan^2 Q_{lz}}dQ_{lz} = -\frac{\pi}{2}, \quad . \quad . \quad (50)$$

where n is half an odd or even integer. Thus the integral over the small squares is $-\pi^2/4$. The same result applies for the antisymmetric solution (7). Thus both ρ_1 and ρ_2 have the ‘ average ’ value (taken over the small squares)

$$\rho = \frac{A}{2\pi^2 L^2{}_z}\left(\frac{K}{1+2K}\right)^{1/2}\left(1-\frac{2K+1}{K\alpha^2}\right)^{-1/2}\left(1+\frac{1+2K}{K\alpha}\right). \quad . \quad . \quad (51)$$

It follows that on the average

$$\frac{\sin 2Q_{tz}}{\sin 2Q_{lz}} = -1 \therefore Q_{tz}+Q_{lz} = n\pi \quad . \quad . \quad . \quad . \quad . \quad . \quad (52)$$

where n is an integer. In fig. 2 we also exhibit the solutions of (7). The two sets of solutions may be shown to be approximately symmetrical about the lines given by (52). Now using (52) as the frequency equation would lead to a density given by (51). Thus it appears, that the independence of the density on the surface is due to the deviations from the bulk distribution, for symmetric and antisymmetric waves, being equal and in opposite directions, while those for the waves of type (2) are equal and in the same direction.

The total number of modes is thus

$$M_B(\omega_m) = \int_{\varphi_0}^{\pi/2}\int_0^{[-P_m{}^2/\cos 2\varphi]^{1/2}} \rho q\, dq\, d\phi \quad . \quad . \quad . \quad . \quad (53)$$

where $q^2 = Q_{tz}{}^2 + Q_{lz}{}^2$; $\tan\phi = \alpha$, no zero wave number correction being required. Therefore

$$M_B(\omega_m)=\frac{A}{\pi^2}\left[\pi\frac{q_{ml}^2}{4}+\frac{q_{mt}^2}{2}\tan^{-1}\left(\frac{K}{1+K}\right)^{1/2}\right] \quad . \quad . \quad . \quad (54)$$

where $q_{ml}=\omega_{m}/c_l$ is the maximum longitudinal wave number. Thus finally adding the contributions for the three types, the total number of modes

$$M(\omega_m)=A\left[\frac{q_{mt}^2}{4\pi}+\frac{q_{ml}^2}{4\pi}+\frac{q_{mt}}{\pi L_z}\{Y_0+\tfrac{1}{4}-I_2\}\right]. \quad . \quad . \quad . \quad (55)$$

Substituting the values for $K=0$, the result agrees with that in B (except for the $\frac{1}{4}$ due to the zero correction) which is obtained from types 1 and 2 alone.

Before calculating the Debye frequency and specific heat of the lattice we extend the treatment to include three-dimensional waves and recalculate M.

§ 3. THE THREE-DIMENSIONAL CASE

In the y direction we now take an additional periodic boundary condition with periodicity $2L_y$ which introduces a factor exp $(iq_y\, y)$ in the displacement, where

$$q_y=n_y\pi/L_y\,;\; n_y=\ldots -3, -2, -1, 0, 1, 2, 3; \ldots \quad . \quad . \quad . \quad (56)$$

Introducing the vector

$$\hat{\mathbf{q}}=q_x\mathbf{i}+q_y\mathbf{j}\,;\quad \hat{\mathbf{Q}}=\hat{\mathbf{q}}\,L_z \quad . \quad . \quad . \quad . \quad . \quad . \quad . \quad (57)$$

where $\mathbf{i}$, $\mathbf{j}$, and $\mathbf{k}$ are unit vectors, in the x, y, and z directions respectively, it can easily be shown that the two-dimensional motion discussed in the last section takes place in the plane defined by $\hat{\mathbf{q}}$ and $\mathbf{k}$. ($\hat{\mathbf{q}}$ replacing q_x in the various formulae.) However there is an additional type (4) consisting of purely transverse bulk waves whose displacement is perpendicular to the plane $\hat{\mathbf{q}}$, $\mathbf{k}$. (These are omitted in B.) They are again symmetrical or antisymmetrical with frequency equations given by

$$Q_{tz}=n_{tz}\pi/2\,;\quad n_{tz}=\begin{cases}1, 3, 5, \ldots \text{ symmetrical,}\\ 0, 2, 4, \ldots \text{ antisymmetrical.}\end{cases} \quad . \quad . \quad . \quad (58)$$

Replacing the parameter Q_x of the family of hyperbola (10) by $\hat{Q}$ gives the number of these for a range $d\hat{Q}$ of $\hat{Q}$ as

$$\rho(\hat{Q})\,d\hat{Q}=\frac{L_x}{\pi}\frac{L_y}{\pi}\frac{2\pi\hat{Q}}{L_z^2}\,d\hat{Q}=\frac{V}{L_z^3}\cdot\frac{\hat{Q}}{4\pi}\,d\hat{Q}. \quad . \quad . \quad . \quad . \quad (59)$$

Using this result the densities and total numbers of modes for the various types are :

(1) $M_R(\omega_m)=VY_0^2q_{mt}^2/4\pi L_z. \quad . \quad . \quad . \quad . \quad . \quad . \quad . \quad . \quad . \quad . \quad . \quad . \quad (60)$

(2) $$\rho=\frac{V}{2\pi^2L_z^2}\left(\frac{2K+1}{K+1}\right)Q'_{tz}\left[1 \quad \frac{\delta'}{Q'_{tz}}\left(1+\frac{K\alpha'^2}{1+2K}\right)\right] \quad . \quad . \quad (61)$$

$$M_M(\omega_m)=\frac{V}{\pi^2}\left[\frac{q_{mt}^3}{6}\left(\frac{1+K}{1+2K}\right)^{1/2}+\frac{q_{mt}^2\pi}{L_z}\left(\frac{1}{16}-\frac{1}{4}I_3\right)\right] \quad . \quad . \quad . \quad (62)$$

where

$$I_3(K)=\int_0^{\pi/2}\left(1+\frac{K}{1+2K}\tan^2\phi\right)\dot{\delta}'(\tan\phi)\,d\phi. \tag{63}$$

(3)

$$\rho=\frac{V}{2\pi^2L_z^{\,2}}\frac{K\alpha}{1+2K}\left(1+\frac{1+2K}{K\alpha}\right)Q_{lz} \tag{64}$$

$$M_B(\omega_m)=V\left[\frac{q_{ml}^{\,3}}{6\pi^2}-\frac{q_{mt}^{\,3}}{6\pi^2}\left\{\left(\frac{1+K}{1+2K}\right)^{1/2}-1\right\}\right] \tag{65}$$

(4)

$$\rho=4L_xL_yL_z/\pi^3=V/2\pi^3 \tag{66}$$

$$M_T(\omega_m)=V\left[\frac{q_{mt}^{\,3}}{6\pi^2}+\frac{q_{mt}^{\,2}}{16\pi L_z}\right]. \tag{67}$$

Thus summing over the four types the total number of excited modes is

$$M(\omega_m)=V\left[2\frac{q_{mt}^{\,3}}{6\pi^2}+\frac{q_{ml}^{\,3}}{6\pi^2}+\frac{q_{mt}^{\,2}}{4\pi L_z}\left(Y_0^{\,2}+\tfrac{1}{2}-I_3\right)\right]. \tag{68}$$

§ 4. THE SPECIFIC HEAT AND ENERGY SURFACE TERMS

The Debye frequency can now be determined by equating the number of degrees of freedom ($3NV$) of the lattice points to the number of excited modes $M(W_m)$, hence

$$3N=(2q_{mt}^{\,3}+q_{ml}^{\,3})/6\pi^2+q_{mt}^{\,2}(Y_0^{\,2}+\tfrac{1}{2}-I_3)/4\pi L_z. \tag{69}$$

Thus when $L_z\to\infty$; $q_{mt}, q_{ml}\to\overline{q_{mt}}, \overline{q_{ml}}$ where

$$2\overline{q_{mt}}^{\,3}+\overline{q_{ml}}^{\,3}=18\pi^2N \tag{70}$$

giving the Debye frequency and temperature ($\overline{\theta}_D$) for a large specimen,

$$\overline{\omega_m}^{\,3}=6\pi^2Nc^3 \text{ or } \overline{\theta}_D\equiv\hbar\omega_m/k=\hbar c(6\pi^2N)^{1/3}/k \tag{71}$$

where the ‘ mean velocity ’ c is defined by

$$3/c^3=2/c_t^{\,3}+1/c_l^{\,3}. \tag{72}$$

Substituting $\overline{q_{mt}}$ for q_{mt} in the surface term of (69) gives

$$\theta_D=\overline{\theta}_D[1-A(K)/N^{1/3}L_z] \tag{73}$$

where

$$A(K)=\frac{\pi(Y_0^{\,2}+\frac{1}{2}-I_3)}{2(18\pi^2)^{1/3}[2+\{K/(1+2K)\}^{3/2}]^{2/3}}.$$

To calculate the intrinsic energy E of the vibrations we take (68) as a general formula for excited modes whose frequency lies between 0 and ω. The number of modes whose frequency lies in the range w, $w+dw$ is $(dM/dw)dw$. It is however, simpler to consider ϵ as a function of $q_t(=\omega/c_t)$. Thus

$$E=\int_0^{q_{mt}}\epsilon(q_t)\frac{dM}{dq_t}\,dq_t \text{ where } \epsilon(q_t)=\frac{\hbar q_tc_t}{\exp(\hbar q_tc_t/kT)-1}. \tag{74}$$

Evaluating this integral with the usual new variable

$$u=\hbar q_tc_t/kT;\quad x=\hbar q_{mt}c_t/kT=\overline{\theta}_D/T \tag{75}$$

and substituting from (73) for the upper limit

$$E=V\frac{qNkT}{x^3}\int_0^x\frac{x^3}{e^x-1}\,dx+\frac{V}{L_z}\frac{qN^{2/3}kT}{x^4}A(K)\left[2\int_0^x\frac{u^2du}{e^u-1}-\frac{x^3}{e^x-1}\right]. \qquad (76)$$

The first term represents Debye's result while the second differs from that given in B only in the constant $A(K)$.

We have evaluated the various constants for three values of K. The results are collected in table 1, where the corresponding Poisson's ratio (σ) is also shown.

Table 1

K	σ	I_3	α_0	Y_0^2	$(Y_0^2+\frac{1}{2}-I_3)$	A
0	$\frac{1}{2}$	1·35	0·2956	1·095	0·245	0·044
1	$\frac{1}{4}$	0·836	0·4641	1·18	0·84	0·14
∞	0	0·588	0·6181	1·31	1·22	0·19

The single value of the constant $A(K)$ given in B is $\approx 0{\cdot}24$ which is about five times as large as the corresponding correct value $A(0)\approx 0{\cdot}044$. However if we use elastic constants corresponding to $K=1$, the results in B will only have to be scaled down by a factor of about 0·6.

From (76) we can obtain the surface free energy F_S of the lattice vibrations

$$F_S=E-T\int_0^T\frac{1}{T}\left(\frac{dE}{dT}\right)dT=-9A(K)k\theta_D N^{2/3}Z(x) \quad . \quad . \quad (77)$$

where

$$Z(x)=\frac{1}{x^3}\int_0^x\frac{u^2du}{e^u-1}. \quad . \quad . \quad . \quad . \quad . \quad . \quad . \quad . \quad (78)$$

This result, with the constant as given in B, is used by Huang and Wyllie (1949) in their paper on the surface energy of a metal for the temperature dependent energy contribution of the lattice.

Finally the specific heat can be written in the form

$$C_v=\overline{C}_v[1+A(K)\nu(x)/N^{1/3}L_z] \quad . \quad . \quad . \quad . \quad . \quad (79)$$

where

$$\nu(x)=\frac{6xZ(x)-[2x(e^x-1)+x^2e^x]/[e^x-1]^2}{\frac{4}{x^3}\int_0^x\frac{u^3}{e^u-1}du-\frac{x}{e^x-1}}$$

and $\overline{C}_v$ is the Debye specific heat. An extensive discussion of this result is given in B where curves are drawn to show the variation of C_v with temperature. These must be corrected by the scaling factor $A(K)/0{\cdot}24$.

§ 5. CONCLUDING REMARKS

It is interesting to observe that the reason why our results are in formal agreement with those of previous calculations is that the number of modes $M(W_m)$ has a surface term proportional to q_{mt}^2 (or q_{ml}^2) as for example in (68). It seems unlikely that more elaborate boundary conditions would alter this situation. Their only effect would be to modify the constant $A(K)$.

If we consider a cubic lattice then $q_m \approx 4/a$ where a is the lattice spacing (taking $c_t = c_l$). Thus the condition that the total energy of the specimen can be split into a bulk and a surface term, i.e. $q_m L_z \gg 1$ is equivalent to one of the conditions for replacing the lattice by a continuous medium, viz. $a \ll L_z$. Thus if the Debye theory is applicable to a large specimen of a material then the above calculation will give surface terms for smaller specimens to the same degree of applicability.

The only experimental evidence having a bearing on this work is the difference in the specific heat of activated charcoal and graphite observed by Simion and Swain (1935). This is attributed to the greater specific surface of the former. In B the specific surface of the activated charcoal is estimated to be about 500–800 m²/g. This area will be slightly increased when our values for $A(K)$ are taken which does not affect the interpretation of the result.

ACKNOWLEDGMENTS

The author would like to take this opportunity of thanking Professor L. Rosenfeld for the interest he has taken in the work at all stages. It was done during the tenure of a grant from the Department of Scientific and Industrial Research.

APPENDIX

We briefly show how far the extension from two to three dimensions carried out in B is not quite correct. Since the authors use a different representation of the modes of vibration we first repeat our own calculation in their representation for the special case $K=0$ treated by them.

In B, representative points are considered in the q_x, q_y, q_z space instead of the Q_{tz}, Q'_{lz} plane for the case $K=0$ when $q'_{lz} = q_x$. This would be inconvenient for other values of K.

Thus

$$q_x = n_x \pi / L_x \,;\; q_y = n_y \pi / L_y \text{ and } q_{tz} = n_{tz} \pi / 2L_z + \delta / L_z \qquad (80)$$

where $\tan \delta = \psi(\alpha')$; $0 < \delta < \pi/2$ giving the density

$$\rho = \frac{V}{4\pi^2}\left(1 - \frac{\delta'(\alpha')}{\hat{q} L_z}\right) \qquad (81)$$

considering symmetrical and antisymmetrical waves together.

Introducing polar co-ordinates with $0q_{tz}$ as axis (q_t, θ, ψ)

$$\tan\theta = q_y/q_x \,;\; \tan\psi = 1/\alpha' = 1/\tan\phi . \qquad (82)$$

$$M_M(\omega_m) = \frac{V}{4\pi^2}\int_0^{\pi/2}\int_0^{2\pi}\int_0^{q_{mt}}\left(1 - \frac{\delta'(\tan\phi)}{q_t L_z \cos\phi}\right) q_t^2 \cos\phi \, d\phi \, d\theta \, dq_t \qquad (83)$$

$$= V\left[\frac{q_{mt}^3}{6\pi^2} - \frac{q_{mt}^2}{4\pi L_z} I_3(0)\right] \qquad (84)$$

which agrees with (62) ($K=0$) after adding the Z_0 correction, In B, the extension to the three-dimensional case is carried out by adding a factor $\exp(iq_y y)$ to the displacement function for the x, z plane. Thus α' is not taken as the tangent of the angle between q_{tz} and $\hat{q}(=q'_{tz})$ but of the angle between q_{tz} and q_x. The authors then take polar co-ordinates q'_t, θ', ϕ' with $0q_y$ as axis

$$\cos\theta' = q_y/q_t, \ \tan\phi' = q_{tz}/q_x. \qquad \ldots\ldots \quad (85)$$

This gives the wrong result

$$\overline{M}_M(\omega_m) = \frac{V}{4\pi^3}\int_0^{\pi/2}\int_0^{2\pi}\int_0^{q_{mt}}\left(1-\frac{\delta'(\tan\phi')}{q_t\cos\phi' L_z}\right)q_t^2\sin\theta'\,d\theta'\,d\phi'\,dq_t$$

$$\overline{M}_M(\omega_m) = V\left[\frac{q_{mt}^{\ 3}}{6\pi^2}-\frac{q_{mt}^{\ 2}}{2\pi^2 L_z}I_2(0)\right] \qquad \ldots\ldots \quad (86)$$

which agrees with their eqn. (29)

$$M(r) \approx \frac{\pi r^3}{6}\eta - \frac{r^2}{4}$$

when account is taken of their notation

$$r \equiv (q_{mt}/\pi)(\nu/\eta)^{1/3} \ \text{and} \ \eta = L_z/L_x.$$

REFERENCES

BRAGER, A., and SCHUCHOWITZKY, A., 1946, *Acta Phys. Chim.*, **21**, 1001.
DEBYE, P., 1912, *Ann. d. Physik*, **39**, 789.
HUANG, K., and WYLLIE, G., 1949, *Proc. Phys. Soc.*, **62**, 180.
LAMB, H., 1917, *Proc. Roy. Soc.* A, **93**, 114.
SIMION, F., and SWAIN, R. C., 1935, *Z. Physik. Chem.*, B **28**, 189.

LVI. *On the Existence of Multiple Resonances in the* ^{63}Cu(γ, n)^{62}Cu *Reaction*

By K. Phillips
Research Department, Metropolitan-Vickers Electrical Co. Ltd., Trafford Park, Manchester*

[Received February 5, 1953]

Summary

By the accurate control of the energy of a 20 mev betatron it has been shown that the activation-energy curve consists of a series of small plateaux indicating the existence of narrow resonances for the photo-neutron reaction in copper.

§ 1. Introduction

In recent years numerous publications, e.g. McElhinney *et al.* (1949), Johns *et al.* (1950) have appeared describing work carried out on photo-nuclear reactions. The usual technique involved in these experiments consists of exposing a suitable foil to the high energy bremsstrahlung from a betatron or other suitable electron accelerator. Many of the nuclei produced in these reactions are radioactive. This activity serves as a measure of the photo-neutron yield and by varying the peak energy of the incident photons an activation curve can be deduced.

By making certain assumptions about the tip of the bremsstrahlung spectrum a rough estimation of the (γ, n) cross section can be made. Previous authors, however, seem to have been content to vary the peak energy of the accelerated electrons by intervals of the order of 0·25 mev. This only indicates the general shape of the excitation curve (see fig. 1) and does not bring out any fine structure which may exist.

This report describes an experiment in which the peak energy of a 20 mev betatron has been varied by 0·02 mev intervals. The ^{63}Cu(γ, n)^{62}Cu reaction has been taken as the subject of investigation firstly because ^{62}Cu has a reasonable half life (approximately 10 minutes) and secondly as this reaction has been investigated so many times previously it has become to be almost a standard reference cross section.

§ 2. Control of the Betatron Energy

The kinetic energy of the accelerated electron in a betatron is determined by the magnetic field at the orbit and the radius of the orbit. The peak x-ray energy is then dependent on the excitation current which passes through the magnet coils, that is provided the expansion of the electron orbit takes place at maximum magnetic field. The magnet current can be controlled manually within a few per cent by means of a buck-boost circuit. A finer control of the energy can be further achieved by expanding the orbit at a fixed value of magnetic field. This has been accomplished by using a current transformer connected in series with the magnet. This transformer provides a voltage, proportional to the magnet current, which is fed to a multiar circuit which produces a square pulse having a front of extremely short duration. The multiar was developed by Williams and Moody (1946) for use as an accurate range marking device in radar. The circuit is simply dependent on the conduction of a diode which only occurs when the voltage of the controlling sine wave has achieved a predetermined value fixed by a stabilized voltage, fig. 2. The voltage can be precisely adjusted by the variation of an accurate potentiometer (nominally 100 kΩ) and by this means it can be seen that the multiar pulse can be made to move up or down the sine wave. Furthermore, provided the current transformer has a zero phase shift the multiar triggering position is independent of the magnet excitation. The square multiar pulse is fed into a pulse shaping circuit which produces a standard trigger voltage. This in turn fires the hydrogen thyratron on the expander modulator, and also operates a megavoltmeter similar to the one described by

---

*Communicated by the Author.

Fig. 1

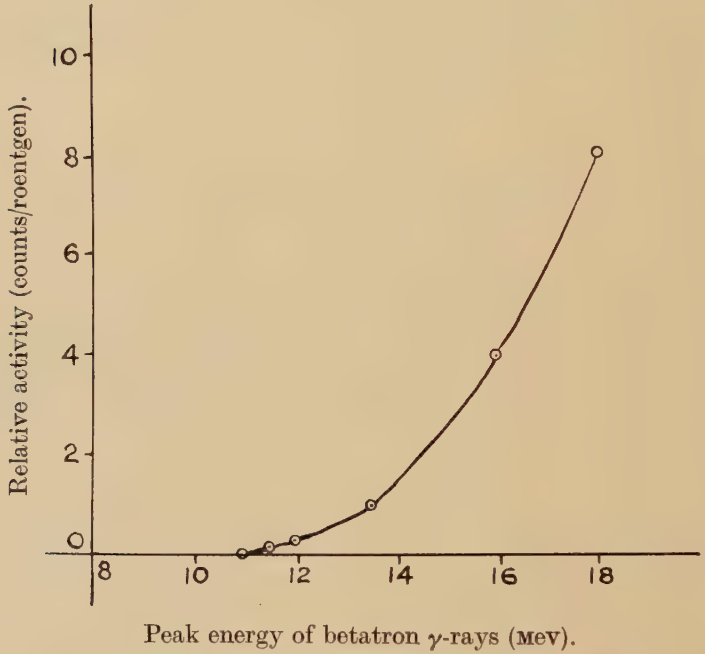

Peak energy of betatron γ-rays (MeV).

A typical activity curve for the $^{63}Cu(\gamma, n)^{62}Cu$ reaction.

Westendorp (1946). The megavoltmeter integrates with time the voltage induced in a loop around the betatron pole pieces, between the limits imposed by the times of injection and expansion. This integration produces a voltage proportional to the product of the field and the orbit radius, i.e. the peak x-ray energy, giving an indication of the electron energy with an accuracy of approximately ±0·20 Mev. Additional checks on this energy were provided by the monitoring C.R.O. and also by measuring the d.c. stabilized voltage fed to the multiar circuit. The methods of energy determination although helpful in carrying out the experiment cannot be expected to give an accuracy of the energy value better than ±1% and have not been relied upon in the present work.

Fig. 2

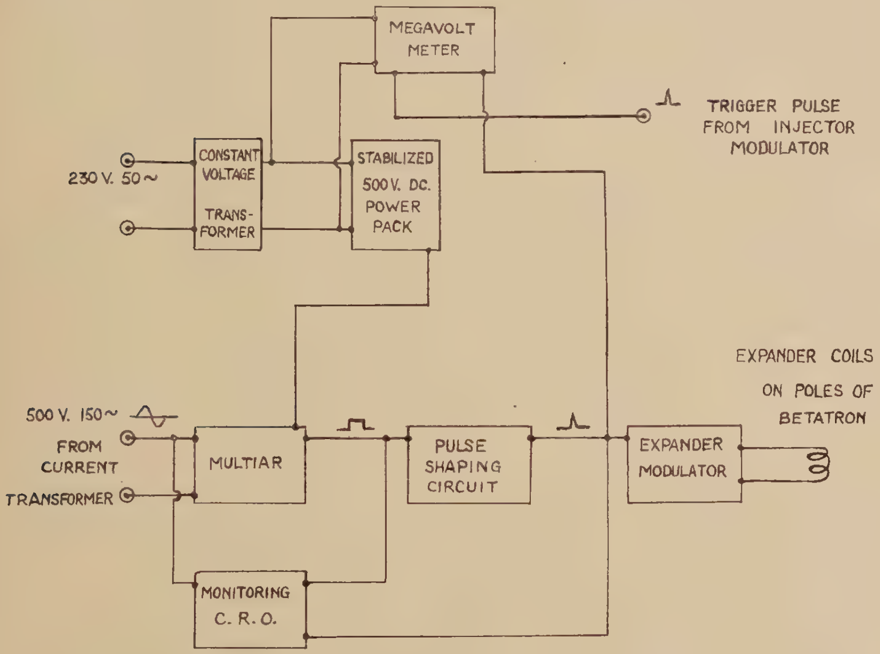
MEGAVOLT METER
TRIGGER PULSE FROM INJECTOR MODULATOR
230 V. 50~
CONSTANT VOLTAGE TRANS-FORMER
STABILIZED 500 V. DC. POWER PACK
EXPANDER COILS ON POLES OF BETATRON
500 V. 150~
FROM CURRENT TRANSFORMER
MULTIAR
PULSE SHAPING CIRCUIT
EXPANDER MODULATOR
MONITORING C. R. O.

A block diagram of the energy control circuit.

§ 3. Discussion of the Accuracy of the Method

As already stated the only two factors governing the control of the firing of the multiar are :

1. The time of firing of the diode in the multiar circuit which is controlled by the d.c. reference voltage.
2. The phase shift in the current transformer.

An attempt to control the first factor was made by using a stabilized power pack which employs the usual series tetrode method providing a stability of 1 part in 5000 at 500 volts output for a wide range of input mains voltage. A further improvement was obtained by the use of a constant voltage transformer; all the electronic circuits obtained their 50 cycles supplies from this transformer.

The phase-shift of the current transformer was made small by careful design, but the first attempt turned out to be somewhat of a failure. The phase shift-excitation characteristic was measured carefully and indicated a phase shift of two degrees at 60 amp falling gradually by a total of 30 minutes at 120 amp. This phase variation of half a minute per amp was good enough for relative energy measurements and many of the preliminary energy checks were carried out using this transformer and keeping the magnet excitation current constant to within a few amp by manual control. The second and more successful transformer, now in use, was constructed of mu-metal laminations and gave a total phase shift of 15 minutes over the same current range and with a correspondingly smaller relative change.

Another factor which may cause variation in the electron energy is the delay between the firing of the diode in the multiar and the triggering of the expander. This time delay has been accurately measured and accounts for a possible increase of 0·01 MeV in the final energy. This error does not affect relative measurements in energy but only absolute values which can be suitably corrected. Summing up, it has been estimated that the relative energy values can be held to within ±0·02 MeV.

§ 4. Experimental Details and Results

The layout of the experiment is shown in fig. 3. The foils made of 1 in. square × 0·060 in. thick spectroscopically pure copper were exposed at a distance of 30 cm from the x-ray targets. The foil itself was fastened by adhesive tape on to a bakelite jig thus enabling similar foils to be placed in an identical position. Some previous workers have tended to place the foils as close to the target as possible. This reduces the exposure required for a given count, but it places a severe restriction on the position of the foils owing to the small size of the x-ray beam, and any variations in foil position would be likely to cause errors.

The foils were exposed for several minutes and the integrated x-ray intensity was measured by means of two 25R Victrometer thimbles placed in a 6-in. diameter polystyrene cylinder placed at 75 cm from the target. Two thimbles were used in an attempt to avoid any errors in measurement and if the ratio of the readings of the two thimbles was not within 2% of the mean value of the x-ray dose the exposure was repeated. Several runs were carried out at each energy point in order to obtain consistent results. The betatron energy was varied by steps of 0·02 MeV.

The activity of the exposed foils was measured by means of an end-window Geiger counter and the usual electronic scalar. The exposure times were controlled so that the numbers of counts were greater than several thousand per ten minute period, thus reducing the probable error to less than 1%. The counter equipment was housed in an area well away from the betatron enclosure, enabling counting to be done while other exposures were being carried out. This procedure was necessary in order to reduce the time of the experiment as several thousand separate exposures had to be made. The plot of foil activity per Roentgen is shown in fig. 4. It can be seen that the excitation curve is of the same general shape as fig. 1 but it actually consists of a series of sharp rises and horizontal plateaux indicating the presence of multiple resonances.* The width of the observed plateaux decreases from approximately 0·4 MeV at an excitation of 14 MeV to about 0·08 at

Fig. 3

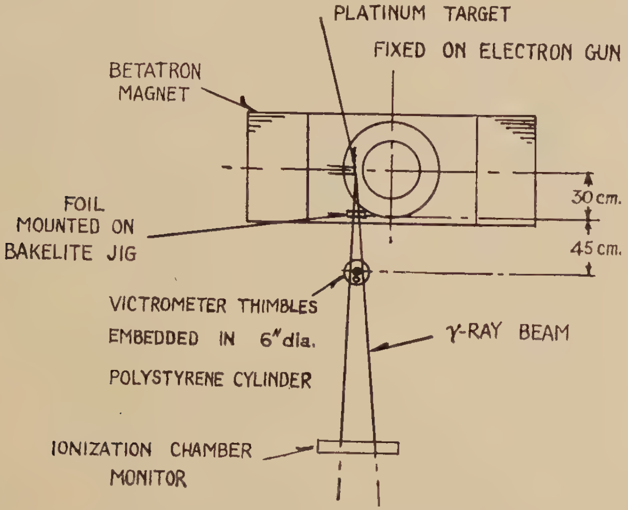

A schematic diagram of experimental arrangement showing the location of the copper foil and the Victrometer thimbles.

Fig. 4

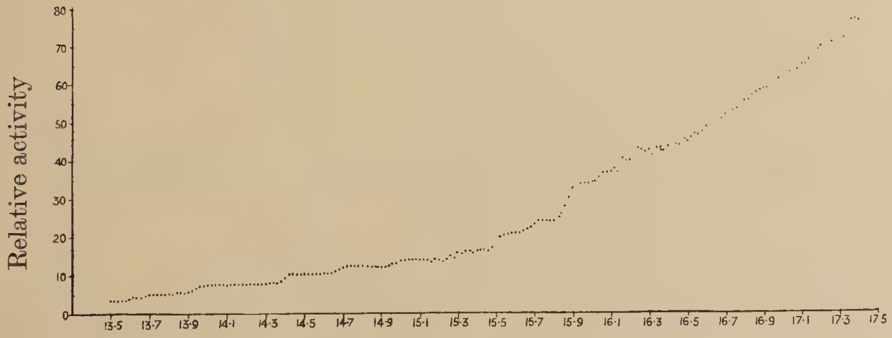

Maximum γ-ray energy (MeV).

The activation curve for the energy range of 13·5 to 17·5 MeV.

---

* A similar effect had been reported recently by Goward and Wilkins (1952) in their studies of the ^{12}C(γ, 3α) reaction in photographic emulsions. The resonances are much broader as would be expected for a lighter element.

16 MeV. There are most likely additional resonances in the higher energy region which cannot be resolved by this method. Above 16 MeV the data hardly warrants drawing a curve but there is some indication that other small steps exist. At the lower end of the curve the statistical inaccuracies increase because of the lower cross section and the corresponding lower betatron yield (the Roentgen output drops by a factor of about 10 when the peak energy is reduced from 20 to 10 MeV). For these reasons the steps become indistinct near to the threshold of the reaction. The energy scale in fig. 4 was deduced by the calibration of the multiar potentiometer against the ^{63}Cu(γ, n)^{62}Cu threshold at 10·9 MeV. It must be borne in mind that this threshold is not known to better than ±0·2 MeV and consequently the energy scale may be in error by as much as ±0·25 MeV.

§ 5. THEORETICAL CONSIDERATIONS AND DISCUSSION OF THE RESULTS

In the experiment described in the previous sections the activity of the copper sample is given as a function of the peak energy of the bremsstrahlung, or the energy of the electrons accelerated in the betatron. In order to interpret fully the shape of these curves it is obviously necessary to know the number of quanta produced in the forward direction. This energy distribution has been deduced by Schiff (1946) from the theoretical work of Heitler (1944). The experimental spectrum has been determined by several workers, see Koch and Carter (1950) and in particular by Phillips (1952) for the betatron used in this experiment. The results in the main correspond to the theoretical results but they suffer from poor statistics at the higher energy end and do not indicate the shape of the curve in that region.

No work seems to have been reported on measurement for the higher energy end of a spectrum in the region of 20 MeV, but Miller and Waldman* (1949) describe the result of the investigation of bremsstrahlung by means of activity measurements on the nuclear isomerism of Indium for the energy range 1·0 to 2·6 MeV. Furthermore the theoretical results are only approximate at the high energy and since the calculations are based on Born's approximation, which requires that $2\pi(Ze^2/hv) \ll 1$ and $2\pi(Ze^2/hv_0) \ll 1$, where Z is the nuclear charge of the x-ray target, e is the electronic charge, v_0 and v are the velocities of the electron before and after the creation of the radiation. It can be seen that even for high energy electrons and elements of high atomic number this condition does not hold, e.g. for platinum $Ze^2/\hbar c = 0{\cdot}54$. (A theory of high-energy bremsstrahlung has been produced by Bess (1950) which avoids any approximations. Unfortunately only one point on the curve is given and the numerical calculations involved are rather intractable.) These approximate results show that the number of quanta falls to zero at the high energy limit. The more exact theory of

---

* I am indebted to Dr. Jennings of University College, London, for bringing this work to my notice.

Sommerfeld and Maue (1935) shows that for non-relativistic energies this is not the case and the number of quanta is finite. Guth (1941) has argued quantitatively that this exact non-relativistic formula may be obtained from the results given by Born's approximation by multiplying them by a function $f(Z, v, v_0)$. On these grounds it seems reasonable to use a similar function to convert Heitler's results into a formula which will provide a good approximation to the actual values. For interpretation of the experimental results it is advisable to introduce the conception of an isochromat. This is defined as the intensity of a narrow band of x-rays of a given energy $h\nu_T$ as a function of the peak x-ray energy (electron energy). The isochromat for the Heitler theory turns out to be a curve steadily increasing with energy as shown in fig. 5 (*a*), whilst the corrected energy distribution has the form of a unit function as in fig. 5 (*b*), i.e. the isochromat is independent of energy.

Fig. 5

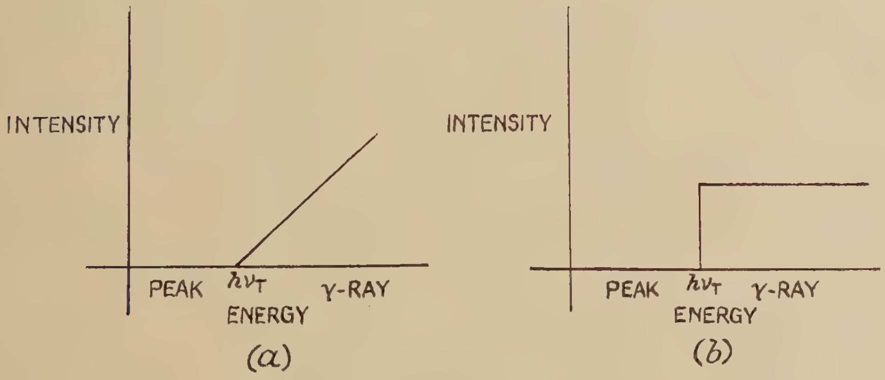

(*a*) The isochromat deduced from the Heitler calculation using Born's approximation. (*b*) The isochromat deduced from the more exact non-relativistic Sommerfeld theory of bremsstrahlung.

From the shape of these isochromats it is easy to show that for a steadily increasing isochromat one would expect an activity function consisting of a series of sloping lines with discontinuities at the various energy levels, see fig. 6 (*a*). For a step like isochromat an excitation curve having a series of sharp rises and plateaux would be expected, fig. 6 (*b*). A slight slope of the front edge would occur owing to the energy spread of the accelerated electrons. The third curve, fig. 6 (*c*), indicates the activity function for thick target radiation. This can be understood by assuming that the thick target isochromat is the sum of a series of thin target isochromats thus producing a sloping activity curve with discontinuities at the different energy levels.

Summing up it may be said that this work indicates :

1. That narrow resonances exist in the ^{63}Cu(γ, n)^{62}Cu reaction and that the cross section therefore should be deduced on the basis of energy

levels in the compound nucleus. This does not eliminate the possibility of a photo-electric effect and it may be concluded that the resulting cross section is due to a series of narrow resonances superimposed on a continuous background.

2. The high energy bremsstrahlung spectrum is of the thin target type, thus confirming previous spectrum measurements.

Fig. 6

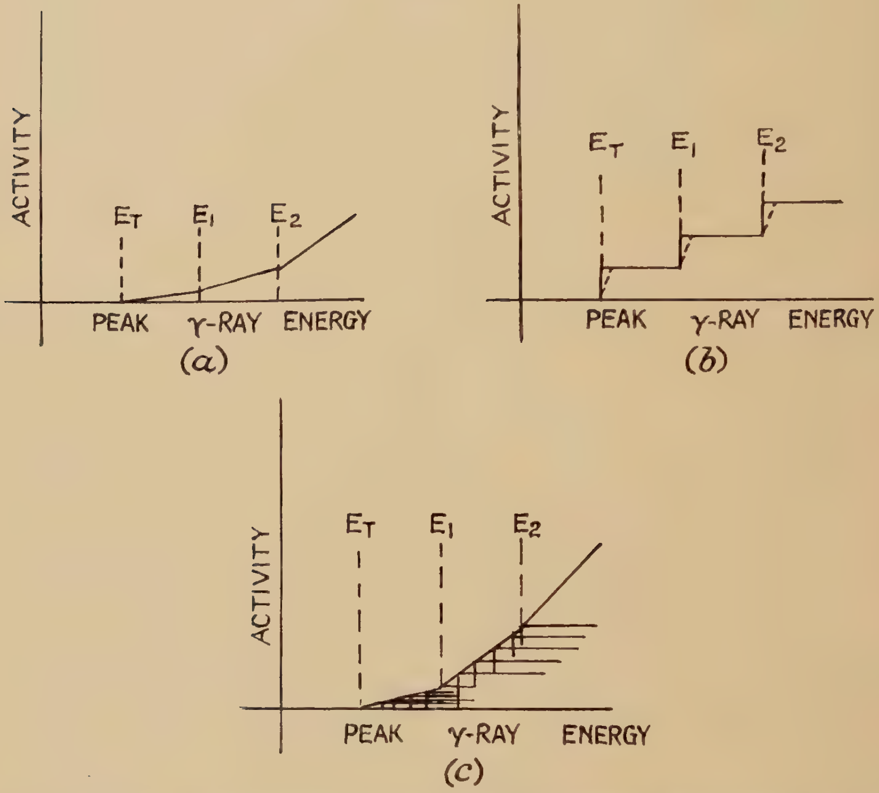

(*a*) The activity curve deduced from a steadily increasing isochromat. (*b*) The activity curve for the case of a step isochromat. Both (*a*) and (*b*) are for thin target radiation. (*c*) The activity curve for a thick target radiation for small thin target steps.

3. The theoretical bremsstrahlung curve of Heitler's is unsatisfactory at the high energy limit owing to the use of the Born approximation, and furthermore the isochromat has the form of a step function. It is worth while noting from fig. 4 that the front of the step is not a sharp discontinuity at each level. As already mentioned this might be caused to a certain extent by the energy spread of the accelerated electrons. From the curve the average energy variation over the rapid rise is approximately ±0·04 Mev —slightly larger than the previously estimated energy spread of ±0·02 Mev.

ACKNOWLEDGMENTS

The author wishes to acknowledge the assistance given to him by all the members of the betatron team and also Mr. F. Harlen for his stimulating discussions on the accuracy of the Victrometer measurements. He also wishes to thank Mr. F. R. Perry for his encouragement and advice, and Dr. Dannatt, Director of Research, and Mr. B. G. Churcher, Manager of Research Department, Metropolitan-Vickers Electrical Co. Ltd. for permission to publish this work.

REFERENCES

BESS, L., 1950, *Phys. Rev.*, **77,** 550.
GOWARD, F. K., and WILKINS, J. J., 1952, *Proc. Phys. Soc.* A, **65,** 671.
GUTH, E., 1941, *Phys. Rev.*, **59,** 325.
HEITLER, W., 1944, *The Quantum Theory of Radiation* (Oxford : Clarendon Press).
JOHNS, H. E., KATZ, L., DOUGLAS, R. A., and HASLAM, R. N. H., 1950, *Phys. Rev.*, **80,** 1062.
KOCH, H. W., and CARTER, R. E., 1950, *Phys. Rev.*, **77,** 165.
MCELHINNEY, J., HANSON, A. O., BECKER, R. A., DUFFIELD, R. B., and DIVEN, B. C., 1949, *Phys. Rev.*, **75,** 542.
MILLER, W. C., and WALDMANN, B., 1949, *Phys. Rev.*, **75,** 425.
PHILLIPS, K., 1952, *Proc. Phys. Soc.* A, **65,** 57.
SCHIFF, L. I., 1946, *Phys. Rev.*, **70,** 87.
SOMMERFELD, A., and MAUE, A. W., 1935, *Ann. d Physik*, **23,** 589.
WESTENDORP, W. F., 1946, *Rev. Sci. Instrum.*, **17,** 215.
WILLIAMS, F. C., and MOODY, N. F., 1946, *J. Instn., Elect. Engrs.*, **93,** IIIA, 1188.

LVII. *Isotopic Spin Selection Rules—I: Radiations from* ^{16}O

By D. H. WILKINSON and G. A. JONES
Cavendish Laboratory, Cambridge*

[Received February 2, 1953]

§ 1. INTRODUCTION

IT is rapidly becoming clear that there exists a very large measure of charge-independence in the interactions between nucleons. This realization has given rise to a revival of interest in the isotopic spin formalism with its provision of another significant parameter for the description of nuclear states. Adair (1952) and Kroll and Foldy (1952) have discussed the effect of conservation of isotopic spin and charge parity in heavy particle reactions; Trainor (1952) has pointed out the existence of isotopic spin rules in the emission of electric dipole radiation and Radicati (1952) has shown that, for any multiple whether electric or magnetic, the rigid selection rule $\Delta T=0, \pm 1$ obtains, with the limitation that for electric dipole transitions in self-conjugate nuclei the selection rule is $\Delta T=\pm 1$. Even if the specifically nuclear interaction between nucleons is charge-independent, complete charge-independence cannot obtain because of the existence of Coulomb forces; we must therefore expect that the isotopic spin is not a good quantum number and that, for example, there will be a mixing of a small amount of a wave-function belonging to a state of $T=1$ in a state that is principally of $T=0$. This will effect a partial relaxation of the isotopic spin selection rules; if they are obeyed as well as may be expected, having regard to the Coulomb perturbation, the hypothesis of charge-independence of the specifically nuclear forces is strengthened, if they appear to be poor rules charge-independence must be only approximate. Alternatively, if we can obtain some independent assurance as to the validity of charge-independence such as may derive from nucleon and meson scattering experiments, violations of the isotopic spin selection rules will afford quantitative information about the properties of groups of nuclear levels which are not directly investigated. Radicati (1953) has investigated theoretically the mixing of isotopic spin states by Coulomb forces in the ground states of certain nuclei (with two and four nucleons outside a closed shell), and finds that, in his examples, we may expect to find mixed with the principal wave-function appropriate to $T=0$ a few tenths of a per cent to a few per cent (in amplitude) of a wave-function appropriate to $T=1$. This means that, under complete specifically nuclear charge-independence, we should find that transitions that are allowed by ordinary spin and parity rules but forbidden by isotopic spin rules occur about 10^3 to 10^4 times less readily than those allowed by isotopic spin rules as well.*

---

* Communicated by the Authors.

This paper reports experiments that place rather crude upper and lower limits to the validity of the isotopic spin rules ; these limits are in agreement with the above-mentioned work of Radicati.

Fig. 1

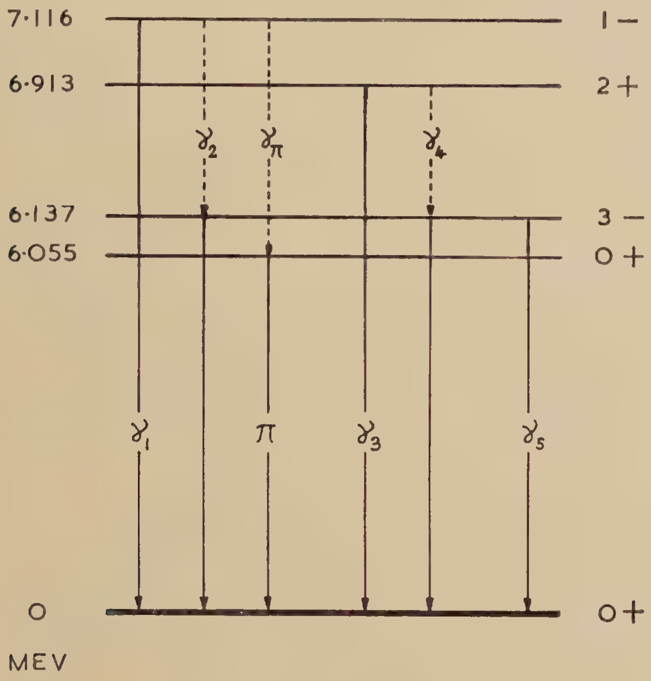

Low-lying levels of ^{16}O. The full arrows indicate known transitions, the dashed arrows those sought in the present investigation.

§ 2. THE LOW-LYING STATES OF ^{16}O

The present investigation concerns itself with the rule that a transition with $\Delta T=0$ is forbidden for electric dipole radiation in a self-conjugate nucleus ; ^{16}O appears to provide examples both of the operation and violation of this rule and so enables us to set rough limits to its validity.

We consider the lowest states of ^{16}O ; these are shown with their relevant characteristics in fig. 1. The energies are taken from Ajzenberg and Lauritsen (1952) ; the spin and parity of the first excited state are due to work by Rasmussen, Hornyak, Lauritsen and Lauritsen (1950), Devons and Lindsey (1949), and Devons, Hereward and Lindsey (1949); those of the (3−) state to Arnold (1950) and Barnes, French and Devons (1950); those of the remaining two excited states to Seed and French (1952), Sanders (1952) and Fagg and Hanna (1952). The known modes of de-excitation are shown by the full arrows; the hypothetical modes of interest in the present investigation are shown by the dashed arrows. Now ^{16}O is a very strongly-bound nucleus and the ground states of its neighbours ^{16}N and ^{16}F (the latter unstable to break-up into ^{15}O and a proton) occur, after allowance for the Coulomb energies and n–p mass difference, 12·8 MEV above that of ^{16}O (Lauritsen 1952, Ajzenberg and Lauritsen 1952). It is therefore certain that all five states of ^{16}O shown in fig. 1 have $T=0$; if we think in terms of charge-symmetry alone, the charge parity of all these states is almost certainly even.

---

* The mixing of isotopic spin states will depend on the proximity of the 'contaminating' states to that in question and so, presumably, be least for the ground states ; the rules, therefore, should become apparently less strict for transitions involving highly-excited states.

It is apparent that γ_1, which must be electric dipole, violates the isotopic spin rule.* If this rule were strict the (1−) level would de-excite by means of the cascade starting with the electric quadrupole γ_2; we have sought γ_2, as will be described later, but have not found it. The (2+) level emits the electric quadrupole γ_3 although we should expect the cascade starting with the electric dipole γ_4 to compete favourably with it; we have sought γ_4 without success and its absence may be an illustration of the isotopic spin rule in action. The quantitative implications of these observations will be discussed after the account of the measurements.

§ 3. THE POPULATION OF THE INITIAL STATES

In order to search for γ_2 and γ_4 we must be able to prepare ^{16}O in the (1−) and (2+) states. The most convenient method is to bombard fluorine with protons when the reaction ^{19}F(pα)^{16}O takes place. This reaction is strongly resonant below 1 MEV of proton energy and by choosing the appropriate resonance we may vary the population of the states shown in fig. 1. Unfortunately, all resonances below 1 MEV that populate the (1−) and (2+) states favour the (3−) state, which merely provides the useless γ_5 as background. We have used the resonances at 874 kev and 935 kev proton energy; the former populates the levels (1−), (2+) and (3−) in the ratios 7 : 19 : 74 while the latter gives the ratios 22 : 3 : 75. (Chao, Tollestrup, Fowler and Lauritsen 1950, Seed and French 1952.)

§ 4. THE MEASUREMENTS

We have examined the gamma-rays directly using NaI(Tl) crystals; the whole gamma-ray spectrum was examined to begin with to make sure that no medium-energy gamma-rays comparable in intensity with γ_1, γ_3 and γ_5 existed. We then examined the low-energy region of the spectrum with some care using a kick-sorter of the type described by Hutchinson and Scarrott (1951). Several examinations were made with good statistics, achieving the order of 100,000 pulses per channel in each one. Each examination was split into many runs, between which irradiations with ^{137}Cs gamma-rays enabled a check to be kept on the overall stability of the system. We have found it best to display graphically not the actual counts per channel, since the very small statistical errors do not permit

---

* This has also been pointed out, in conversation, by Professor W. E. Burcham.

Fig. 2

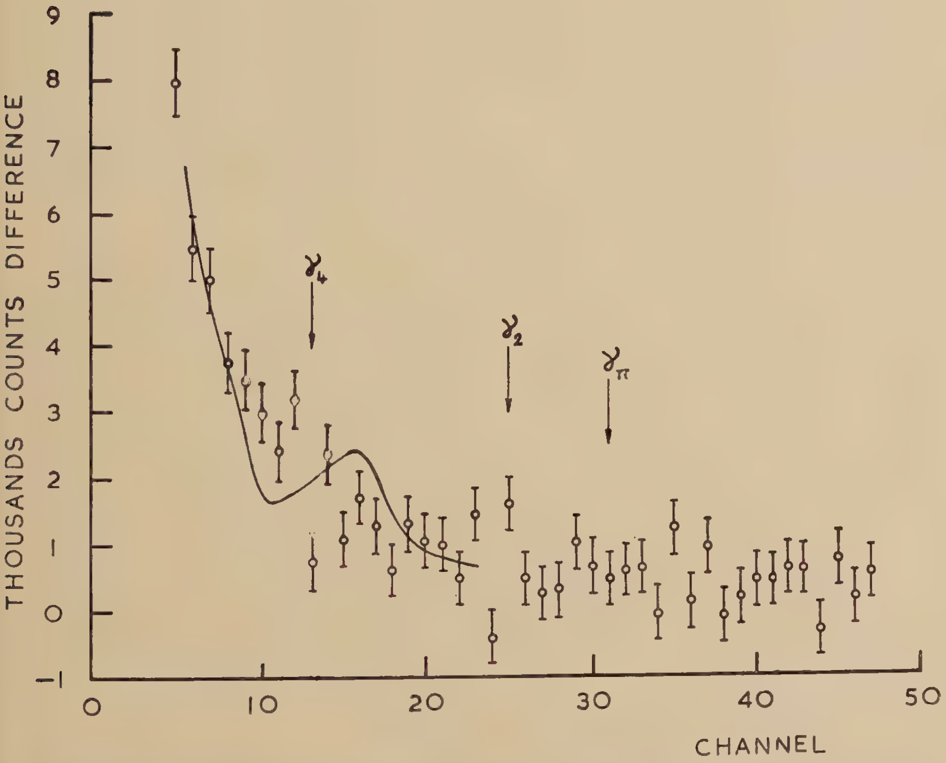

Differential distribution of NaI(Tl) crystal pulses in successive channels at proton bombarding energy of 874 kev (thin target). The arrows indicate the expected positions of the various low energy gamma-rays (see fig. 1). The full line shows the expected differential distribution due to a branching ratio of 5×10^{-3} : 1 for γ_4 relative to γ_3. The error limits represent standard deviations.

of any easy demonstration of the sensitivity of the method, but rather the differences between actual recorded counts in successive channels ; this gives a differential distribution. Figure 2 shows such a differential distribution for a single examination of the spectrum at the 874 kev resonance, using a thin target and the detector at 90° to the proton beam.* The arrows indicate the positions at which the various low-energy gamma-rays of fig. 1 are expected to occur and it is obvious that none is present in excess of the statistical fluctuations. As an illustration of the sensitivity of the method we have indicated by the full line the differential distribution to be expected if the branching ratio of γ_4 relative to γ_3 were $5\times10^{-3}:1$. Other examinations were consistent with this conclusion that γ_3 is at least 200 times stronger than γ_4. The branching from the (1−) level is best sought by bombardment at 935 kev; the results were similar to those of fig. 2 and suggested that the branching ratio of γ_2 relative to γ_1 is less than $8\times10^{-3}:1$. γ_π which might lead from the (1−) to the pair-emitting (0+) level is not found. The experimental branching ratio is less than $10^{-2}:1$; the ratio expected from the ratio of the energies of γ_1 and γ_π is about $3\times10^{-3}:1$ so the absence of γ_π is not noteworthy. The present method is not the best available for seeking γ_π, and we hope to make it the object of a separate investigation.

---

* It is very unlikely that strong angular distributions obtain at either resonance ; those for the high-energy gamma-rays are known to be feeble (Devons and Hine 1949, Sanders 1952, Chao 1950).

§ 5. DISCUSSION

In order to discuss the significance of the absence of γ_2 and γ_4 we must have some idea of the relevant branching ratios to be expected 'in the absence of isotopic spin rules'. It is not possible to obtain more than a very rough orientation on this point and this we derive from the predictions of the single-particle model (Weisskopf 1951, Blatt and Weisskopf 1952). This model is clearly not directly applicable to the present nucleus, but its predictions will at any rate provide an order-of-magnitude estimate. It appears that the predictions of this model are rather reliable for electric dipole transitions in light nuclei (Wilkinson 1953).

According to the single-particle model γ_1 should be $2\cdot4\times10^7$ times more probable than γ_2; we find it to be at least 120 times more probable so the isotopic spin rule has not slowed up the transition by as much as a factor 2×10^5, i.e. if we take the ground state of ^{16}O to be pure $T=0$, the relative amplitude of the $T=1$ state admixed to the predominantly $T=0$ state of 7·12 Mev is greater than 2×10^{-3}.

According to the single-particle model γ_3 should be 6 times less probable than γ_4; we find it to be at least 200 times more probable so the isotopic spin rule has slowed up γ_4 by at least a factor 1200, i.e. the relative amplitude of the $T=1$ states admixed to the predominantly $T=0$ states at 6·91 Mev and 6·14 Mev is less than 3×10^{-2} (assuming equal 'contaminations' of the two states).

If, then, we may give our results their most naive interpretation it appears that these isotopic spin or charge parity states are pure to within somewhere between 0·2% and 3% in amplitude:* this agrees very well with

---

* The principal factors likely to disturb seriously our present estimates of the expected ratios 'without isotopic spin rules' are correlations which would inhibit electric dipole transitions and the possible relevance of the alpha-particle model (Dennison 1940, Seed and French 1952) which would do the same. It is unlikely that the former effect is serious for so light a nucleus with an excitation of 7 Mev (*see* Wilkinson (1953)); about the latter little can be said at the present time. If either of these effects is of importance both limits must be increased; they are probably correct to within a factor of about five.

Radicati's estimate of a few tenths of a per cent to a few per cent as the contamination in amplitude due to Coulomb forces, and so may be taken as some strengthening of the hypothesis of the charge-independence (or charge-symmetry) of the specifically nuclear component of the nucleon–nucleon interaction.

References

Adair, R. K., 1952, *Phys. Rev.*, **87,** 1044.
Ajzenberg, F., and Lauritsen, T., 1952, *Rev. Mod. Phys.*, **24,** 321.
Arnold, W. R., 1950, *Phys. Rev.*, **80,** 34.
Barnes, C. A., French, A. P., and Devons, S., 1950, *Nature, Lond.*, **166,** 145.
Blatt, J., and Weisskopf, V. F., 1952, *Theoretical Nuclear Physics* (John Wiley).
Chao, C. Y., 1950, *Phys. Rev.*, **80,** 1035.
Chao, C. Y., Tollestrup, A. V., Fowler, W. A., and Lauritsen, C. C., 1950, *Phys. Rev.*, **79,** 108.
Dennison, D. M., 1940, *Phys. Rev.*, **57,** 454.
Devons, S., Hereward, H. G., and Lindsey, G. R., 1949, *Nature, Lond.*, **164,** 586.
Devons, S., and Hine, M. G. N., 1949, *Proc. Roy. Soc.* A, **199,** 56.
Devons, S., and Lindsey, G. R., 1949, *Nature, Lond.*, **164,** 539.
Fagg, L. W., and Hanna, S. S., 1952, *Phys. Rev.*, **88,** 1205.
Hutchinson, G. W., and Scarrott, G. G., 1951, *Phil. Mag.*, **42,** 792.
Lauritsen, T., 1952, *Annual Review of Nuclear Science* (Stanford), p. 67.
Radicati, L. A., 1952, *Phys. Rev.*, **87,** 521 ; 1953, *Proc. Phys. Soc.* A, **66,** 139.
Rasmussen, V. K., Hornyak, W. F., Lauritsen, C. C., and Lauritsen, T., 1950, *Phys. Rev.*, **77,** 617.
Sanders, J. E., 1952, *Phil. Mag.*, **43,** 630.
Seed, J., and French, A. P., 1952, *Phys. Rev.*, **88,** 1007.
Trainor, L. E. H., 1952, *Phys. Rev.*, **85,** 962.
Weisskopf, V. F., 1951, *Phys. Rev.*, **83,** 1073.
Wilkinson, D. H., 1953, *Phil. Mag.*, **44,** 450.

LVIII. *Bose–Einstein Condensation in Helium Films*

By J. M. Ziman
Clarendon Laboratory, Oxford *

[Received January 30, 1953, revised MS. received February 20, 1953]

Abstract

It is shown that an ideal Bose–Einstein gas confined to a layer of any finite thickness behaves like a ‘two-dimensional gas’ in that the temperature of the B.E. condensation is size dependent and tends to zero as the area of the layer tends to infinity. Such an effect is not observed in real helium films. If it is assumed that liquid He must be treated as if made up of independent B.E. assemblies, each smaller than a fixed length L_0 ($\sim 7\times 10^{-6}$ cm), the observed variation, with thickness, of the temperature of onset of superfluidity, in unsaturated films, may be closely predicted. The zero-point motion in each restricted assembly is then close to the critical transfer velocity of superflow, and L_0 is of the same order of magnitude as the thickness of the saturated film. This assumption brings the ideal B.E. gas model nearer to the real structure of liquid He, but the interpretation of L_0 as a ‘scattering length’ does not give agreement with estimates from kinetic theory.

§ 1. Introduction

It is well known that one interpretation of the lambda-point transition in liquid helium is that it is equivalent to the condensation process which can be shown to occur, theoretically, in an ideal Bose–Einstein gas. The details of the process are not well predicted, but the absence of any similar phenomena in ^{3}He, which obeys Fermi–Dirac statistics, seems very strong evidence that this hypothesis is fundamentally correct (see review articles by Dingle 1952, Daunt 1952). The mathematical argument for the condensation has been exhaustively studied by numerous authors, and there now seems little doubt that in an infinite assembly of B.E. particles there is a discontinuity in certain thermodynamic properties at a definite temperature. It is usually assumed that a macroscopic sample of liquid helium may be treated as if it were part of such an infinite assembly, and that the appearance of superfluidity corresponds to the condensation process.

There are serious difficulties, to which we shall return later, in this treatment of a liquid as if it were a perfect gas. For the moment we observe that the phenomena of superfluidity are not confined to the bulk liquid, but have been observed, at sufficiently low temperatures,

---

* Communicated by the Author.

in films only a few atomic layers in thickness (Bowers, Brewer and Mendelssohn 1951, Long and Meyer 1953). If the assumption is valid that the onset of superfluidity corresponds to a B.E. condensation, this should be true as much for a thin film as for the bulk liquid. It is, therefore, of some interest to study the mathematical properties of an ideal B.E. gas, not, as in the usual theory, in an infinite cubical box, but confined to a layer of finite, even microscopic, thickness, and to see whether these properties agree in any way with the observed properties of thin films of helium.

If we treat a film as a two-dimensional gas, which would, at first sight, seem a reasonable approximation, we find that there is no B.E. condensation at all, according to the standard argument, in an infinite square. For a finite assembly of this type, Osborne (1949) has shown that there exists an ‘ accumulation ’ temperature, akin to a condensation temperature, and varying as $1/\ln N$, where N is the number of atoms in the system.

The problem of the ideal B.E. gas in a layer of finite thickness has also been discussed by Osborne (1949), who has argued that the usual demonstration of the B.E. condensation breaks down only when the layer has become thinner than a critical distance, q, which is given, approximately, by the condition that the mean thermal energy, kT, of each atom shall be of the same order of magnitude as the zero-point energy $p^2/2M$, where p is the momentum conjugate to q, satisfying the uncertainty relation $pq \sim h$. It would seem evident from first principles that for films thinner than q the higher energy levels, corresponding to momenta $2p$, $3p$, etc., normal to the plane of the film, would not be excited, and the system behaves as if it were two-dimensional.

From this argument, one would evidently conclude that if one took a film of large, but finite thickness (e.g. 1 cm) and infinite extent, it would show an ordinary B.E. condensation, but that as one squeezed the faces together the transition temperature would be gradually reduced, and would tend to zero when the critical thickness was reached. Such a lowering of the onset of superfluidity in thin films is actually observed; the original object of this research was to calculate it explicitly, for it appeared that the results were implicit in Osborne's work, and merely required analysis.

However, it turned out that the difficulty of estimating the errors in Osborne's replacement of sums by integrals led to the adoption in the present work of a different technique, by means of which the following paradoxical result has been obtained: the condensation temperature of a B.E. gas confined to a layer of fixed thickness, however large, tends to zero as $1/\ln N$, when N, the total number of particles, tends to infinity (the density being kept constant). In other words, a film of finite thickness always behaves as if it were ‘ two-dimensional ’. It is impossible to assume that a real film is just a small part of an indefinitely large assembly; the size of the assembly affects the transition temperature.

The obvious way of escaping from this difficulty is to assume that there exists a natural upper limit to the size of the assembly, and that macroscopic quantities of liquid helium are to be thought of as made up of large numbers of such maximal assemblies, each independent of its neighbours. There is some theoretical justification for this device, and it will be shown that we can obtain a good estimate of the variation of the lambda point with film thickness, without changing the usual results for the properties of the bulk fluid. This natural limiting size is a cube of side about 7×10^{-6} cm and it is shown that a fundamental length of this order of magnitude plays an important role in many distinct phenomena observed in He II.

§ 2. BOSE–EINSTEIN GAS IN RECTANGULAR BOX

As usual, we take a system of B.E. particles, each of mass M, whose wave functions are confined to a rectangular box of dimensions L, L, D, where the thickness $D \ll L$. The energy levels of the system are then given by

$$E_{lmn}=(l^2+m^2)\alpha kT+n^2\beta kT, \quad . \ . \ . \ . \ . \ . \ . \quad (1)$$

where $\alpha=h^2/8ML^2kT$ and $\beta=h^2/8MD^2kT$ and l, m, n, are integers.

Following Fowler and Jones (1938), we use the method of the Grand Partition Function, which tells us that the total number, N, of particles is given by

$$N=\sum_{j,l,m,n=1}^{\infty}\exp\left(\mu j-jE_{lmn}/kT\right), \quad . \ . \ . \ . \ . \quad (2)$$

where μkT is the chemical potential of the gas particles. Thus, from (1) and (2), we have

$$N=\sum_{jlmn}\exp j\{\mu-(l^2+m^2)\alpha-n^2\beta\}. \quad . \ . \ . \ . \quad (3)$$

For a fixed value of j, the remaining terms represent a product of Theta Functions, to which we may apply Jacobi's transformation (Whittaker and Watson 1952, p. 475). This may be written

$$\sum_{s=1}^{\infty}\exp\left(-xs^2\right)=\tfrac{1}{2}\sqrt{(\pi/x)}\Big\{1+2\sum_{s=1}^{\infty}\exp\left(-\pi^2s^2/x\right)\Big\}-\tfrac{1}{2}. \quad . \ . \ . \quad (4)$$

Now, if $x\leqslant\pi/2$, the error in taking $\tfrac{1}{2}\{\sqrt{(\pi/x)}-1\}$ in place of the right-hand side of (4) is at most of the order of one part in 500. Again, if $x>\pi/2$, the error in taking $\exp(-x)$ alone, in place of the sum, is of the same magnitude. Thus, it is possible, to a sufficient degree of accuracy, to take these simple expressions alone to represent the Theta Function for appropriate values of x.

To use this approximation in the evaluation of (3), we must divide the summation over j into three regions :

$$(a)\ 1\leqslant j\leqslant\pi/2\beta, \quad (b)\ \pi/2\beta<j\leqslant\pi/2\alpha, \quad (c)\ \pi/2\alpha<j.$$

We here assume that $\pi/2\alpha$ and $\pi/2\beta$ are integers; this can easily be arranged, since α and β are small, except for very thin films. No difficulty arises if this condition is not fulfilled; we merely taken the nearest integers instead.

We may now write (3) in the form

$$N \approx \frac{1}{8}\sum_{j=1}^{\pi/2\beta} \exp(\mu j)\{\sqrt{(\pi/j\alpha)}-1\}^2\{\sqrt{(\pi/j\beta)}-1\}$$
$$+\frac{1}{4}\sum_{j=\pi/2\beta+1}^{\pi/2\alpha} \exp\{j(\mu-\beta)\}\{\sqrt{(\pi/j\alpha)}-1\}^2+\sum_{j=\pi/2\alpha+1}^{\infty} \exp\{j(\mu-2\alpha-\beta)\}. \quad . \quad . \quad . \quad (5)$$

It is evident that each of the terms arising from the sums over regions (a) and (b) is bounded, unless $\mu \to \infty$, or α, or β vanishes. But the last term has a singularity when

$$(2\alpha+\beta-\mu)=\epsilon \to 0, \quad . \quad . \quad . \quad . \quad . \quad . \quad . \quad . \quad (6)$$

where the sum behaves like $1/\epsilon$. To obtain the thermodynamic properties of the assembly, we must solve (5) for μ, as a function of N, etc. Evidently, when N is small, μ is negative. As N increases, so does μ, until it approaches the value $2\alpha+\beta$. But here any large value of N can be fitted by taking ϵ sufficiently small. On the other hand, the first two sums are monotonically increasing functions of μ, and cannot, for $\mu \leqslant 2\alpha+\beta$, exceed a fixed value N_0 obtained by evaluating them for $\mu=2\alpha+\beta$, i.e. $\epsilon=0$. Thus, when $N>N_0$ we must have $1/\epsilon \sim N-N_0$, which is of the order of magnitude of N, a large number. But, when $N<N_0$, (5) can be satisfied by taking $\epsilon=c(1-N/N_0)^2$, i.e. of the order unity. This is because the leading term in the first sum then behaves like a 'generalized Zeta Function' as in the usual theory of the B.E. condensation, and can be expanded in a power series in $\epsilon^{1/2}$, of the general type $N_0(1-a\epsilon^{1/2}+\ldots)$ (Robinson 1951). In other words, as the density increases (at constant temperature) a point is reached at which the chemical potential ceases to rise visibly, but becomes almost constant. This represents a condensation process; physically it means that all subsequent particles beyond N_0 go into the lowest energy level. Since we are always keeping N finite, there is no question of a mathematical discontinuity in the gradient of μ say, but we have an abrupt change, over a small interval, which would be physically indistinguishable from a true singularity.

To find the conditions for the condensation to occur, we must solve the equation for N_0, i.e.

$$N_0=\frac{1}{8}\sum_{j=1}^{\pi/2\beta} \mathrm{e}^{j(2\alpha+\beta)}\left(\sqrt{\frac{\pi}{j\alpha}}-1\right)^2\left(\sqrt{\frac{\pi}{j\beta}}-1\right)+\frac{1}{4}\sum_{j=\pi/2\beta+1}^{\pi/2\alpha} \mathrm{e}^{2j\alpha}\left(\sqrt{\frac{\pi}{j\alpha}}-1\right)^2, \quad . \quad . \quad . \quad (7)$$

where the right-hand side is a function of temperature through α and β.

The exact evaluation of the various sums in (7) is exceedingly complicated. However, if we write it in the form

$$\frac{8N_0\alpha\beta^{1/2}}{\pi^{3/2}}=\sum_{j=1}^{\pi/2\beta}\mathrm{e}^{j(2\alpha+\beta)}\left(\sqrt{\frac{1}{j}}-\sqrt{\frac{\alpha}{\pi}}\right)^2\left(\sqrt{\frac{1}{j}}-\sqrt{\frac{\beta}{\pi}}\right)$$
$$+2\sqrt{\frac{\beta}{\pi}}\sum_{j=\pi/2\beta+1}^{\pi/2\alpha}\mathrm{e}^{2j\alpha}\left(\sqrt{\frac{1}{j}}-\sqrt{\frac{\alpha}{\pi}}\right)^2, \quad . \quad . \quad . \quad (8)$$

the left-hand side is a function only of the number density of particles, N_0/L^2D, and of the temperature, whilst the right-hand side may be expanded as a function of α and β, which we take to be small. An outline of the method of expansion is given in the appendix. The result may be written

$$(T_\lambda/T)^{3/2}=1+\beta^{1/2}(-0{\cdot}19+0{\cdot}648\ln\beta-0{\cdot}432\ln\alpha)+0{\cdot}432\alpha^{1/2}\ln\beta, \quad (9)$$

where
$$(N_0/L^2D)(h^2/2\pi MkT_\lambda)^{3/2}=2{\cdot}612, \quad . \quad . \quad . \quad . \quad . \quad (10)$$

i.e. T_λ is the temperature of the B.E. condensation in an infinite cube, at density N_0/L^2D, according to the usual theory.

This formula may be expressed in a more self-evident manner if we use the spacing of atomic layers in the film as our unit of length. This unit is $3^{1/4}2^{-1/3}(L^2D/N_0)^{1/3}$ (Frederikse and Gorter 1950), which is 3·72 Å in ordinary liquid He. Then we have $\alpha=1{\cdot}17(T_\lambda/T)L^{-2}$, $\beta=1{\cdot}17(T_\lambda/T)D^{-2}$, i.e. $\alpha^{-1/2}$ and $\beta^{\,1/2}$ are approximately the length and thickness of the box in numbers of atomic layers, when the temperature is near the lambda point of the bulk fluid. In these units we have

$$\left(\frac{T_\lambda}{T}\right)^{3/2}=1-\frac{1}{D}\left(\frac{T_\lambda}{T}\right)^{1/2}\left\{0{\cdot}15-0{\cdot}504\ln\left(\frac{T_\lambda}{T}\right)+1{\cdot}512\ln D-1{\cdot}008\ln L\right\}$$
$$-\frac{1{\cdot}008}{L}\left(\frac{T_\lambda}{T}\right)^{1/2}\ln D. \quad . \quad . \quad . \quad . \quad . \quad . \quad . \quad . \quad . \quad . \quad (11)$$

§ 3. SHAPE-DEPENDENCE OF CONDENSATION TEMPERATURE

Equation (11) gives the temperature, T, of the B.E. condensation in a block of dimensions $L\times L\times D$ in ' layer units ', in terms of the transition temperature T_λ in an infinite cube of bulk liquid of the same density. Now let us consider some special cases.

(*a*) If $L\to\infty$, whilst D remains constant, it is obvious that T tends to zero. This result is not a spurious consequence of the approximations; it can be seen to be due to the second sum in (8) which has a singularity at $\alpha=0$. In the limit of large N, it is easy to show that

$$(T/T_\lambda)^{3/2}\propto 1/\beta^{1/2}\ln N.$$

This corresponds to Osborne's result for a two-dimensional gas, but now we see that every layer of finite thickness shows the same behaviour, the difference being that the thicker the system the larger must be the value of N to achieve a given lowering of the condensation temperature. Osborne's critical thickness occurs at $\beta=1$, when the system does indeed have exactly the properties of a two-dimensional gas, but in the limit, as $N \to \infty$, this is irrelevant, and all layers of finite thickness behave alike.

(*b*) If both L and D tend to infinity together, in any way, $T \to T_\lambda$ and we have the usual theory of the bulk fluid.

(*c*) If L and D are equal and finite, two terms in (11) cancel. The resulting formula is not quite correct, however, because we have assumed throughout that $\alpha \ll \beta$, i.e. $D \ll L$. The necessary adjustments are easily made, and we obtain

$$(T_\lambda/T)^{3/2} = 1 - L^{-1}(T_\lambda/T)^{1/2}\{-1{\cdot}15 - 0{\cdot}504 \ln (T_\lambda/T) + 1{\cdot}512 \ln L\}. \quad (12)$$

This formula is, of course, an approximation valid only for large L; we need only consider the case $\ln L > 1{\cdot}15/1{\cdot}51$, where it is evident that $T > T_\lambda$. The maximum possible value of T/T_λ is 1·25, and the ratio tends rapidly to unity as L increases. Thus, the lambda point in a finite cube is slightly higher than in the infinite assembly, except when the sides of the cube are only a few angströms in length, i.e. when it contains only a few score atoms.

(*d*) If $D \ll L$, and L is constant, the dominant factor on the right-hand side of (11) is that containing $\ln L$, and it is clear that T/T_λ decreases as D decreases. The trend is monotonic, and $T \to 0$ as $L \to 0$. (One might object that we have then violated the condition that β be small, used in evaluating (9). Study of (8) for the case $\beta > \pi/2$ shows that the first sum may be neglected, and the second sum behaves like $\beta^{1/2} \ln \alpha$, the same dominant term.)

§ 4. THE 'SCATTERING LENGTH'

It is evident from the above analysis that we can make no progress in studying the lambda-point phenomena in real films of helium if we insist that they shall form parts of infinite assemblies. If we were to consider every observed helium film as a complete assembly, we should find the condensation temperature varying with the size of, say, the glass plate on which it is formed, which is not in agreement with observation. In any case, the calculated values of T from formula (11) turn out to be much smaller than the observed values, if we put in the macroscopic lengths of the apparatus, of the order of 1 cm, for L.

The only way out of this difficulty is, apparently, to make the following new assumption: a macroscopic assembly of liquid helium must be treated as if it were made up of independent sub-assemblies, none of whose linear dimensions may be greater than a fixed length, L_0. Thus, for the bulk liquid we consider a cube, of side L_0, with the particles confined strictly within its boundaries, and construct the macroscopic volume by piling up a number of identical, physically independent cubes. When a film is thinner than L_0, we take rectangular blocks, of side L_0, to cover the area.

The effect of this assumption on the theoretical properties of the bulk liquid is negligible, so long as L_0 is moderately large. We then have case (*c*) above, and it is clear that the effect is merely to raise the predicted lambda point by a small amount. Since the theoretical condensation temperature of a B.E. gas of the density of liquid helium is, in any case, about 50% larger than the observed value, this further small change is quite unimportant.

On the other hand, by choosing a suitable value of L_0, we may be able to fit the observed variation of the condensation temperature with film thickness. That is, we solve (11) as in case (***d***) above, and interpret D as the thickness of the film. T cannot be taken at its face value as the transition temperature in the film, because of the discrepancy between the observed and calculated values of T_λ for the bulk fluid. It is reasonable to assume however, that the cause of the discrepancy acts proportionately in bulk fluid and in film, and we can 'renormalize', by comparing observed and theoretical values of T/T_λ. If we insert the experimental values of D and T/T_λ (Brewer and Mendelssohn 1953) into (11) we obtain a series of values of L, ranging between 150 and 250 atomic layers. This represents a variation of only 10% in ln L, which is the significant parameter in the theory, whilst D goes from 4 to 10 layers. The value L_0=200 layers=$7{\cdot}4\times10^{-6}$ cm has been chosen as the best estimate for the scattering length, and in the figure the theoretical variation of the transition temperature with the thickness of the film is compared with the experimental curve.

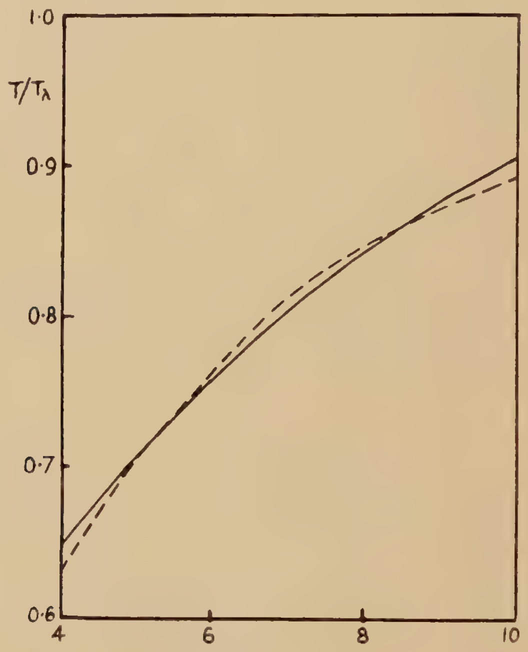

D (Atomic Layers).

Transition temperature as function of film thickness.

——— observed — — — calculated

It will be seen that the agreement is remarkably close, particularly in the central regions of the curves. L_0 is the only adjustable parameter in the theory, yet the curves can be made nearly to coincide over quite a large range of values. We should not be surprised to find discrepancies at the lower end, because there the theory is not properly valid, terms in $\beta \sim D^{-2}$ having been neglected.

§ 5. CONCLUSION

It is clear that by introducing a standard ‘ scattering length ’ of the order of 7×10^{-6} cm into the theory of liquid helium we can improve the usual theory in two entirely distinct ways. We avoid the paradox that a physically thick layer, of infinite extent, would behave differently from a sample of an infinite cube and we obtain a very good theoretical estimate of the variation of the transition temperature with film thickness.

There are other considerations which lend some support to this hypothesis. The scattering length is of the same order of magnitude as the thickness of the saturated helium film below the lambda point, i.e. about 3×10^{-6} cm. Now we have shown (eqn. (6)) that the chemical potential of the helium atoms below the lambda point is given by $kT(2\alpha+\beta)$. α is fixed by our choice of L_0, but β depends on the thickness D of the film, and has a minimum value, α, when $D=L_0$. Thus, there is a distinct gain in negative free energy if the film thickens to this extent—but no further gain from any greater thickness, since we should then have $D>L_0$, which contradicts our assumptions (or, rather, we should have to construct new fundamental cubes on the surface of the layer). This minimum chemical potential is the same as that in the bulk liquid, as it must be in a saturated film. Above the lambda point, the small gains obtained in the chemical potential in this way are outweighed by large entropy terms, and there is no reason to depart from the normal theory of adsorbed gases, which gives a thin film.

Another difficulty of the standard theory which is avoided concerns the interpretation of the ‘ condensed ’ atoms as superfluid atoms, for if these are assumed to lie in the lowest energy state of an infinite container, they would have zero momentum, and would be incapable of flow (Mendelssohn 1945). But, in our interpretation, the ‘ condensed ’ atoms lie in the ground state of a box of side L_0, and it can easily be shown that this corresponds to their having a ‘ zero-point velocity ’ of 70 cm/sec, if L_0 is about 7×10^{-6} cm. This is of the same order of magnitude as the observed maximum velocity (30–50 cm/sec, Bowers and Mendelssohn 1952), for flow through superleaks, and provides a simple explanation of the fact that this velocity does not seem to depend on the dimensions of the apparatus.

The agreement may well, of course, be fortuitous. Leaving aside the question, to which we shall return below, whether this equating of zero-point velocity to superflow velocity is tenable, we are still no nearer to explaining why the flow of the condensed atoms should be frictionless. To discuss this, we should need to allow exchange of particles between neighbouring boxes, and it is difficult to see how this can be formulated in a consistent manner. But in this respect we are no worse off than in the usual B.E. gas theory; all that we have done is to assign a new distribution of energy levels to the whole assembly by insisting that the wave functions shall vanish at each of a set of plane boundaries.

It has recently been suggested (Brewer and Mendelssohn 1953) that the anomalous behaviour of unsaturated helium films below the lambda point of the bulk fluid may be explained by the formation of ‘ clusters ’ at least 10^{-6} cm in diameter, of the bulk fluid. This is supported, at least qualitatively, by the present theory, since we provide a reason for the clusters to grow to a certain thickness L_0, but not larger.

Throughout this paper, the object has been to show that the usual theory of B.E. condensation is paradoxical, and cannot be applied consistently to the case of thin layers. We have shown what modification is necessary to resolve the paradox and to give some agreement with the observed properties of helium films. It is worth discussing briefly whether there is any *a priori* justification for the assumption we have made—the introduction of a standard length.

In treating liquid helium as an ideal gas, we have neglected two important factors: the van der Waals attractive forces between the atoms and their finite impenetrable volumes. The attractive forces, although responsible for the condensation to the liquid state, are very weak, and it seems reasonable to take account of them by assuming that inside the liquid they give rise to a smeared-out uniform potential, which rises sharply at the boundaries and reflects the atoms back into the occupied volume. This model gives a good theoretical estimate of the vapour-pressure curves of ^{3}He and ^{4}He (Daunt 1952). But it cannot be correct to treat the atoms as if they were free to bounce unchecked from side to side of the whole container. It is true that the density of liquid helium is low, and the spacing between the atoms much larger than the gas-kinetic diameter, but there must be collisions and scattering of one atom by another. After having gone a certain distance, an atom will have ‘ forgotten ’ its original momentum, owing to this scattering. That is to say, it cannot be correct to discuss the energy levels as if they were those of the whole container, the only conditions on the wave functions being that they should vanish on the walls. The picture of plane waves persisting unchanged from one side of the box to the other must be modified to allow for this incoherent scattering. Our assumption is tantamount to simulating the scattering by inserting walls, distant L_0 apart, and insisting that the wave functions shall vanish on these walls also. The detailed shape of these elementary volumes is not important; the asymptotic distribution of the eigenvalues of the wave equation depends only on the general dimensions of the assembly (Courant and Hilbert 1931, p. 373).

The distance L_0 may thus be interpreted as a ‘ scattering length ’. But if we attempt to calculate it directly, from kinetic theory, it turns out to be far smaller than the value we have adopted. It will, of course, be rather larger than the mean free path for collisions, as calculated from the geometric cross-section of the atoms, owing to the persistence of velocity ; the effect of an impenetrable wall on an impinging particle is much more drastic than that of a glancing collision with a like particle, so that the walls must be rather further apart to give the same scattering effect. But even then, about 10^{-7} cm would seem to be an upper limit, at the density of liquid helium.

That such a calculation must be fundamentally correct is shown by the fact that the ‘ zero-point energy ’ in liquid helium is large, corresponding to a velocity of about 10^4 cm/sec, whereas, on our model, as pointed out above, this would only be about 70 cm/sec. This is a fundamental difficulty in all theories based on the B.E. condensation (Mendelssohn 1945). Since the zero-point motion is just ‘ uncertainty momentum ’, the velocity is inversely proportional to the scattering length, for which a value of about 5×10^{-8} cm is thus suggested.

Thus, although we have taken a step in the right direction to bring the B.E. gas model nearer to the physical reality of liquid helium, there is still a large gap which cannot be bridged ; if L_0 is of the order of a few angströms, the condensation phenomena are inexplicable—if it is as large as 7×10^{-6} cm, the model has no firm basis in kinetic theory. We apparently need a theory in which lengths of both these magnitudes occur, in order to explain, on an equal footing, all the phenomena.

I am indebted to Dr. K. Mendelssohn and Mr. D. F. Brewer for several valuable discussions, and for the experimental data shown in the figure.

APPENDIX

The evaluation of the various sums occurring in (8) is carried out along the following lines. A typical term would contain, say,

$$U_r = \sum_{j=1}^{\pi/2\beta} j^{-r} e^{jb},$$

where $b \leqslant \beta$. Thus, $jb \leqslant \pi/2$ for the values of j included in the sum, so that the exponential term may be expanded in a power series. We have

$$\begin{aligned} U_r &= \sum_{j=1}^{\pi/2\beta} \sum_{s=0}^{\infty} j^{-r}(jb)^s/s! \\ &= \sum_{s=0}^{\infty} (b^s/s!) \sum_{j=1}^{\pi/2\beta} j^{s-r}. \end{aligned}$$

But, by the Euler–McLaurin theorem (Whittaker and Watson, p. 128),

$$\sum_{j=1}^{\pi/2\beta} j^{s-r} \sim \int_1^{\pi/2\beta} x^{s-r}\,dx + \tfrac{1}{2}\{1+(\pi/2\beta)^{s-r}\} + \sum_{t=1}^{\infty} \frac{(-1)^{t-1}}{2t!} B_t \left[\frac{d^{2t-1}}{dx^{2t-1}} x^{s-r}\right]_1^{\pi/2\beta}.$$

We need only retain the lowest power of β, which comes from the upper limit of the integral, i.e.

$$U_r \sim \sum_{s=0}^{\infty} \{b^s/(s-r+1)s!\}(\pi/2\beta)^{s-r+1}$$
$$=(2\beta/\pi)^{r-1} \sum_{s=0}^{\infty} (\pi b/2\beta)^s/(s-r+1)s!,$$

and the series converges rapidly.

For the leading term of (8), for which $r=3/2$, it is better to use

$$\sum_{j=1}^{\pi/2\beta} j^{-3/2}=\zeta(3/2)-\sum_{j=\pi/2\beta+1}^{\infty} j^{-3/2},$$

giving a correction term, of order $\beta^{1/2}$ to the known Zeta Function. The logarithmic terms arise when $s-r=-1$ in the above expansions and the series can then be evaluated by the theorem of Euler's limit.

In principle, the calculation can be carried to higher orders of approximation, using the asymptotic Euler–McLaurin expansion, but it becomes exceedingly complicated. The most important terms in (9) are those involving $\ln \alpha$ and $\ln \beta$, and these have coefficients which are exactly $2/\sqrt{\pi}\zeta(3/2)$ and $3/\sqrt{\pi}\zeta(3/2)$ respectively. The number 0·19 is the resultant of many sums and differences of terms like U_r but it evidently would not affect the theory very greatly if it were a few per cent in error.

REFERENCES

BOWERS, R., BREWER, D. F., and MENDELSSOHN, K., 1951, *Phil. Mag.*, **42,** 1445.

BOWERS, R., and MENDELSSOHN, K., 1952, *Proc. Roy. Soc.* A, **213,** 158.

BREWER, D. F., and MENDELSSOHN, K., 1953, *Phil. Mag.*, **44,** 340.

COURANT, R., and HILBERT, D., 1931, *Methoden der Mathematischen Physik*, 2nd ed. Vol. 1 (Berlin : Springer).

DAUNT, J. G., 1952, *Advances in Physics*, **1,** 169.

DINGLE, R. B., 1952, *Advances in Physics*, **1,** 111.

FOWLER, R. H., and JONES, H., 1938, *Proc. Camb. Phil. Soc.*, **34,** 573.

FREDERIKSE, H. P. R., and GORTER, C. J., 1950, *Physica*, **16,** 402.

LONG, E., and MEYER, L., 1953, *Advances in Physics*, **2,** 1.

MENDELSSOHN, K., 1945, *Proc. Phys. Soc.*, **57,** 371.

OSBORNE, M. F. M., 1949, *Phys. Rev.*, **76,** 396.

ROBINSON, J. E., 1951, *Phys. Rev.*, **83,** 678.

WHITTAKER, E. T., and WATSON, G. N., 1952, *Modern Analysis*, 4th ed. (Cambridge : University Press).

LIX. CORRESPONDENCE

Anomalous Surface Tension in Helium II

By D. F. Brewer and K. Mendelssohn, F.R.S.
The Clarendon Laboratory, Oxford

[Received March 17, 1953]

In trying to interpret recent observations on the formation of the helium II film (Brewer and Mendelssohn 1953), we have suggested the presence of bulk liquid at pressures well below the saturation pressure. In order to account for such a phenomenon, a quantity of the dimension of a length, d, characteristic for liquid helium II, was introduced. The significance of d is that of the de Broglie wavelength of the lowest energy state, i.e. the distance within which the position of a helium atom in this state cannot be determined. It may then be energetically advantageous for clusters of bulk liquid to be formed of the order of magnitude of d. It was also concluded from the experiments that d would be at least $\sim 10^{-6}$ cm. The existence of such a characteristic mean free path in liquid helium II has since been made plausible on theoretical grounds by Ziman (1953). We have further concluded that such a model should lead to an anomalous surface tension effect. The macroscopic surface tension does not show a discontinuity at the lambda point (Allen and Misener 1938), as is indeed to be expected owing to the absence of a latent heat. However, if our model is correct, one can expect the surface tension to become size-dependent when dimensions of the order of d are approached, because of the extra energy available for liquid clusters of this size. An experiment was therefore designed to investigate this question.

A cylindrical container C (fig. 1) 12 cm long and of internal diameter 2·3 cm was closely packed with about 1000 plane circular glass plates with an estimated gap of $\sim 10^{-4}$ cm or less between neighbouring plates. At the bottom of C a glass tube T was attached. The whole container, which could be filled with gas through the line L, was immersed in liquid helium.

Helium gas was introduced into C just below the lambda point until some bulk liquid appeared in T. The temperature of the helium bath was then raised to just above the lambda point. In doing this, some liquid should evaporate from T, but as the gas space as well as the relative increase in temperature were small, this effect was insignificant. In addition, one must expect the helium film of $\sim 10^{-6}$ cm thickness to disappear from the surface of the glass plates, and this should lead to a small rise of the liquid level in T.

An increase of bulk liquid in the tube *T* was indeed observed, but the amount exceeded that calculated for the film by between 10 and 20 times.

Since ordinary capillary condensation due to the normal surface tension will change very little in the small temperature interval ($<0{\cdot}1°$) through which the temperature of the container *C* was raised, the appearance of this large amount of bulk liquid must be connected with the lambda phenomenon. It seems indeed that below the lambda point, a large amount of liquid helium II was held in the gaps between the plates. As the lambda temperature is exceeded, the significance of *d* is lost, and with it the extra energy holding the liquid in clusters of small dimensions.

Fig. 1

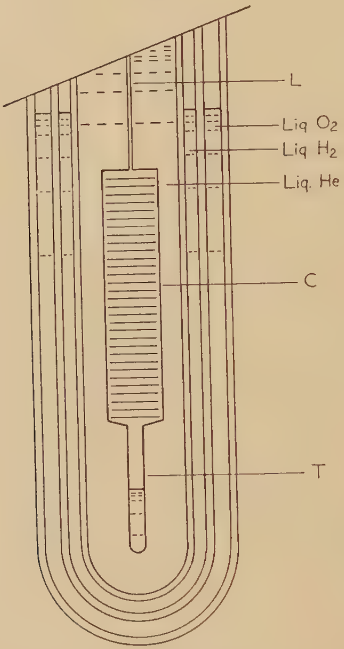

While thus our experiments indicate that the postulated effect exists, certain features of it require further elucidation. For instance, another appreciable quantity of bulk liquid appears as the temperature is raised from 2·2° to 2·5°K. It is not clear whether this is due to the fact that at the lambda point, further expulsion of liquid from the plates becomes very slow, or whether the effect actually extends into the region of the slow anomalous increase of entropy between the lambda point and 2·6°K. Moreover, it may be significant that in the present as well as in the earlier experiments, the plane of the solid surface on which the helium was deposited was horizontal. Finally, the relation between the clustering effect and the well known film phenomenon is not quite clear.

The most likely explanation seems to be that the tendency to form liquid clusters of the order of the de Broglie wavelength is the primary effect of which the film presents only one particular aspect.

The existence of an anomalous surface tension effect in liquid helium II will go far in explaining a number of curious features in earlier experiments. It has been shown (Bowers and Mendelssohn 1950) that the anomalously high transfer rates sometimes observed (de Haas and van den Berg 1949) were due to surface contamination by solidified gases, and that surface roughness in general leads to higher transfer rates (Chandrasekhar and Mendelssohn 1952). It is now clear that cracks in surfaces in contact with liquid helium II are filled with bulk liquid. The new effect is probably also responsible for the unexplained high adsorption of helium below the lambda point observed by Long and Meyer (1949) in packed rouge powder. The peculiar transport phenomena observed by the same authors (1952, Method II) in helium films of only $1\frac{1}{2}$ statistical layers may also possibly be due to anomalous capillary condensation in the superleak over the surface of which the flow was thought to occur.

References

Allen, J. F., and Misener, A. D., 1938, *Proc. Camb. Phil. Soc.*, **34,** 299.
Bowers, R., and Mendelssohn, K., 1950, *Proc. Phys. Soc.* A, **63,** 1318.
Brewer, D. F., and Mendelssohn, K., 1953, *Phil. Mag.*, **44,** 340.
Chandrasekhar, B. S., and Mendelssohn, K., 1952, *Proc. Phys. Soc.* A, **65,** 226.
de Haas, W. J., and van de Berg, G. J., 1949, *Rev. Mod. Phys.*, **21,** 524.
Long, E. A., and Meyer, L., 1949, *Phys. Rev.*, **76,** 440 ; 1952, *Ibid.*, **85,** 1030.
Ziman, J. M., 1953, *Phil. Mag.*, in the press.

Flow of an Inviscid Supersonic Jet past an Infinite Wedge

By D. C. Pack and L. Roberts
Department of Mathematics, University of Manchester

[Received 13 March, 1953]

The general character of the two-dimensional inviscid flow, past an infinite wedge, of an infinite stream with supersonic velocity at infinity in the upstream direction, is well-known. When the wedge is too blunt or the stream not sufficiently fast, there is a shock-wave astride the flow at some distance upstream from the wedge. On the line of symmetry, between the central point of the shock-wave and the tip of the wedge, the speed is subsonic, and at the tip itself there is a stagnation point. When the wedge is narrow enough or the stream sufficiently fast, the shock-wave system is attached to the tip of the wedge. There is a small range of wedge angles and Mach numbers for which the flow between the shock-wave and the wedge is subsonic, but almost always when the shock-wave is attached the flow up the sides of the wedge is uniform and supersonic and the shock-wave straight.

Although there have been many papers on the subject of flow past a wedge with a finite length of sloping edge in an infinite stream, the authors are not aware of any discussion of the flow, past an infinite wedge, of a stream of finite thickness such as a jet. Examination shows that this problem has some interesting features.

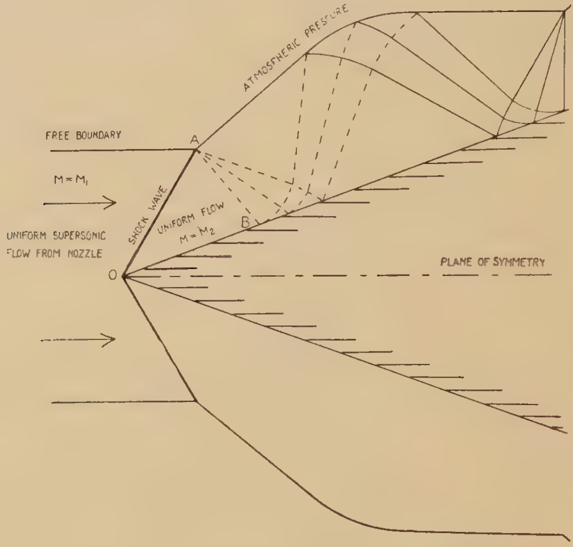

Consider (see the figure) an infinite wedge impinged upon by a uniform jet of gas flowing with supersonic speed (Mach number M_1) at atmospheric pressure from infinity. The speed is supposed to be great enough to produce an attached straight shock-wave with supersonic flow up the sides of the wedge if placed in an infinite stream with the same speed. The shock-wave will be straight for the jet also; for, upstream of the characteristic AB from the point at which the shock-wave meets the boundary, the fact that the jet is not of infinite width can have no influence. The shock-wave deflects the bounding stream-lines and increases the pressure. This increase must instantaneously be removed by means of a Prandtl–Meyer expansion down to atmospheric pressure. This is indicated in the upper half of the figure, by the pencil of Mach lines from A (the broken Mach lines denote expansions, solid Mach lines compressions).

It will be observed that the situation behind the shock-wave is exactly that which occurs when a jet emerges with uniform supersonic velocity from an orifice, the velocity in this case being the velocity (corresponding to Mach number M_2) behind the attached shock-wave. The flow is uniform up to AB. The subsequent motions on the upper and lower faces of the wedge are respectively the upper and lower halves of the supersonic jet described above, and are therefore quasiperiodic with shock-waves occurring in a well-known manner (Pack 1948). (The figure illustrates one complete period of the jet structure, assuming absolute periodicity.)

Professor Lighthill has pointed out to the writers that an experiment designed to reproduce the state of affairs outlined above would be of great interest. The orthodox supersonic jet is quite well understood, although not many experiments have been carried out on the two-dimensional form. The flow up the wedge side considered in this note contains a half-jet bounded, not by another half-jet, but by a solid wall. The usual plane of symmetry in the gas has been replaced by the solid boundary of the wedge. This solid boundary introduces a boundary-layer effect, and it would be profitable to see what differences are induced in the flow by its presence, by comparing studies of the flow in this situation with jet flows obtained by the usual means.

Theoretical work is being undertaken on other and more difficult problems relating to the flow of supersonic jets past bodies when the bow shock-wave is detached.

REFERENCE

PACK, D. C., 1948, *Q.J.M.A.M.*, **1**, 1–17.

ERRATUM

The Role of Preferred Orientation in Elasticity Investigations, by G. BRADFIELD and H. PURSEY, 1953, *Phil. Mag.*, **44**, 439.

Equation (2) should read :

$$\alpha=\frac{-125c(c_{11}+2c_{12})(K-1/5)}{2(c_{11}-c_{12}+3c_{44})(c_{11}+4c_{12}-2c_{44})}\,.$$

LX. *Notices of New Books and Periodicals received*

Thermal Diffusion in Gases. By K. E. Grew and T. L. Ibbs. [Pp. xi + 143.] (Cambridge Monographs on Physics ; C.U.P. 1952.) Price 22*s*. 6*d*. net.

The need for a book of this character has been evident for some time. Most of the large and scattered body of experimental and theoretical work on the thermal diffusion effect in gases and liquids, up to the end of 1951, is here mentioned and correlated. The study of thermal diffusion as a means of investigating intermolecular forces is most fully dealt with and the book will become the standard monograph on this study, alongside de Groot's monograph on the Soret Effect and the Furry and Jones (1946) paper on the Clusius–Dickel column.

The first two chapters are devoted to an outline of the discovery, nature and theoretical treatments of the thermal diffusion effect in gases. Relevant parts of the Chapman–Cowling theory are presented in detail and developed in terms of various molecular models. The third and fourth chapters cover the experimental methods and results of 'two-bulb' experiments, and in the fifth chapter an excellent and detailed discussion and comparison is made of these results with the theory. An account of the diffusion-thermoeffect is given in the next chapter. This is most welcome, as it is probably the first detailed description of Waldmann's work to appear in English, and as it also includes a phenomenological theory of the effect. The Clusius–Dickel column is dealt with next, necessarily rather briefly, in 16 pages. The simple theory of the operation of the column is given, together with some examples of its use for concentrating isotopes. It is a pity that no reference is made to Clusius' production of 99·8% ^{15}N, nor to Jensen's theory of the column which is that usually quoted by Clusius. The last chapter covers the Soret Effect, again briefly, and includes work published since the appearance of de Groot's monograph in 1945. The appendices include a useful list of values of α for nearly all mixtures examined experimentally. R.H.D.

The Method of Descartes. (A study of the Regulae.) By L. J. Beck. (Oxford : Clarendon Press, 1952.) [Pp. 316.] Price 30*s*.

This work is a thorough commentary on the *Regulae* and to a great extent on the *Discours*. Mr. Beck argues, among other things, that the latter cannot properly be understood without the former. His exposition of Descartes' ideas of method and of their importance for Descartes' works in philosophy, mathematics and physics is lucid and illuminating. Mr. Beck's book will, the reviewer believes, prove to be of real use to those who wish to understand the guiding conceptions of Descartes. S. K.

British Association Mathematical Tables, Vol. X, Part 2.—*Bessel Functions of Positive Integer Order.* By W. G. Bickley, L. J. Comrie, J. C. P. Miller, D. H. Sadler and A. J. Thompson. [Pp. xl+255.] (Cambridge University Press, 1952.) Price 60*s*.

The publication of this volume is an event of major importance to table-users. Vol. X, Part 1, containing Bessel functions of orders zero and unity, appeared in 1937 ; Part 2, now issued, contains the functions J_n, Y_n, I_n and K_n for further integral n up to 20. The delay in fulfilling a scheme conceived so long ago is easily understood, not only by reason of the size of the task but because of many unavoidable interruptions. However, the authors have produced a set of tables of lasting value, and which in design and presentation reach the highest standard. R. A. B.

[*The Editors do not hold themselves responsible for the views expressed by their correspondents.*]

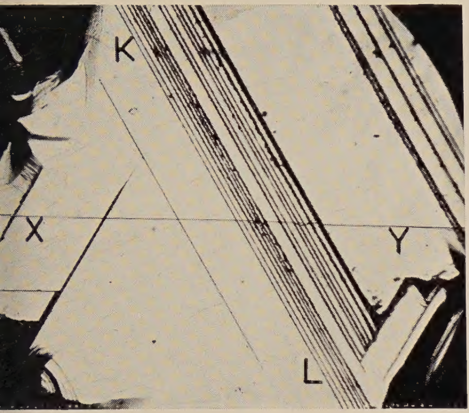

Fig. 1 ×30

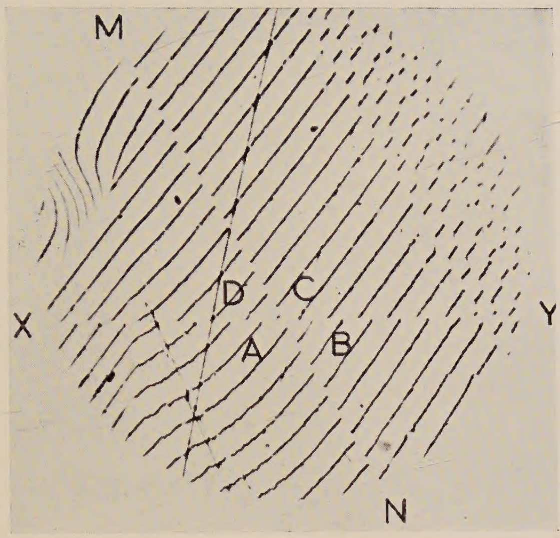

Fig. 2 ×100

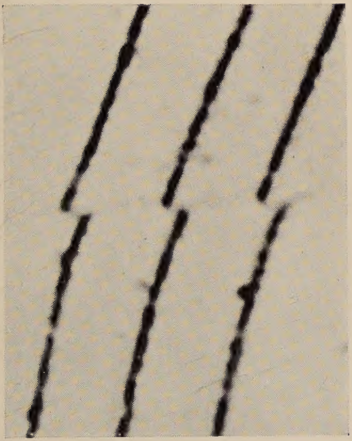

Fig. 3 ×2000

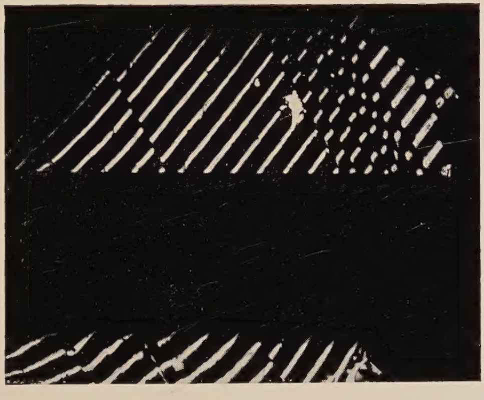

Fig. 4 ×90

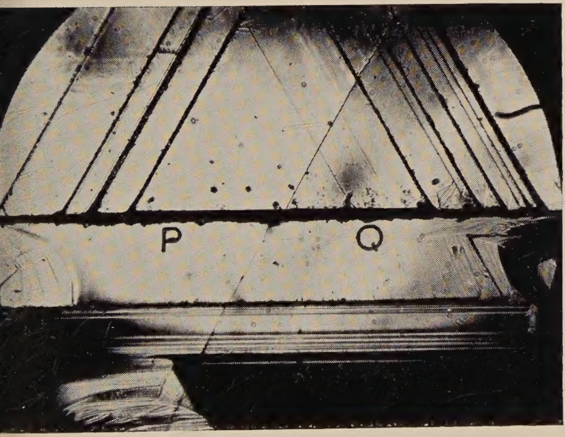

Fig. 5 ×30

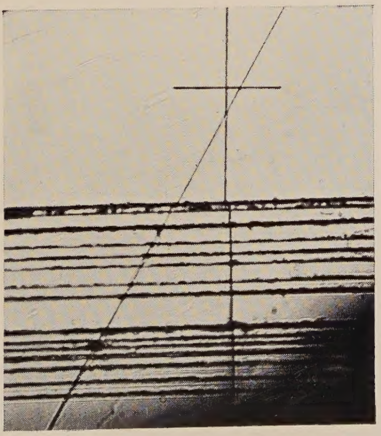

Fig. 6 ×90